VOLTAGE CONTROL IN SMART DISTRIBUTION NETWORK WITH DISTRIBUTED ENERGY RESOURCES

Thesis

Submitted in partial fulfilment of the requirements for the degree of

DOCTOR OF PHILOSOPHY

by

SWATHI TANGI

DEPARTMENT OF ELECTRICAL AND ELECTRONICS ENGINEERING

NATIONAL INSTITUTE OF TECHNOLOGY KARNATAKA

SURATHKAL, MANGALORE - 575 025

JULY 2023

DECLARATION

By the Ph.D. Research Scholar

I hereby *declare* that the Research Thesis entitled "VOLTAGE CONTROL IN SMART DISTRIBUTION NETWORK WITH DISTRIBUTED ENERGY RESOURCES" which is being submitted to the National Institute of Technology Karnataka, Surathkal for the award of the Degree of Doctor of Philosophy in Department of Electrical and Electronics Engineering, is a *bonafide report of the research work carried out by me*. The material contained in this Research Synopsis has not been submitted to any University or Institution for the award of any degree.
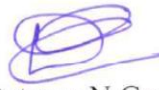
T. Swathi

Swathi Tangi, Reg. No. 165143EE16P03,

Department of Electrical and Electronics Engineering

Place: NITK, Surathkal

Date: 6/7/2023

CERTIFICATE

This is to *certify* that the Research Thesis entitled "VOLTAGE CONTROL IN SMART DISTRIBUTION NETWORK WITH DISTRIBUTED ENERGY RESOURCES" submitted by SWATHI TANGI, Registration Number: 165143EE16P03 as the record of the research work carried out by her, is accepted as the *Research Synopsis submission* in partial fulfilment of the requirements for the award of Doctor of Philosophy.

06/07/2023

Dr. Dattatraya N Gaonkar

Research Guide

6/07/2023

Chairman, DRPC

ACKNOWLEDGMENT

DEDICATION

To my devoted late father Shri Tangi Bhaskararao, who gave everything to make me the person I am today. God the almighty grants him eternal rest for his soul.

ABSTRACT

With the rise of distributed or embedded generation in distribution networks (DN) and local energy producers' involvement, distribution systems have become active and grown more complex. These events caused the distribution network to transition from a passive to an active configuration, increasing its difficulty and causing long-term changes in its characteristics. The state estimate procedure for the active distribution network (ADN) is typically more complex than the transmission network due to factors like the distribution network's high R/X value, high distributed generation (DG) penetration, improper node-to-node communication, and others. In this scenario, significant responsibility for the distribution network operators is implementing advanced management systems with precise monitoring, control, and protection systems to ensure reliable operation. In this regard, distribution state estimation (DSE) plays a predictable role in measuring and monitoring distribution networks. This study intends to investigate the areas of measurement system configuration and state estimation in the ADN utilizing the phasor measurement unit technology (PMU).

The front side of a state estimator is a supervisory control and data acquisition (SCADA) system that gathers system information. The SCADA system periodically queries the data collection devices. Nevertheless, the data extracted does not adequately reflect the system's behaviour when it alters during the assessment. In contrast to state estimation using a conventional SCADA system, synchro-phasors allow the status of the power system to be observed. High-speed, consistent data is delivered by the promising synchro-phasor technology. With the introduction of global position system (GPS) receivers, this platform has grown increasingly appealing and cost-effective. Synchro-phasors offer voltage and current measurements with a similar frame of reference; one such standard time source is the GPS. The PMU data is either gathered by the phasor data concentrator or directly sent from the PMU over the communication network. To perform wide-area monitoring protection and control, stability analysis, and grid state estimation, the central station may use the synchronized phasor data gathered by the PMU. As a result, more academics are starting to research the use of PMU technology to keep up with the demands of an active distribution network. This research has been conducted with this motivation.

Given the importance of PMUs in current grid networks, first, this work attempts to simplify the selection of the optimum locations for PMUs in various configurations. Hence,

for full observability of the distribution test feeders, an integer linear programming technique is utilized in the simulation with a minimum number of PMUs with and without zero injection buses (ZIBs). A methodology is suggested to analyze the voltage estimation using the current PMU count while taking zero injections into consideration after the best PMU locations have been determined. As expected, the results reveal that employing zero injection buses (ZIBs) reduced the number of PMUs in the network and had no appreciable impact on the system's voltage profile.

Second, although the quantity of PMUs required is reduced by zero injections, the zero-injection bus approach for PMU placement in ADNs has some limitations. Due to the heavy load on distribution networks, loads can change drastically, and DG is gradually being incorporated into it. To accurately estimate the distribution network states and monitor the network's system response, no node or bus can be disregarded. Henceforth, a technique is presented for computing the voltage magnitude of the radial distribution network using PMU technology while disregarding ZIs. To validate the suggested approach, a forward and backward sweep (FBS) load-flow algorithm is employed. In addition to the proposed voltage estimation technique, an algorithm is developed to validate the results of integer linear programming (ILP) performance in radial test feeders for complete system observability with a minimal number of PMUs.

Third, the dynamics of the distribution networks, as well as the entire power system, may be impacted by DG expansion. Unbalanced voltage is among the many problems with power quality that are the most serious. When network voltages are unbalanced, voltage management becomes challenging because the unbalanced voltage's negative sequence component results in oscillations with a double fundamental frequency in both reactive and active power injections. To address the issue, this work proposed the multi-agent system (MAS) based control technique to find the best voltage regulator for the operation of unbalanced radial distribution networks.

To evaluate the viability of the developed techniques, the standard IEEE Distribution network systems are considered. MATLAB programming is employed to simulate case studies.

Keywords: embedded generation, active distribution network, load-flow algorithm**,** integer linear programming, phasor measurement unit, multi-agent system, observability, zero injection bus, negative sequence component, unbalanced voltage, global position system, voltage estimation

TABLE OF CONTENTS

LIST OF FIGURES

LIST OF TABLES

NOMENCLATURE

g_i	Observability of the i_{th} bus
P_x, Q_x	Real and reactive powers at each bus
Z_x	Line data
V_x	Initial voltage of each bus
Y_p	Interrelation setting of the PMUs at the p_{th} placement bus
h_p	node observability at the p_{th} placement bus
V_{new}	New bus voltages using the branch currents
i_{new}	New branch currents again using the new bus voltages
Y_p	interrelation setting of the PMUs at the p_{th} placement bus
V_{new}	new bus voltages using the branch currents
i_{new}	branch currents using new bus voltages
$[Z_{rybn}]$	Primitive Impedance Matrix
I_{Li}	load current injection for bus I
$V_r\,(I_r)^*$	Power fed into the phase - r of line at the sending end bus
$V_{r\prime}\,(I_r)^*$	Power fed into the phase - r of line at the receiving end bus
P_{Gi}^{DG}	Supplied DG active power to the network at node i
Q_{Gi}^{DG}	Supplied DG reactive power to the network at node i
$SL_{ri},\ SL_{yi}\ \&\ SL_{bi}$	total apparent power of phases $r,\ y\ \&\ b$ at i^{th} node
S_{ri}^{DG}	DG power at i^{th} node of a 3- phase feeder

V_{unf}	percentage unbalance of voltage
I_{unf}	percentage unbalance of current
V_1, V_2	Positive and negative sequence components of voltage
I_1, I_2	Positive and negative sequence components of current
Z_{ryb}	phase impedance matrix
P_m, Q_m	real and reactive power of a node in a 'k' bus network
$|V_n|, |V_m|$	voltage magnitudes of the n_{th}, m_{th} nodes
δ_m, δ_n	voltage phase angles at node m, n
$|Y_{mn}|, |\theta_{mn}|$	node admittance magnitude and angle at node m, n
$\partial|V_m|$	change in voltage at a node 'm' in response to the change in P and Q on every system node 'n'
$P_{loss[mn]}, Q_{loss\,[mn]}$	active and reactive power losses that have occurred throughout branch "mn"
Q_{nc}	shunt capacitors' total compensation
Q_{nL}	network's net reactive load
q_k	Total number of PMUs in a 'k' bus network
L	Column matrix
E	incidence matrix
n	number of buses
b	Branches
p	PMU bus locations
r	remaining buses
N_B	Total number of branches
β	set of branches connected between the source and node i
IL_{ri}, IL_{yi} & IL_{bi}	currents at i^{th} node of phase r, y and b

$PL_{ri,}^{with\_DG} \ PL_{yi}^{with\_DG}$ & $PL_{bi}^{with\_DG}$	active power demand of a 3- phase feeder at i^{th} node of phase r, y and b at which a DG unit is placed
$QL_{ri,}^{with\_DG} \ QL_{yi}^{with\_DG}$ & $QL_{bi}^{with\_DG}$	reactive power demand of a 3- phase feeder at i^{th} node of phase r, y and b at which a DG unit is placed
$PL_{ri,}^{without\_DG} \ PL_{yi}^{without\_DG}$ & $PL_{bi}^{without\_DG}$	active power demand of a 3- phase feeder at i^{th} node of phase r, y and b without DG units
$QL_{ri,}^{without\_DG} \ QL_{yi}^{without\_DG}$ & $QL_{bi}^{without\_DG}$	reactive power demand of a 3- phase feeder at i^{th} node of phase r, y and b without DG units
$PG_{ri,}^{DG} \ PG_{yi}^{DG}$ & PG_{bi}^{DG}	DG active power injection at i^{th} node of phase r, y and b
$QG_{ri,}^{DG} \ QG_{yi}^{DG}$ & QG_{bi}^{DG}	DG reactive power injection at i^{th} node of phase r, y and b
$S_{ri,}^{DG} \ S_{yi}^{DG}$ & S_{bi}^{DG}	DG apparent power of phases r, y & b at ith node
$S_{ri,} \ S_{yi}$ & S_{bi}	total apparent power with DG integration at i^{th} node of a 3- phase feeder
$I_{Lr,} \ I_{Ly}$ & I_{Lb}	load current with DG integration at i^{th} node of a 3- phase feeder
P_{mn} & Q_{mn}	active and reactive power through branch "mn"
R_{mn} & X_{mn}	Line resistance & reactance of branch "mn"
P_{nL} & Q_{nL}	Load active and reactive power at node 'n'

ABBREVIATIONS

AC   : Alternating Current

ADN   : Active distribution network

CT   : Current Transformer

CVR   : Conservation Voltage Reduction

DC   : Direct Current

DER   : Distributed Energy Resource

DG   : Distributed Generation

ESS   : Energy Storage System

EV   : Electric Vehicle

FBS   : Forward and Backward Sweep

GPS   : Global Positioning System

IC   : Internal combustion

ICT   : Information and Communications Technology

ILP   : Integer Linear Programming

IoT   : Internet Of Things

KCL   : Kirchhoff's Current Law

KVL   : Kirchhoff's Voltage Law

LTC   : Load Tap Changer

LV   : Low Voltage

M2M   : Machine-to-Machine

MAS   : Multi-Agent System

OLTC   : On-load Tap Changer

PEMFC   : Proton-Exchange Membrane Fuel Cells

PEV   : Plug-in Electric Vehicle

PMU   : Phasor Measurement Unit

PT   : Potential Transformer

PV   : Photovoltaic

PWM   : Pulse Width Modulator

RES   : Renewable Energy Sources

SCADA   : Supervisory Control and Data Acquisition

SG   : Smart Grid

SVC   : Static Var Compensator

SVR   : Step-Voltage Regulator

UPS   : Uninterruptible power supply

V2G   : Vehicle to Grid

VAR   : Voltampere-Reactive power

VVO   : Voltage/Var Optimization

ZIB   : Zero-Injection Bus

Chapter 1

INTRODUCTION

1.1 Overview

Regarding the global challenge of climate change and security of energy supply, smart grid and renewable energy sources are crucial. The transition from the existing traditional or centralized supply to decentralized generation and the intelligent electric grid has great potential and may be able to solve several problems concerning energy safety, reliability, and the drawbacks of outdated power system installations. The current electric grid technology should be transformed into a smart grid which is adaptable for interconnection with distributed energy resources (DERs) to meet the expanding need for electric energy, increase efficiency and effectiveness, and reduce emissions.

The progress of sizable central power plants and overhead transmission networks can be replaced more quickly and affordably with DERs. Customers can benefit from lower prices, more dependable services, better power quality, higher energy efficiencies, and alternative energy sources. Utilizing green power such as solar photovoltaic, wind, biomass, hydroelectric power, and geothermal as well as distributed energy generation methods made from renewable resources, can positively impact the environment. Electric generating units utilize DERs in the electric distribution network at or close to the final consumer. They perform duties that are comparable to autonomous or electrical supply units. Generators, backups, and on-site power systems are all part of the well-known DER technology.

One of the critical research issues in electrical engineering is the ongoing expansion of the distribution network due to rising load demand and the significant evolution of DG. Distribution networks become active systems after DG penetration, which possibly will have an impact on the dynamics of the overall power system, notably the distribution networks. Forecasting, planning, and operation of the electricity system are now more unpredictable than before the advent of DG. Power quality will be a significant concern in networks with more power electronics interacting with DGs and nonlinear loads. An unbalanced voltage is

one of the most critical problems with power quality. An excessive voltage rise is another concern brought on by distributed generation's extensive use of the distribution system (DS).

1.2 Smart grid

Ecological safety and energy conservation are becoming global challenges due to the varied consequences of global warming and the increase in energy consumption. In technologically evolved towns and governments, the amount of power consumed rises to levels that, if unregulated, would no longer be under control. The smart grid addresses the transition to greener technologies like distributed generation and microgrids. With digital network skills, a smart grid is an electrical system that promotes the two-way transmission of power and information and can recognize, react, and act in response to multiple challenges. Smart grids give electricity users the tools to become valuable partners and can self-restore.

Making methodical application of energy constraints requires using strategic power management to distribute energy for various locations. Nevertheless, an intelligent grid can improve the status of our power system by rewarding energy needs through zone-specific requirements and offering the convenience of energy from diverse sources without requiring human interaction. For the above, supervisory control and data acquisition (SCADA) and other sensing devices are being used. Many factors spur the attempt to transition from traditional electric networks to smart grids, and an intelligent grid offers several benefits. These include the devolution of the role of the "prosumer," changing rules, the emergence of microgeneration and microgrids, advancements in monitoring, variations in the amount of power generated, and others. An intelligent grid expansion creates wireless sensor systems, which are currently cutting-edge technological development. These sensors evaluate the local assessment, gathering information to create a comprehensive picture of the ecosystem. The intensity of the sensors forces the nodes to cooperate in tasks including choice, data gathering, and location supervision.

1.2.1 Smart grid drivers

Several market factors and new possibilities recommend upgrading the smart grid to increase reliability and efficacy.

- **Initiatives to increase the efficiency of consumption of energy and distribution**

Utility companies strive to minimize losses in the system by balancing supply and demand. Distribution systems in use today do not provide demand-driven supply modifications.

Electricity costs greatly depend on when users use it because it cannot be stored effectively. By closely observing and influencing consumption, smart meters enable utilities to establish demand response plans to control the supply and demand of power.

- **Organizations promoting or requiring the use of smart appliances**

Smart meters are now fundamental components of many governments' national energy strategies. Most of these are intended to increase efficiency and lower carbon dioxide emissions. Other countries are funding pilot projects, and some have mandated nationwide deployment.

- **Endeavors to combine distributed generation and sustainable sources**

Alternative energy sources to address power shortages include renewable energy sources like wind and solar. Households with microgeneration systems, such as solar panels on their roofs, may more easily feed electricity back to the grid thanks to smart meters.

- **A heightened state of competitiveness in the electricity industry**

Energy retailers now face more competition due to the liberalization of energy markets across the globe. Thanks to data from smart meters, the energy sector can compete more fiercely on prices and services. Retailers may also provide graded billing plans and smart meters to incentivize off-peak usage and increase utility sustainability. In-home surveillance and remote demand response also allow businesses to stand out.

- **Smart meters are used as an instrument for economic legislation**

To lessen the effects of the world economic downturn and generate jobs, the adoption of "green" innovations, such as smart meter designs, is supported by many economies.

- **Security of cashflow**

Utility providers can lower non-technical transmission and distribution losses by utilizing smart meters. Saving money can be a strong motivator in impoverished nations where electricity is routinely stolen.

- **Client endears**

Many developed countries have long preferred online resource management, which is defined as a service that allows customers to remotely control electrical equipment and receive information about current electrical consumption.

1.2.2 Smart grid characteristics

The smart grid provides a comprehensive justification for the problems with the electrical supply; some of its aspects have been discovered to include the following features.

- **Enables customers to participate informedly**

By changing the way, they use and acquire power, consumers contribute to maintaining a balance between supply and demand and ensuring stability. These changes are brought about by buyers now having options that encourage various purchasing philosophies and behaviors. These preferences include cutting-edge technologies, the most recent information on their electricity usage, and modern techniques for rating and enticing electricity use.

- **Embraces all available energy - storage alternatives**

A smart grid can support large, integrated power plants and the expanding variety of distributed energy resources located near consumers. The use of these resources, which include renewable energy, sizable cogeneration, and energy storage, will quickly spread throughout the entire value-added chain, from sellers to vendors to buyers.

- **Empowers offerings, commodities, and businesses**

Markets that are appropriately designed and operated successfully create the opportunity for purchasers to choose from among participating facilities. Energy, size, location, duration, rate of changeover, and excellence are some specific grid factors that need to be explicitly managed. Markets have a significant role to play in the control of these variables. Customers, vendors/operators, and regulators need the flexibility to modify business regulations to meet the working and market conditions.

- **Offers power quality to meet a variety of demands**

Only some businesses, especially not every household consumer, need the same power. An intelligent grid offers variable energy results. The servicing and maintenance agreement may include the cost of outstanding power quality attributes. Improved management methods look at critical areas, enabling quick analysis and responses to events that affect power quality, like lightning, switching transients, line failures, and harmonic resources.

- **Maximizes adequacy and effectiveness and equipment utilization**

A smart grid integrates the newest technologies to serve its objectives better. For instance, active evaluations, which regularly detect and analyze resources' capacities, enable them to be used at higher loads and can lead to improved capability. Situation-built protection, which calls for apparatus maintenance at precisely the right time, can increase maintenance effectiveness. Machines that control systems can be updated to reduce errors and remove the impediment. Operational competency increases when choosing the least expensive energy distribution method made possible by these kinds of system-power appliances.

- **Ensures resiliency to intrusions, interruptions, and catastrophic events**

The ability of a system to respond to unexpected actions by segregating problematic essentials while the rest of the system is restored to regular operation is known as resilience. These self-corrective actions result in minimal facility disturbance for customers and service providers to complete the distribution setup.

1.2.3 Smart grid research initiatives

The demand for electrical energy has grown significantly due to technological advancement, raising concerns about its production and distribution. By increasing the need for more regularity, yield, safety, and ecological and energy sustainability objectives, this increased demand is complicating power systems. These intelligence-related characteristics of a power grid ultimately give rise to the term "smart grid" as we know it today and the intangible practice used to expand the power distribution infrastructure to be more affordable, reliable, and viable.

- **Management and information exchange**

Currently, issues with consistency and safety in wired and wireless communication environments plague smart grid (SG). The biggest challenge is a communication network setup essential for supporting the grid monitoring structure. Wireless is the most cost-effective alternative to wired communications in any architecture network. Since two-way communication is one of the most significant differences between traditional grids and SGs, communication plays a crucial role in SGs. Recently, an outstanding effort has been made to promote wireless-based internet of things (IoT), or more specifically, machine-to-machine (M2M) communication, for widely ranging sensory devices. Grid supervision is one of the critical elements of an extensive framework's flexibility. Outage supervision, which may

prevent a grid system cascading catastrophe, is a vital aspect of grid observation. These days, the dynamic concerning situational consciousness through an extensive area measurement system is altering due to the growing usage of Phasor Measurement Units (PMUs).

- **Monitoring and assessment**

Sensing devices are essential components of SG. These tiny crossings serve as detecting points and make it easier to see machinery and energy resources from a distance. Synchro phasors, also known as PMUs, are fast devices that offer synchronized measurements of voltage and current phasors in real-time. These phasor measurements are used for observation, safety, and control purposes in complex power systems. PMUs can track record grid circumstances with incredible precision and are significantly faster than SCADA systems. Digital indicators used in smart grids can detect usage in real-time, provide dynamic estimating, help with demand response, and remotely fix or disconnect the electricity. The newest development in power metering technology is smart meters. Additionally, alternative electric meter alternatives can help reduce peak pressure and improve energy efficiency.

- **Security**

The Smart Grid technology, which combines network and communication technologies, enables several advancements while increasing energy. Nevertheless, numerous hazards connected to computer networks can affect intelligent grids. The intricate networks of SGs, composed of numerous connected appliances and units, are the source of smart grid security. Smart meters, innovative electricity supply, and demand equipment, components in hazard-prone locations, outdated equipment that might not work with modern equipment, device-to-device communication, ad unarranged communication, Etc., are the most common liabilities in SGs.

- **Electric vehicles (EV)**

With new communication features, the innovative grid model has wholly transformed the electricity system. One of the smart grid's processes, the Vehicle to Grid (V2G) model, uses EVs to improve the operation of the electricity system. The V2G technique enables power exchange between EVs and the power grid, providing the power grid with several crucial functions. In the meantime, EV vendors can profit handsomely from participating in V2G support. The bidirectional power exchange between electric vehicles and the power grid is made possible by vehicle-to-grid knowledge, which offers the power system several services, including reactive power benefit, peak load reduction, spinning reserves, and power grid management.

- **Information assurance and emulators**

The use of information and communications technology (ICT) in the grids to monitor and manage electricity generation and demand is the main element of the smart grid. ICTs will allow the current power system to support two-way energy and data flow, isolate and address power outages more quickly, enable the incorporation of renewable energy sources into the grid, and give customers tools to improve their energy efficiency. This results in the communication mechanism being progressively more critical and the functioning of the entire power system becoming more dependent on the effectiveness of the communication networks. Regarding the status of the communication network, its impact on the evolving features of the power system demands to be considered cautiously. Due to the complexity and costs, it appears impractical to evaluate various communication structures and skills on real-time systems; nonetheless, a model can be used as a backup plan before actual execution.

1.2.4 Smart grid technologies

A smart grid lets users take real-time control over electricity generation, transmission, and distribution by utilizing a wide range of methods and network infrastructure. The following are the leading smart grid technologies that make it possible to operate energy more effectively, maximize the use of available resources, and enhance smart grid functions.

1.2.4.1 Distributed energy resources

Utility companies have several options for adding more DERs to grid networks while utilizing technology to protect the network and supply quality. Regardless of the safety risks and grid problems they cause, one of the fundamental reasons utilities use DERs is the requirement to streamline their grid networks considering evolving and possible industrial models. Customers are gradually becoming more knowledgeable about sustainability and the benefits of renewable energy for the environment, human health, and the economy. As a result, they want their services to provide them with a more affordable and cleanly produced product. Additionally, it is anticipated that DERs will make it simpler for energy companies to follow the international policy of emission reductions and environmental protection. While DER systems like battery storage, demand response, and vehicle-to-grid will help utilities manage flexibility for the system's dependability, renewable energy will enable them to retreat fossil fuel-based plants. Nevertheless, DERs are likely to deliver services with numerous possibilities to substitute the baseload capacity formerly sourced from fossil fuels.

Customers with electric vehicles (EVs) and onsite battery storage systems can store power when renewable energy generation is high and unload the capacity on the primary grid when the load surpasses generation on the grid system.

- **Types of DER technologies**

Energy generation and storage components are typically located at or close to the point of use in DER technologies. The information about technologies currently on the market but are also undertaking a substantial amount of additional research and development can be found in the following subsections.

  ➢ **Photovoltaic systems**

Through the photovoltaic (PV) effect, PV systems transform sunlight into electricity. The cells change their electrical characteristics when sunlight is exposed, producing voltage and current. The connection of the cells in series or parallel ensures that they have the necessary voltage and current. The solar PV system absorbs solar energy and converts the photons into electrical energy. The direct current produced by the panel is then converted into alternating current using a solar inverter. Due to its ability to operate "behind the meter," where it can directly replace grid purchases, and its incredible scalability, PV technology is a fantastic option for distributed generation. In addition, PV systems export electricity back into the power grid. Nevertheless, laws governing this may vary depending on the jurisdiction and where the PVs are located on the grid. The size of the system and the level of demand at the host site will determine this.
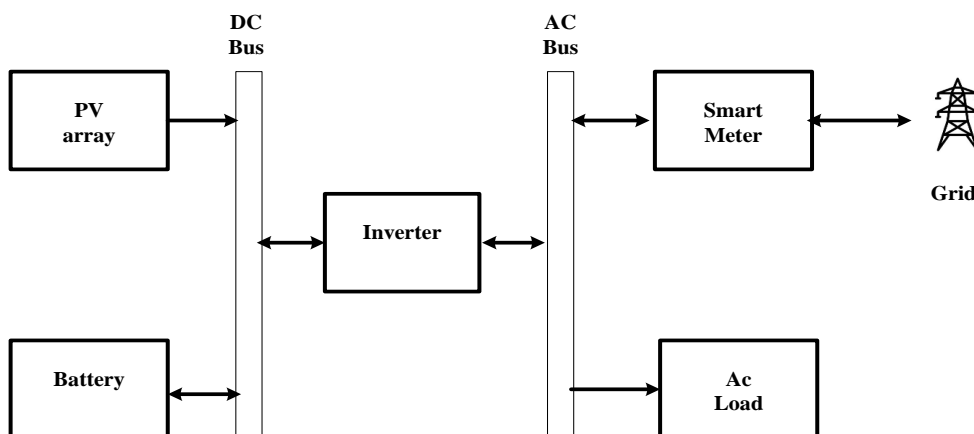
Figure 1.1: Grid tied solar PV system

➢ Wind systems

A method of generating electricity using the wind patterns found in the earth's atmosphere is known as wind energy. Modern wind turbines can produce power by using the wind's kinetic energy. It is environmentally friendly to generate electricity from wind energy because no carbon emissions are involved. Wind energy is the best source for generating electricity in remote areas where existing power lines cannot be extended due to the cost and environmental concerns. Comparing wind turbines to traditional power plants, the former is more portable. Modern technology has significantly improved the efficiency of capturing wind energy. There are only setup fees and minimal running costs because the wind is free. In this instance, significant funding has been provided for manufacturing, research, and development, as well as specific financial incentives, which have benefited wind energy production. The higher quality of wind energy captured has increased connected capacity, efficiency, and volume.
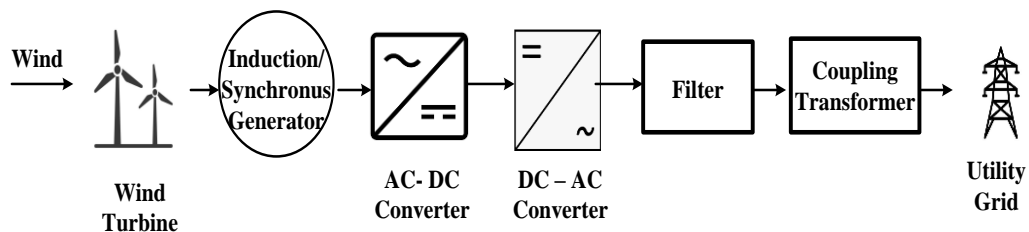
Figure 1.2: Grid connected wind system

➢ Microturbines

One of the valuable technologies for non-renewable energy sources is the microturbine. Microturbines use a range of fuels and small-scale gas turbines paired with their generators to generate electricity at very high speeds. The majority of microturbines generate alternative electricity by utilizing high-speed permanent magnet generators. For energy efficiency purposes, heat from fuel combustion in turbines is utilized. There is a high rotational speed present. They can produce a few kilowatts up to tens or hundreds of kilowatts of power. Axial-flow or centrifugal-radial-inflow units can be used as microturbines. The success of microturbines depends on several critical characteristics, including their small size, low price, higher efficiency, ease of use, quick start, and minimal environmental impact. It would be an excellent option for supplying baseload and combined-cycle generation to various consumers if these characteristics could be achieved.
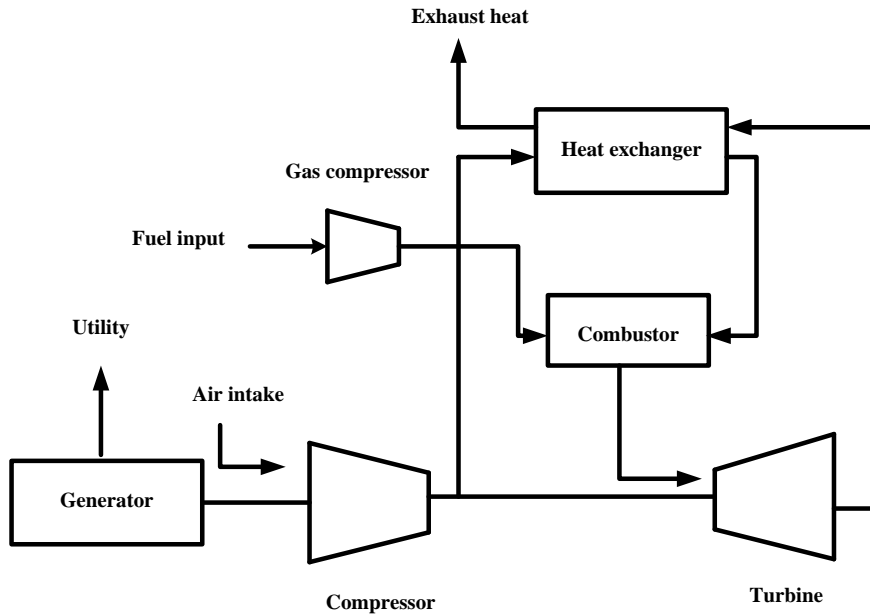
Figure 1.3: Microturbine system

➢ **Hybrid systems**

Hybrid Systems are incorporations of the technologies created for unique or specialized tasks. When it comes to energy sources that cannot be dispatched, or those whose accessibility we have no control over, renewable energy technologies, like wind and solar systems, for specimen, differ. To save energy for use when a service requires it, combine them in a hybrid arrangement, such as a PV with battery backup. Hybrid non-renewable DER schemes are also used; one example is a battery-powered network encircled by a microturbine that uses it as backup energy for prolonged outages while allowing the system to function through brief outages on the batteries.
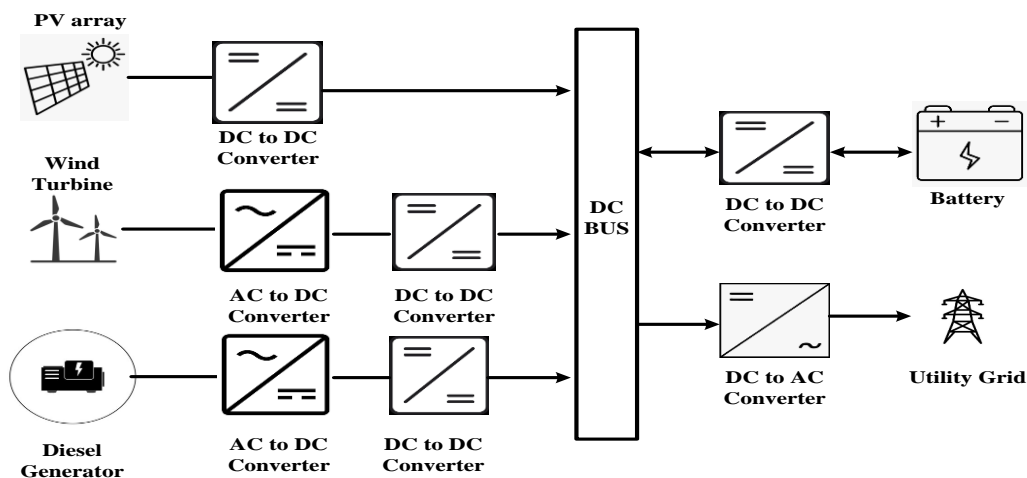
Figure 1.4: Block schematic diagram of hybrid system

➢ **Fuel cells**

The electrochemical technology used in fuel cells allows chemical energy conversion into electrical energy. When compared to conventional power generation networks, they provide a higher electrical efficacy. Base load, off-grid usage, and fuel tractability are additional advantages. Its other features, including its noise-free operation and modular manufacture, enable it to be used for small-scale applications, off-grid power generation in distant locations, and maritime and space applications. The commercialization of proton-exchange membrane fuel cells (PEMFC) technology has resulted in tremendous growth. Due to their achievement and robustness, which have reached acceptable levels, PEMFCs are among the most capable and low-emission technologies for switching to alternative energy sources. For the market to be accessible and to appropriately lower consumer costs, improvements are still required.
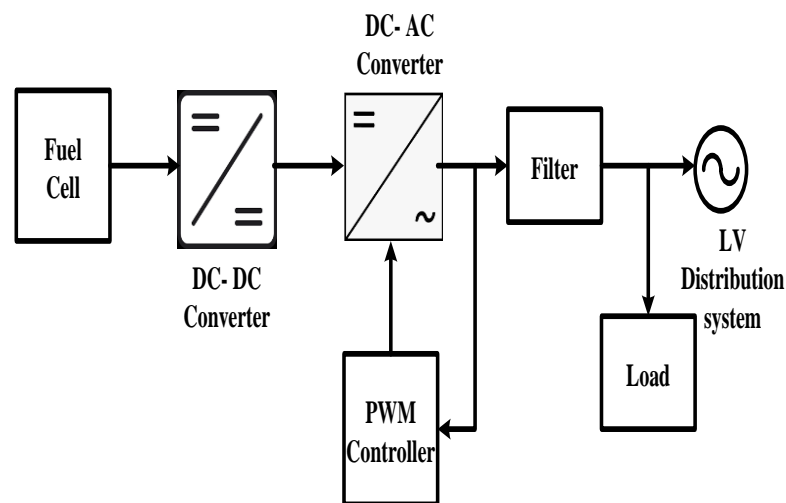
Figure 1.5: Schematic diagram of fuel cell connected to low voltage distribution network

➢ **Energy storage systems**

Storage systems' requirements must come from the electric grid or alternative supply, such as a renewable DER, and must be stored and made readily available. The storage technologies that are currently available have a wide range of features. The most popular type of electricity storage is batteries.; uses range from low-power ones like long-distance communications to high-power ones like supporting utility grids. Another standard storage option is an uninterruptible power supply (UPS), which typically consists of batteries converts energy stored to alternating current and send it as desired.
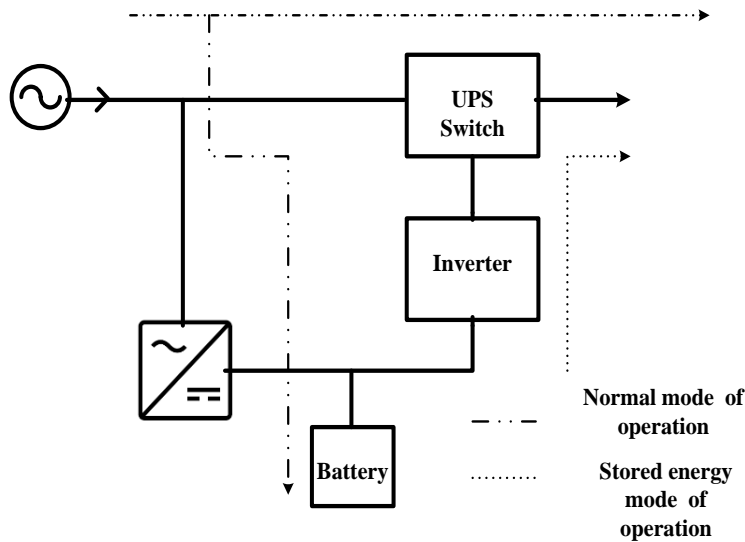
Figure 1.6: Block diagram of energy storage systems

> **Internal Combustion Engines**

The internal combustion (IC) engine is the most economical and reliable power source in heavy machinery and transportation. Gasified biomass is best used in IC engines, particularly for dispersed power generation, such as diesel engines. Transportation is where IC engines are most used. Alternatives are keeping an eye out to take its place as environmental worries increase. The automotive industry is the leading producer of IC engines within this alliance, and it is in this sector that a notable impact can be made in the future.
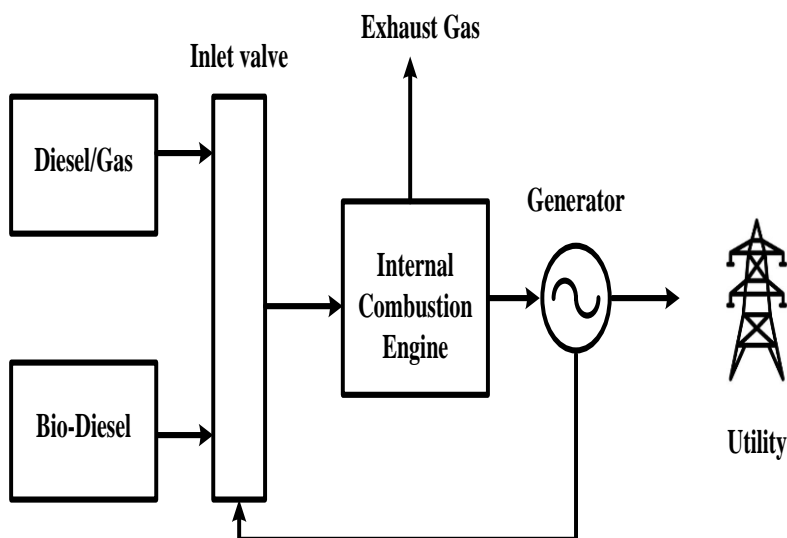
Figure 1.7: Block diagram of internal combustion engines

➢ **Stirling engines**

An external combustion engine called a stirling engine heats and cools the working gas inside the cylinders to convert thermal energy into kinetic energy. Since non-flammable combustion even causes cyclical force oscillation, the Stirling engine has a reasonable possibility of producing low noise and vibration levels. A working gas is continuously warmed and cooled by a closed-loop system that powers the Stirling engine. The gas expands when it is heated. This is used to move a piston, which in turn causes a crankshaft to turn. In this manner, heat energy is transformed into shaft power, mechanical energy. In addition to combustion fuels, surplus heat, and solar heat energy, they can be heated using various resources. Currently used in the commercial sector as cryogenic cooling systems, they are being developed into quiet, low-emission automobile engines.
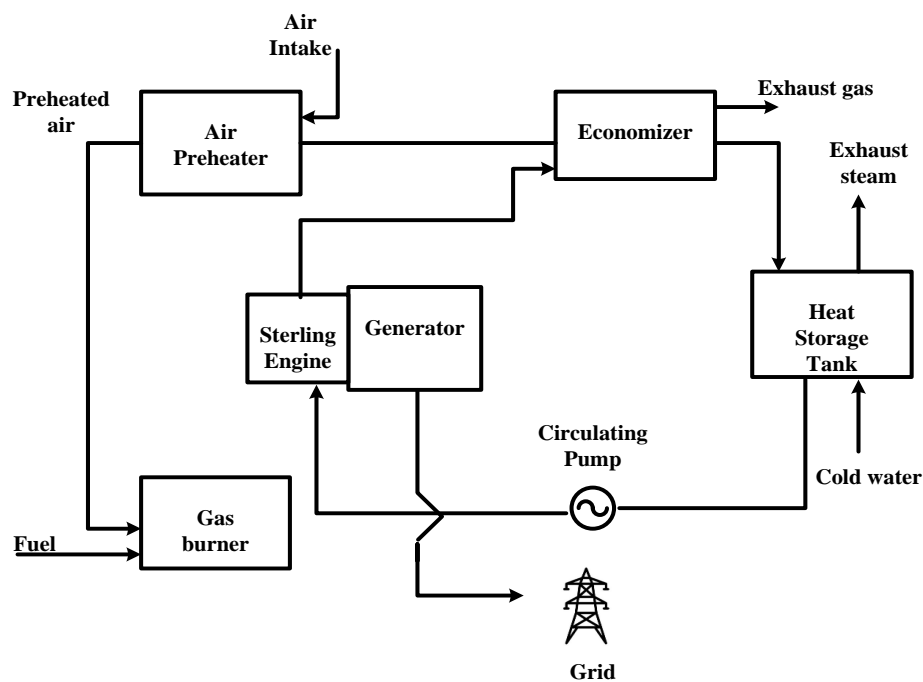
Figure 1.8: Block diagram of Stirling engines

➢ **Small hydro**

Small hydroelectric facilities are considered renewable since they use less water to run and have a less environmental impact than large hydroelectric projects. Like their larger counterparts, small hydropower plants operate. When water falls from a height, a turbine turns its kinetic energy into mechanical energy, which drives a generator to produce electricity. Grid coupling is an option for power plants that generate more than 100 kW, but

smaller power units can only supply a small area. The needs for household loads where a modest power quality produced at marginal cost is sufficient are generally met by the small micro- and pico-power plants. Small hydroelectric power generating systems have grown in significance in developing countries for supplying energy to remote and rural areas. Small hydropower generation from countries with sizeable hydro capacity can be recognized and encouraged to help meet the world's expanding energy demand.

> **Biomass**

Plants, both terrestrial and aquatic, as well as their by-products, produce biomass, which is an organic material. This process releases energy when biomass is burned because sugars are transformed into carbon dioxide. As a result, energy can be extracted and released from biomass more quickly, making it a renewable energy source. Currently, biomass makes up about 14% of the global electricity supply, with 38% of that energy used in emerging economies, especially in the rural and traditional market segments. An organic material called biomass feedstock generates heat, gas, and electricity. Climates that are humid and blessed with brilliant sunshine and rain provide the ideal conditions for biomass production—additionally, the great agricultural potential results in enormous agro-remains that can be used to meet energy needs.

> **Geothermal**

Geothermal technology draws heat from the earth's subsurface, which can be used directly for heating and cooling systems or converted into electrical energy. However, resources that can withstand high or low temperatures are necessary to produce power. These are frequently found close to tectonically active zones where hot water and steam can be obtained at shallow depths or delivered to the earth's surface. Its key advantages are geothermal energy's low cost and ability to operate year-round at high capacity. This enables it to provide dispatchable electricity for business purposes and, if rewarded, auxiliary services to the electricity system. These characteristics become increasingly crucial as solar and wind energy become more widely used. Closed-loop geothermal power facilities of the present day emit no greenhouse gases. Throughout their energy output, geothermal power plants use less water than most conventional electricity-generation methods. New technologies, such as enhanced geothermal systems, which are still in the experimental stage, are being developed to support more extensive geothermal energy expansion.

➢ **Solar thermal**

One way to use solar energy for heating and cooling is through solar thermal energy. It takes in the heat energy from the sun's beams directly. In domestic settings, solar thermal energy is widely used as a specific space and water heating method. The technology for solar thermal systems has been developed to a robust and profitable standard, making them suitable for use in cooler climates and specific uses. On the other hand, solar district heating plants are a significant application of solar thermal energy. The solar thermal plant, made up of a sizable field of solar collectors, distributes the heat produced by the sun to urban houses, smaller neighbourhoods, or big cities. The cost, sturdiness, and effectiveness of these technologies are, nonetheless, the main issues that must be resolved.

• **DG interfacing technologies**

Conventional grids are designed to support fewer centralized producing units that can supply a sizable number of scattered loads. Power flow used to be essentially unidirectional, but that is no longer the case. Small generating units are now connected to distribution networks to meet the growing electricity demand, although these networks were not designed to accommodate power generators. The need to enhance the use of renewable energy, which is more suitable for a dispersed application, has spurred this transition from traditional grids to grids that no longer have unidirectional power flow, as seen in figures 1.9 and 1.10.
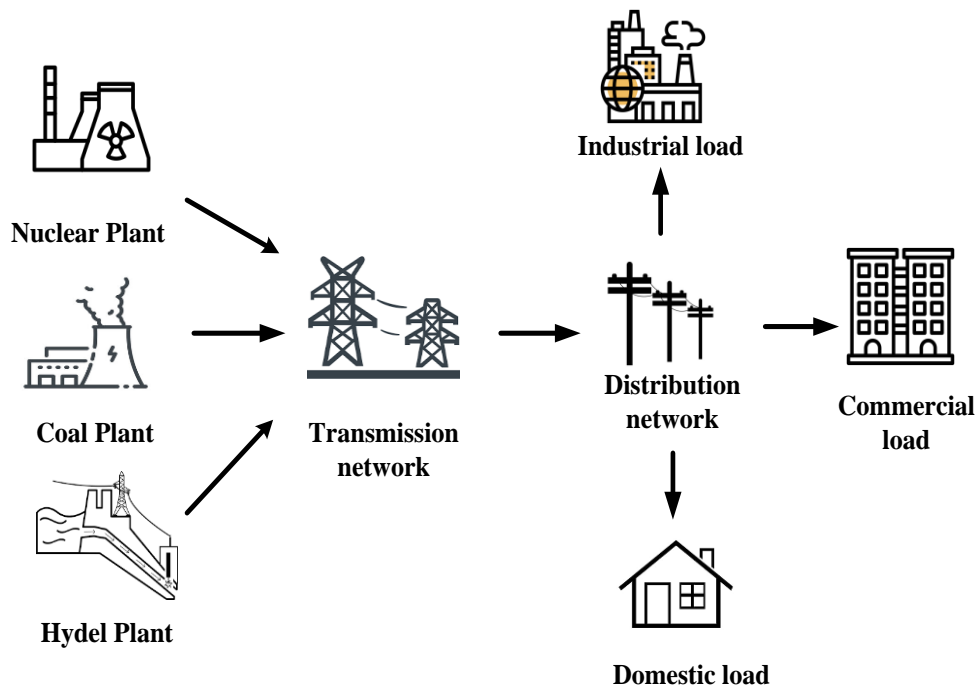
Figure 1.9: Schematic diagram of conventional power grid
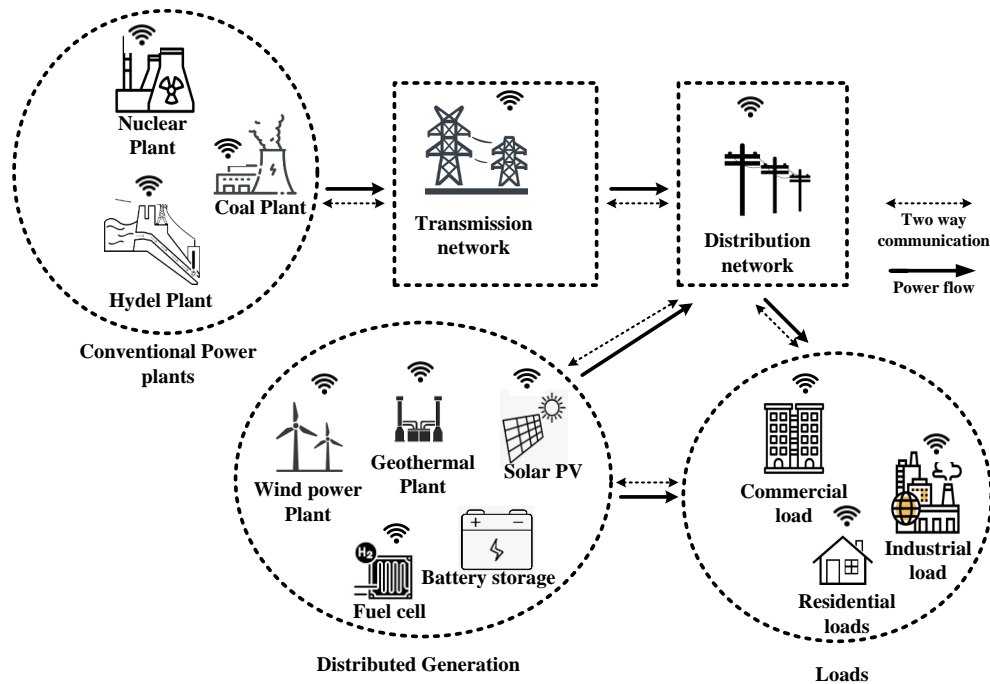
Figure 1.10: Schematic diagram of smart grid

Most studies indicate that up to 15% penetration of distributed generation may be achieved without significantly altering the grid, with connectivity control being the only concern. The DERs should be interconnected either in islanding mode, parallel with the grid, or a combination of the two. While the grid operates in parallel, as is typical, if a grid malfunction results in an island's establishment, the DER is permitted to operate independently. To preserve reliability and deliver high-quality power, it is necessary to study the characteristics of the alternative resource before integrating it into the grid. Much research is being done to use the energy from DERs and to increase the productivity of these sources because it has significant advantages, such as being affordable and environmentally benign. The chief objectives of interconnection are to guarantee the reliability, safety, and service quality of the power systems, to deliver uniform technical supplies, procedures, and transparent arrangements, and to assure interconnections are timely, foreseeable, and cost-effective as possible.

➤ **Synchronous generators**

Synchronous generators are frequently used for variable-speed applications of wind turbines; due to their moderate rotating synchronous speeds, the electricity is generated at grid frequency. For wind turbines that run at variable speeds, synchronous generators might be a helpful alternative. They are not required to have a pitch control system. The pitch control system increases the turbine's price, which also impacts the pressure on the turbine and

generator. When synchronous generators operate at varying speeds, power will be produced at varying voltages and frequencies. The output voltage of the synchronous generator can be managed by using an automatic voltage regulator to excite the field voltage. However, regulated capacitors are necessary for induction generators to regulate voltage. For the generating mode of operation, their operating speed must be greater than the synchronous speed.

➢ **Induction generators**

A rotating field that rotates at synchronous speed is induced in the stator of the induction machine when the stator winding is given to the AC supply. However, the induction motor typically operates at a lower speed than synchronous. Therefore, it needs an outside push to accelerate past synchronous speed. The rotor experiences a current; as a result, the induction machine functions as both a self-starting motor and a generator. However, the isolated induction generator does not need ac supply for reactive power. A capacitor bank placed across the terminal offers reactive power for both the generator and the load. The device stops generating when its terminals experience a short circuit. It requires minimal maintenance because of its robust build. These generators are utilized in mini-hydropower plants and wind turbines. When a power factor load is lagging, the voltage drops quickly. Reactive power is what it needs from the main supply.

➢ **Power electronic converters**

Power electronic converters are in the business of taking electrical energy from the power grid and converting it into the form that a motor needs. The electronic converter may be defined according to the specific power supply and driving motor. Power electronic converters have a long history and are used in various applications. The drive of electrical machines, primarily used at the beginning for industrial applications but now widely used in many home applications, is one of the best uses. The market for power electronic converters was only slightly impacted by the beginning of the renewable energy story. To improve aerodynamic power conversion, connecting wind turbines with power electronic converters is essential. At the same time, photovoltaic energy also started to develop, requiring a power electronic interface for the obvious and necessary direct current/alternating current conversion. Along with renewable energy, the influence of power converters on the grid is improved by the advancement of several high-voltage direct current link projects. Power electronic converters significantly impact the grid, and numerous studies have shown that

the new grids that incorporate many of these new devices operate well. Additionally, the current connection type will not be sufficient in the future.

1.2.4.2 Wide area monitoring systems (WAMS)

WAMS is a recent acronym first used in late 1980s power system research. They have been widely viable in power tracking, operating, and controlling functions. WAMS fuses the capabilities of communication systems with the features of advanced metering infrastructure to monitor, operate, and regulate power systems over a broad geographic region. This overall ability helps to obtain data from the complete system at the same time and location. Numerous WAMS functions may utilize this data, which is gathered from the overall network, adequately. These data show that WAMS is already a significant change in the modern era for overcoming problems with power systems connected to reform, liberalization, and decentralization. Phasor measuring units (PMUs), which have supplied synchrophasor measurements since 1994, have indeed been employed in WAMS. Synchrophasor measures would add advanced WAMS functions that traditional measurements have not accomplished, or they may introduce certain existing features. In many smart grid solutions, phasor measurements are state-of-the-art.

1.2.4.3 Phasor measurement unit technology

A PMU is employed to estimate voltage or current magnitude and phase angle in the power system network utilizing a standard time base for synchronization. The resultant measurement is recognized as a synchrophasor. Synchronized measurement sets acquired from synchronized phasors be responsible for an enormously upgraded technique for tracing power system dynamic behavior for enhanced electrical system protection, monitoring, stability, operation, and control [Tangi and Gaonkar 2021].

An anti-aliasing filter amplifier processes the measured data of the power system parameters fed from potential and current transformer in analog formats (low pass filter). The simultaneous sampling of the separate signals provided by instrument transformers is accomplished using sample and hold circuits and analog multiplexing. The sampled signals are delivered to the personal computer data acquisition board, transforming them into digital form before processing as shown in figure 1.11.
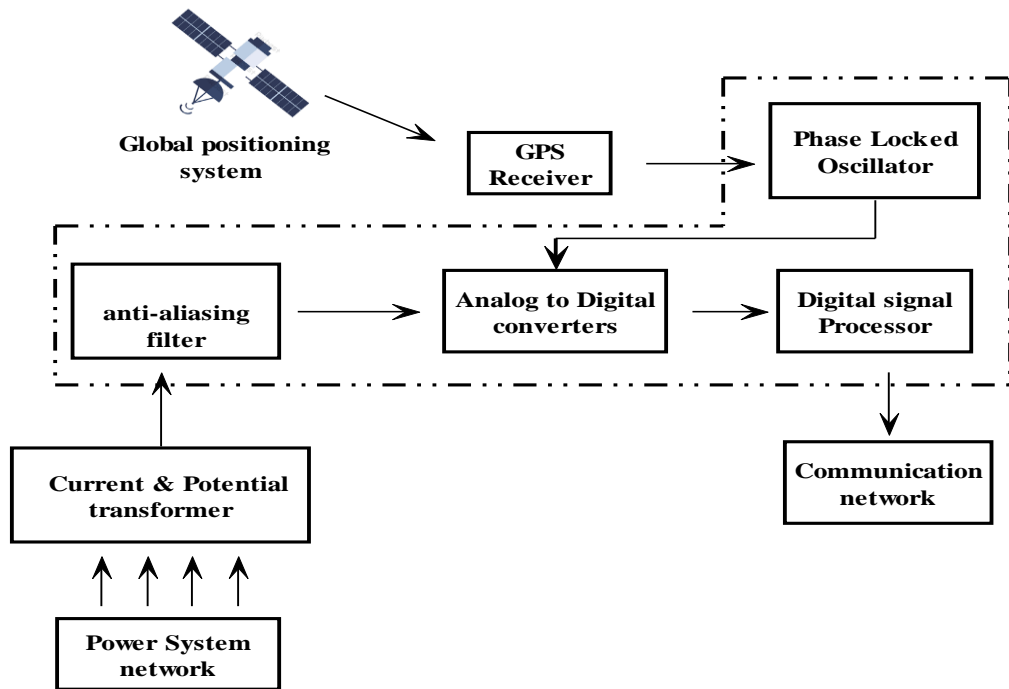
Figure 1.11: Block schematic of the PMU

- **PMU application in power system**

Several research institutions worldwide are actively engaged in efforts to develop applications for the synchronized phasor measuring technology due to its recent development. Many of these applications can be classified simply using the following criteria:

  ❖ Power system real time supervising
  ❖ Advanced network safety
  ❖ Cutting-edge control structures
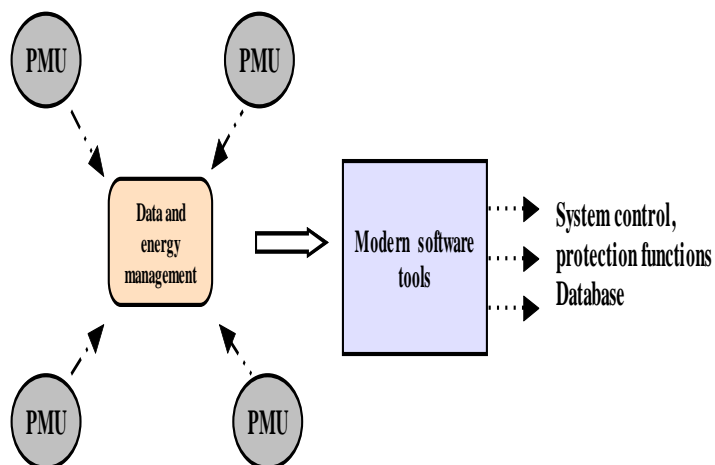
Figure1.12: PMU applications in power system

- **PMU outlook**

    PMUs enable innovative utility issues and offer power system operators a variety of potential benefits, notably:

    ❖ The condition of the power system can frequently be estimated with high accuracy, allowing for corrective actions, and monitoring dynamic events from a single position.

    ❖ To guarantee the customer's power supply is of adequate quality.

    ❖ The accurate snaps of the system states provided through global positioning system (GPS) synchronization greatly improve post-disturbance assessments.

    ❖ It is possible to build advanced protection based on synchronized phasor readings, with choices to enhance the system's overall responsiveness to catastrophic occurrences.

    ❖ It becomes possible to do advanced control utilizing remote feedback, which enhances controller efficiency.

1.2.5 DG integration challenges in smart grid

A power source connected to the utility grid and located close to or at the consumer's location is a distributed generation. These sources are relatively tiny when compared to centralized power plants. The incorporation of DG into a distribution system is required due to end consumers' ongoing need for a reliable energy source. Nonetheless, adding DG poses several challenges in terms of issues with stability, power quality and protection. These problems must be solved for the DGs to be successfully integrated into the current system.

- **Voltage control**

The significant emergence of DG into the distribution network due to an increase in energy consumption represents a comprehensive strategy to increase the performance of distribution networks. However, it has been evidenced that the rising degrees of DG penetration into a power system includes both favourable and adverse effects. The characteristics of the power system have altered due to the incorporation of DGs; specifically, power flows have altered from a single direction to reversible. When a generator is attached to a radial feeder, its power flow exportation lowers the power coming from the central substation, lowering the voltage drop all along the feeder. Whenever the output of the generated power surpasses the feeder demand, electricity flows to the primary substation from the generator, causing a voltage increase along the feeder.

- **Fault clearing**

The distribution systems that use a radial configuration, where there is a single resource, and the feeders radiate out from the supply, demand only one protective device must be operational for a fault to be cleared. With DG, various resources are available, so ensuring fault clearance by simply using the utility circuit breaker is impossible. Due to the extensive architecture of existing distribution networks, DGs must become accustomed to how the utility operates. To enable the typical fault-clearing process, the protective devices connected to the DGs must detect and isolate the fault.

- **Reclosing**

Reclosing devices are often deployed in the power system because operational failures are typically transient. The coordination between initial reclosing and distribution protection will be compromised by incorporating DG into distribution networks. If there is a transitory failure in the line, the breaker trips immediately and then trip again to restart the energy supply. In the incident of a feeder transient fault, the DG unit may fail to trip and extinguish the fault arc before the circuit's reclosing shot. The reclosing effort would be ineffectual and put the automatic rebuilding of that circuit at risk if the DG kept supplying power to the feeder. On the other hand, out-of-phase reclosing may happen when the feeder circuit breaker is recombined if the fault completely clears, and the DG energizes the circuit. High voltages may be present when the power is cut off and flow through the circuit breaker connecting the DG to the utility supply. When automatic reclosing occurs, the temporary disruption will allow the DG to accelerate or decelerate out of phase with the utility supply. All these consequences demonstrate the importance of adopting an islanding protection strategy quickly and consistently to avoid out-of-phase reclosing or an ineffective reclosing attempt that would result in extended outages.

- **Interference with relaying**

Circuit breakers and reclosers are designed to inspect a region down the radial feeder known as the device's "reach," which is determined by the minor fault current the protection system will sense. The range of the relay may be restricted by DG infeed, which can lower the current it senses. High impedance faults will be discovered once they cause more damage to the utility's appliances and more danger of ongoing customer invasion, which are signs of

more severe issues. While DG improves network dependability, during fault conditions, it might harm dependability in some circumstances.

- **Islanding**

An islanding incident happens when the power grid serves a portion or region of the distribution network, and the DG gets cut off from the grid supply for whatever reason. It can be challenging to forecast in advance how to detect an islanding scenario. The conditions amid which an island is formed decide the likelihood of a trustworthy identification. In the most common scenario, the DG unit cannot provide the isolated portion of the network on its own, voltage and frequency drop, and the problem is quickly identified. Comparable to this, DG units might even supply too much power, causing overvoltage that is simple to detect. An island can generally be spotted if the generation does not fit the transient demand too closely. Voltage and frequency might stay within acceptable ranges if the island's demand is equal to its supply by the DG unit(s). The network might continue to be isolated. The ideal load generation balancing is entirely feasible in most situations in a distribution network with variable loads. The probability of balance is challenging because DG production also changes depending on the energy supply. Depending on the shift in loads and supply and the generator's dynamic response, the island could last only briefly or for a while. Nevertheless, even the brief islanding might quickly lead to a catastrophic reclosing.

- **Storage needs**

Due to their dependence on supply, forecasting the output of renewable DGs takes time and effort. In a liberalized environment, agreements must be made in advance, and power is sold in a competitive market governed by rules. Henceforth, a DG vendor must know how much electricity he can produce each hour of the following day in advance. Then, to compensate for this variable output, storage capacity is required.

- **Power quality problems**

The electrical connection between the network and its users is called the "power quality." It consists of two main parts: the voltage quality understands how the source voltage influences the device, and the current quality understands how the equipment current affects the system. The system's power quality is generally improved by standby unit and on-site power supply offered by DG. Nevertheless, few difficulties could ascend when distributed generators, with their diverse forms and technologies, are connected to the utility distribution network. These problems include voltage control, voltage flicker, voltage sag, prolonged interruptions, and harmonics.

❖ **Voltage flicker**

Operating an induction machine or a step change in the DG output, which results in a significant voltage difference on the feeder, may cause DG to create a voltage flicker. When using intermittent energy sources like wind and solar energy systems, the production varies according to how strong the wind and sun are. The standard flicker graph (IEEE Standards 519-1992) assesses the size and frequency of voltage changes occurring per unit period to ensure they are below the visibility tolerance range. Mitigation is crucial if they are above the tolerance range. Reduced voltages on induction generators during start-up operations and stricter synchronization for synchronous DG are examples of mitigation techniques. Inverters are managed to lessen high-magnitude currents and output level volatility.

❖ **Voltage sags**

A DG may or may not be able to counteract voltage sags, depending on its design and location. Synchronous generators can help keep the voltage steady and prevent voltage drops in neighbouring facilities. However, any effects on the feeder's surrounding loads might be avoided, owing to the associated transformer impedance. In the event of a sag, distributed generators equipped with inverter technology can be configured to produce reactive power for voltage correction.

❖ **Prolonged interruptions**

Most distributed generators were installed in the network to provide backup power during a power outage or to cover emergencies when a section of the distribution system went down. Over time, these generators will improve system dependability. However, not all DG systems can meet the load requirements if the utility system cannot. An example of a renewable DG that might not operate in stand-alone mode has an unregulated inverter and insufficient storage. When the DG is connected in parallel with the utility distribution system, several operational conflicts may impact the system's reliability.

❖ **Harmonics**

The network to which it is connected may experience harmonics introduced by DG. The type and severity depend on the power converter technology and connector configuration. Insulated-gate bipolar transistors, which use pulse-width modulation technology and can produce clean output that meets the IEEE standards for harmonics, are the basis for most

contemporary inverter designs. There are several harmonics produced by earlier line-commutated inverters that are thyristor-based. Depending on the configuration of the generator windings and grounding, synchronous DGs may generate harmonics. Since the two-thirds pitch generates far fewer third harmonics than other pitches, synchronous generators frequently specify their windings at this pitch. Nevertheless, a two-thirds pitch machine might permit higher harmonic current to flow from those other resources connected with it since it has a lower third harmonic resistance.

- **Stability**

The tendency of an electrical system, for a specific starting operating mode, to return to a position of ability to operate equilibrium after being exposed to external intrusion is known as power system stability. Most network parameters are bound, meaning that almost the whole system is unaffected. Power system experts initially experienced stability issues with generator rotor angle stability, which made it difficult for the system to maintain synchronism following a disruption. The DG's impact on stability includes its influence on voltage, frequency, and angle stability. The distribution system prioritizes voltage stability above other factors. Under normal working circumstances, if the generation can meet demand and offset losses, there is no problem. Aside from that, unanticipated events like a sudden increase in the load might lead to unpredictable conditions. Voltage drops at the buses are the most prevalent sudden events, leading to voltage instability throughout the system. When DGs are installed incorrectly, they can enhance the system losses and lead to voltage instability at some buses by creating varying voltage levels.

1.2.6 Voltage regulating devices

Voltage control is one of the critical operational challenges associated with significant levels of renewable-based DG penetration. Renewable energy sources (RES), like wind and solar energy, can negatively interact with conventional techniques of operating on-load tap changers and significantly affect the voltage profile of smart grids (OLTCs). Another factor is the increasing use of Plug-in electric vehicles (PEVs), which places more demand on voltage-regulating devices because of their variable and intense power profiles. These combined generation and load power profiles may result in under voltages, over voltages, significant network losses, severe tap functions, impractical outcomes for OLTCs, and restrictions on integrating PEVs and RES. Therefore, for efficiency, safety, and uniformity,

the voltage magnitudes of the busbars must be maintained within legal boundaries. A system's voltage stability can be increased while power losses can be reduced with the help of proper voltage and reactive power optimization. Many different types of voltage control equipment and power quality devices must be used at numerous sites in the smart grid to perform voltage control efficiently and promptly. In this section, a few voltage control devices are presented.

- **OLTC transformer**

The on-load tap changer (OLTC) oversees regulating the feeder voltage. OLTCs are often installed at the substation, from which a feeder is drawn. An operator will define a specific voltage operating point to control the voltage of a regulated bus. The windings of a transformer can be utilized to alter the transformer's turn ratio gradually. The OLTC manages the voltage of the controlled bus according to the established dead band criteria. The comparator compares the regulated bus voltage to a user-defined set point. The tap is not changed if the detected voltage is within the dead band. If the measured voltage exceeds the dead band, the taps are relocated after an operator-defined time. An autotransformer with a ± 10% voltage regulation ability is a voltage regulator (VR). By altering the tap location as the load current changes, the VR keeps the load output voltages at the target output. The OLTC notion is comparable to the dead band and delayed time concepts.

- **Load ratio transformer**

Tap-changing transformers are a crucial technique for controlling the voltage at all voltage levels throughout the system. It is common practice to use autotransformers with tap-changing capabilities to change the voltage from one subsystem to another. They can be autonomously or automatically managed. The taps on the network transformer provide a simple way to control reactive power transfer between system elements. These are mainly used for improving voltage profiles and minimizing real and reactive power losses. Its control influences voltage changes at a transformer's terminals. Moreover, it affects the transformer's reactive power flow. The network configuration and load/generation distribution will impact the voltages on other buses. If the overall voltage level is to be adjusted, coordinated control of all the transformers connecting the subsystems' tap changers is essential.

- **Shunt reactors**

Shunt reactors are utilized to mitigate the consequences of line capacitance, mainly to prevent voltage increases during open circuit operation under modest loads. These dissipate reactive power. These qualities make it easier to use them in distributed generating and distribution systems when there is a possibility of power flow being reversed. Additionally, these reactors minimize energization beyond voltage.

- **Shunt capacitors**

Shunt capacitors enhance over voltages and provide reactive power. They are applied in various dimensions and are employed throughout the system. For power factor adjustment, these were initially utilized. They are an extremely cost-effective way to provide reactive power. The main advantages of shunt capacitors are their versatility in terms of installation, use, and price. They are easily implemented at numerous systemic sites, which boosts transmission and distribution performance. The main disadvantage of shunt capacitors is the inverse relationship between reactive power output and voltage. As a result, reactive power production is reduced at low voltages when it is most likely to be required. Shunt capacitors frequently used may result in poor voltage control and a loss of small signals.

- **Static Var compensator**

A static VAR compensator is constructed using reactors and capacitors, and it is run by thyristor actuators adjacent to a set capacitor bank. A shunt transformer links it in parallel with the power line. Shunt-connected variable susceptance, which is automatically modified to achieve voltage control, can be thought of as the model for SVC. The susceptance varies subject to the restrictions when the reactive power demand at the bus changes. On the other hand, the reactive power depends on the square of the bus voltage. As a result, as the voltage drops, so does the reactive power generation. Additionally, to complete a coordinated process, advanced voltage control techniques, methodologies, and software tools must be used.

1.3 Literature review

This section examines the technical literature relating to the effects of DG integration on the voltage profile of the distribution system and voltage control methods for a smart distribution network.

1.3.1 Impact of DG integration on the voltage profile

Due to the distributed generation (DG) industry's rapid expansion, the DG penetration limit is now an ever-evolving difficulty. A transformer with an on-load tap changer (OLTC) or a feeder step-voltage regulator (SVR) may become activated in extreme situations by a short-term voltage variation brought on by the irregular DG sources' variable DG power. A feeder DG trip will also cause a sudden, massive voltage step change. DG's most enormous, permitted penetration in distribution networks is constrained by these factors [Wang et al., 2017]. A method to calculate the adverse effects on voltage profile that a variety of DG penetration sizes may have in very meshed LV secondary networks was proposed by [Chen et al., 2012]. To consider, the obscurities of incoming connections, DGs are mounted probabilistically. An impedance-based observing technique was presented by [Mortazavi et al., 2015] to identify different distribution network conditions in the presence of varying PV penetration levels. The apparent impedance observed at the connection location is determined using straightforward regional measurements of bus voltages and line current in this supervised practice. In [Azzouz et al., 2017], fuzzy-based voltage regulators are recommended to solve the problems caused by high-level DG penetration-induced voltage breaches. Simple tap operation provides proper voltage management with equal DG and energy storage system (ESS) active power savings.

1.3.2 Challenges of distribution system voltage control and the control mechanisms

Customers of distribution services must receive quality power. The primary purpose of the voltage equipment is to prevent under-voltage and overvoltage by voltage regulation at the fundamental frequency. The nodal voltage profile or maintaining an acceptable voltage range are other terms for this issue.

- **Traditional control topology**

Distribution network operators use various voltage control technology to improve the node voltage profiles in distribution systems in [Farag et al., 2012]. On-load tap changers are typically installed in the substation transformers. SVR may also be wired into the feeder's centre to boost the voltage produced by a transformer with load tap changing (LTC). The loads that consume a significant amount of reactive power can also impact voltage dips. In the substation, next to the feeders, or close to loads, reactive power compensation devices, such as permanent or flexible capacitor banks, and multiple power electronics-based compensators, such as static var compensators (SVC), STATCOM, Etc., are installed in

[Liao and Milanović 2017]. Direct voltage control devices are occasionally seen in low-voltage distribution networks. In the low-voltage distribution system, smart inverters and other intelligent grid techniques have advanced recently to provide grid-backing auxiliary functions. However, these newest voltage control devices impact how traditional voltage control devices operate, so they must work together to maintain a precise voltage profile and reduce system loss in [Luo et al., 2014].

- **Enhanced control topology**

To reduce local voltage changes and worries about voltage rise brought on by the addition of solar power at the end of interconnection, intelligent inverters can provide independent volt/var control or power factor management [Ranamuka et al., 2016]. However, the market enticement strategy has yet to be accepted for reactive power produced by non-utilities. Additionally, the provision of reactive power capacity frequently necessitates excess inverter power, necessitating overly large hardware or active power generating limitations [Procopiou et al., 2016].

- **Enhancement of voltage/Var**

Distribution networks are continuously incorporating new voltage control techniques. Services are offered at conservation voltage reduction (CVR) to increase the efficiency of the distribution system and conserve power considering the energy and electrical catastrophe issues in [Hossein et al., 2020]. At most distribution equipment, as technology and communication have advanced, efforts to reduce energy consumption have shifted to near-real-time regulation of voltage and voltampere-reactive power concentrations (VAR) or voltage/var Optimization (VVO). Control techniques for VVO are offered in both centralized and decentralized forms. LTC transformers, voltage regulators, and fixed/switched capacitor banks are used in centralized VVO techniques to manage voltage and reactive power flow. Numerous centralized VVO techniques exist. These auto-adaptive regulators are built on either closed-loop control with real-time voltage measurement or earlier communication systems to improve the power flow in response to the utility's instructions. Decentralized or agent based VVO methods, have drawn more people to question the scalability of control [Manbachi et al., 2013; Moghe et al., 2016].

- **1.3.3 Voltage control methods for a smart distribution network**

The voltage control apparatus and sensors are located at the transformer's transmitting ends and substations in conventional distribution network architectures. However, because of the

complex power conditions and two-way power inflows, the voltage control mechanisms in the smart grid need to be improved in [Shankar and Singh 2022]. Additional accurate voltage data is anticipated to keep the voltage under control for a short while. The current-voltage control techniques used in active distribution networks (ADNs) may be categorized as dispersed, quasi-coordinated, or centralized control strategies in [Bidgoli and Van Cutsem 2017]. The OLTC and voltage regulator are just two examples of the numerous network devices that can be synchronized using a wide range of communication mechanisms according to the centralized or coordinated control approach, which gives voltage control from the substation to the rest of the network [Luo et al., 2021]. On the other hand, the quasi-coordinated and decentralized or distributed control techniques must be able to manage the local DG unit with a minimal number of other system components while operating it efficiently [Adeyanju et al., 2021]. These solutions enable the system to function more broadly despite budgetary restrictions brought on by the lower demand for communication tools. Several voltage control methods have been suggested in the literature to control voltage when DGs are present. A review of the voltage control methods used to concern ADNs is covered in this section. Based on how information is exchanged between the involved entities, the applied control methods can be divided into two main categories: centralized and decentralized. In centralized control, a central coordinator collects all the necessary grid measures, maybe via intelligent sensors and remote terminal devices, finds the answer to the control issue, and then relays that information back to the rest of the system. The primary coordinator is the only network device capable of starting a control signal. Every regulator in the network only needs to connect with nearby nodes when using dispersed/ decentralized control. Therefore, access to the grid's overall data is optional to make control decisions [Mai et al., 2021].

- **Centralized control schemes**

A centralized voltage control technique is created to best utilize the PSO algorithm to control the reactive power of DG units, and the suggested sensitivity strategy in [Zad et al., 2015]. In [Sun et al., 2020] uses the idea of maximizing worldwide and controlling locally to provide a combined central and local voltage control technique based on a two-stage voltage control framework. A unique worst-case voltage scenario based centralized voltage-controlling system to reduce the voltage variations of all buses in distribution networks is proposed in [Ma et al., 2021]. A two-stage interval optimization-based optimization strategy to reduce voltage fluctuations and improve the economy of the distribution network with

energy storage integrated soft open spots and high DG penetration is suggested in [Hu et al., 2022]. To synchronize OLTCs and smart inverters on operational time scales, this research suggests an optimization-based voltage control technique in [Li et al., 2020]. To provide an all-encompassing voltage control system for LV distribution grids that combines PV inverter and OLTC operating under high DG integration situations is explained in [Efkarpidis et al., 2016]. A two-stage hierarchical demand response (DR) method for controlling the voltage at distribution feeders while responding to transmission system DR requests in [Zhu et al., 2018]. The authors of [Sheng et al., 2015] used the branch and bound methodology with the trust region sequential quadratic programming method to an iterative approximation of the optimization with trust region guidance to solve the mixed integer nonlinear programming issue. In [Shabestary et al., 2019] proposes a fully decentralized asymmetric ride-through mechanism. An effective voltage control technique in smart grids with limited communication infrastructure, distributed voltage control is developed in [Abessi et al., 2015]. In [Li et al., 2017] develops a time-series optimization model based on SOP for coordinated voltage and VAR management. The suggested model considers the collaboration of SOP and numerous control devices to end voltage violations while reducing the operating expenses of ADNs. A brand-new Volt/Var control framework for managing distribution networks is suggested in [Mejia et al., 2021]. To optimize the voltage profile and offer additional functionalities to the distribution networks, this framework implements a multilevel control mechanism that organizes the reactive power injection from the EV chargers organized in parking spaces. In [Sun et al., 2022] suggests a three-stage suitable voltage control technique to ensure optimal system reliability in distribution networks by coordinating PV inverters with conventional voltage control equipment. In [Kulmala et al., 2014], two correlated voltage regulation methods are proposed and investigated that can be applied in distribution networks with varied distributed energy sources. An efficient, efficient, coordinated system for active distribution systems' voltage control was proposed in [Mehmood et al., 2018].

- **Decentralized or Dispersed control schemes**

To better control the voltage across the network, a distributed voltage control method is suggested in this research for intelligent distribution networks with high penetrations of inverter based DGs [Guo et al., 2021]. A completely dispersed control approach exploiting a multiple agent scheme is used to control voltage through voltage outings in ADNs, and to reduce network losses in [Wang et al., 2018]. In [Li et al., 2019] suggests a collective

decentralized and local voltage control approach to handle with the recurrent voltage variations. The authors [Hu et al., 2021] propose a new control approach for real-time voltage regulation in both balanced and unbalanced distribution networks to exploit online and step-less reactive power vehicle to grid facilities. In [Liu et al., 2019] presents a fully distributed optimization method to deal with the voltage violation problem caused by large-scale PV access in local distribution networks. a method based on sensitivity concept is presented to control the network voltage by means of the reactive power switched between the network and the DGs in [Brenna et al., 2012]. a distributed method for online voltage regulation in a radial distribution network has been explained where the obligation for synchronic update of decision variables in the distribution network in some prevailing algorithms has been effectively detached in the projected method [Hu et al., 2019]. a distributed voltage control which divides the system into few sub-systems is presented as a competent voltage control technique in the smart grids with low communication organization in [Abessi et al., 2015]. To optimize the voltage profile along the distribution system's feeders, the study suggests a decentralized optimization-based design of the set-point for the DG control method in [Di et al., 2013]. In [Li et al., 2019] proposes a kriging metamodel-based local voltage control technique for DGs with reactive power optimization. First, the procedures for calculating the input variables are provided in detail to develop the object model for localized voltage regulation, and various parameters' impacts on the domain model's correctness are examined. A battery energy storage central control solution for rooftop PV systems to lessen voltage rise/drop problems in LV distribution networks with significant PV source integration is offered in [Zeraati et al., 2016]. A unique distributed control technique based on a framework for back-and-forth communication is created to coordinate numerous multi-energy storage systems for multi-time-step voltage regulation in [Yu et al., 2020]. For upcoming distribution networks, a unique distributed cooperation voltage regulation mechanism is put forth in this research. The suggested method can reduce the number of agents necessary for voltage control and the change in power needed for voltage regulation, which reduces the demand for re-dispatching, or the effect of voltage regulation on energy exchange in [Fu et al., 2022]. A fully decentralized multi-agent system-based adaptive reactive regulation approach to enhance the power grid's energy efficiency and voltage profiles under various operational scenarios is suggested in [Zhang et al., 2014].

Distribution systems are enormously complicated due to their large number of nodes, proximity, low magnitude, angle variances among nodes, rapid oscillations, and absence of precise documentation. As a result, these complications have increased the demand for new,

highly accurate, and precise monitoring systems that aid in developing insight into distribution networks and empower distribution managers to respond to such interruptions. The results of the survey spurred further investigation with the aim of establishing methodologies for estimating the voltage magnitudes states of the balanced and unbalanced conditions of the radial distribution networks using PMU technology.

1.4 Motivation

The distribution grid is impacted by the large-scale integration of DG units in several ways, including system voltage, protection, grid stability, and grid planning. Electric Power Systems operators have historically monitored that the power system works in a safe area using SCADA readings and results from the static state estimator. It is extremely challenging to precisely evaluate the system's overall and current operating state since the numbers collected from the SCADA system and the SE are not synchronized. The use of SE for real-time network dynamic behaviour monitoring is made possible by the new PMU technology.

Researchers have explored and investigated the conventional optimal PMU placement (OPP) problem for many years with the goal of making the power system fully observable. The smart selection of the minimum number of PMUs is a significant aspect of the OPP problem. The high investment and installation costs of PMUs as well as the lack of the necessary communication infrastructure in the system are further barriers to this system-wide installation of PMUs. Due to this, it has become clear that choosing the right number and position of PMUs to install in a system in order to assure its full observability is a significant issue that has been the subject of intensive research over the past decade. In the literature, numerous techniques, and various algorithms for the best placement of PMUs have been introduced. Deterministic methods and meta-heuristic optimization techniques can be used to classify them in general into two major classes. The ideal PMU placement is formulated as an integer programming (IP) or binary Search issue in deterministic techniques. Therefore, a key factor in arriving at the best solution is carefully defining the proper restrictions to assure the viability of the objective function. Among the heuristic methods that have been developed so far for the purpose of optimum PMU placement, which include methods like simulated annealing, genetic algorithm, tabu search, particle swarm optimization, ant colony optimization, tree search topology and differential evolution etc.

To guarantee the feasible benefits out of PMU placement in the network and improving its dynamic monitoring, along with optimal placement of PMUs, zero injection

conditions can be rigorously met without compromising predictive performance. Since the power distribution network is dynamic and always changing, the intermittent nature of integrated DGs and the continual changing of loads fundamentally highlight this. This causes a shift in flows and injections at every bus in the network in turn. A crucial component of contemporary control centre operations is state estimate (SE). SE determines the voltage magnitudes and angles at each power system bus.

1.5 Authors contributions

The following research contributions have been developed in this work:

1. A methodology has been developed and presented in this work for optimal placement of PMUs in a distribution network while considering zero injection buses to improve system observability.

2. Developed a methodology for estimating the voltage magnitudes without considering zero injection bus constraints for the balanced radial active distribution network using PMUs.

3. An algorithm is developed to validate the results obtained from the integer linear programming (ILP) functioning in radial test feeders for complete observability of the system

4. A multi-agent system (MAS) based coordinated control technique has been developed to optimize the voltage profile in a 3-phase radial unbalanced active distribution network considering and power losses and unbalanced factors.

1.6 Organization of the thesis

The following chapters compose the thesis:

Chapter 1 covers introduction to the subjects covered in the thesis. Along with the objectives that have been set, it includes a literature review on these topics.

Chapter 2 analyses the computational errors introduced by the enormous weights used in traditional state estimation methods for zero injection constraints. The proposed approaches are intended to guarantee that these zero injection criteria can be strictly achieved while calculating the voltage profile and observability of the various distribution networks without sacrificing computation efficiency. The viability of the suggested solution is evaluated using conventional IEEE distribution networks.

Chapter 3 analyses the challenges posed by conventional offline approaches regarding network reliability and operation. By considering the drawbacks of the zero-injection bus concept, an online voltage magnitude estimation technique utilizing PMU technology is

proposed to estimate the ADN characteristics (voltage and current) with the DG fluctuation effectively. A forward and backward sweep (FBS) load flow algorithm is used to authenticate the proposed methodology. The recommended technique's applicability is examined using the balanced IEEE Distribution network systems.

Chapter 4 assesses the impact of unbalanced loading, DG integration, and voltage regulation requirements. Imbalanced active distribution networks must be carefully examined to reduce adverse effects from internal unbalances and the addition of intermittent sources like DG. A coordinated voltage regulation method is developed using a MAS control structure to overcome the abovementioned issues. The suggested method improves coordination between DGs and shunt capacitors (SCs), which optimizes the voltage profile and lowers overall power losses and voltage and current imbalance factors of the unbalanced 3-phase radial distribution network. PMUs measure the state parameters of the above-regulated distribution network to ensure improved real-time monitoring. The results of the load-flow measurements made by PMUs are compared to those made by the FBS load-flow algorithm to validate the suggested methodology. An unbalanced 3-phase distribution network feeder is used to evaluate the practicality of the proposed method.

Chapter 5 summarizes the outcomes mentioned in the previous chapters. Additionally, the potential for future study in this field is also covered.

Chapter 2

VOLTAGE ESTIMATION USING PMU TECHNOLOGY CONSIDERING ZERO INJECTION BUS CONSTRAINTS

2.1 Introduction

A power system's synchronized current and voltage phasors can be measured using equipment like phasor measurement units (PMUs). PMU is among the most crucial measuring tools for advanced intelligent power systems. PMUs, which could also continually record samples of the electrical system's system parameters, have drawn much interest in distribution networks. These examples can be used for real-time security, supervision, and regulation. Due to the scattered varying energy supplies, the distribution system exhibits distinct dynamics (like wind and solar energy). Furthermore, the smart grid paradigm would convert the current unidirectional power distribution system to a bidirectional one. PMUs must always be deployed at the necessary nodes for complete visibility of the voltage or current phasors.

PMUs give network administrators greater visibility and allow them to pick up incidents that SCADA might have missed in [Amoateng et al. 2021]. Most high-voltage buses in real power systems are zero injection buses without load or generation. They ensure that such zero injection conditions can be rigorously met without compromising predictive performance. The network's transhipment nodes are related to zero injection. Zero injection nodes inject no current into the network. If zero injection nodes are also designed, the total number of PMUs in the PMU deployment challenges can be significantly decreased. An effective zero injection limitation computing technique is required to determine the power system's state in [Guo et al. 2013]. In observability assessment, zero-injection pertains to the system's effects or impacts on buses where no power is supplied. The number of PMUs could be decreased by simulating the zero-injection buses (ZIBs) present in the situation. As a result, fewer PMUs are needed to analyse the network when zero-injection buses are present in [Mohamed et al. 2019]. ZIBs are regarded as a bus with exceptionally effective power monitoring since they have no supply or demand in [Chauhan and Sodhi 2019]. Integrating

the implications of ZIBs and load flow observations to figure out the right amount of deployed PMUs, that not just serves to save cost but much more significantly improves the cyber resilience of the power grid, could be challenged in PMU placement optimization [Shi et al. 2019]. The term "set of ZIB nodes" refers to the ZIB and any associated buses. If there are N buses in this collection, then using the ZIB's functionality to make an unobservable bus observable using the measurability of N-1 buses is sufficient [Patel et al. 2022].

The following are a few studies that have addressed the significance of zero injection nodes in the literature: This study proposes an optimal PMU placement (OPP) problem setting with zero injection buses (ZIBs) in typical system states and considers contingency due to PMU outage [Bečejac and Stefanov 2020]. Adding ZIBs will result in lines being removed from the system, influencing the PMU placement problem outcomes that aim to achieve reliability against a line failure in [Koochi et al. 2020]. A comprehensive PMU-observability framework of the network topology is created in [Bai et al., 2021], built on the OPP paradigm and taking ZIB into account. In [Almasabi et al. 2019], considers both the price and how significantly the PMU placements will enhance system observability in the existence of potential vulnerabilities. This paper offers zero injection observation depth (ZIOD) to illustrate how Zero injection (ZI) impact propagates. By constraining ZIOD, the authenticity of ZI observation is ensured [Lu et al. 2018]. Reference [Kumar et al. 2015] explained the best locations to strategically install a certain number of PMUs are determined for a system that considers uncertainty and topological aspects. The attack-resistant OPP technique proposed in this research uses reinforcement learning guided tree search to arrange PMUs in a specific order, with the exploration of placement orders being done via reinforcement learning's sequential decision-making [Zhang et al. 2022]. The unique aspect of this work is positioning the PMUs so that weak buses can be observed with the most significant possible number of PMUs to determine the system's full observability and stability under various conditions, such as taking zero injection nodes into account and experiencing a single PMU outage in [Müller et al. 2020]. The of two distinct stages: in phase 1, the coordination sites in the search tree are examined by depth-first search, and in phase 2, the primary simplex is configured using the basic feasible solution from phase 1 till the global optimum is identified in [Babu et al. 2021]. The strategy for deploying micro-phasor measuring units in a distribution network that can operate in different configurations is outlined in [Dua et al. 2021]. This study introduces the idea of observability propagation depth to improve the OPP formulation that effectively addresses constrained quantitative measurements [Guo et al. 2020]. Concerning the PMU outage contingency, the nonlinearity

in state estimation dependability and resiliency issues are addressed in [Kiio et al. 2022]. This work presents an algorithm that can account for realistic requirements such as redundancy in monitoring crucial system components and calculating the tap ratios of the transformers in use [Pal et al. 2017]. To assign and identify smart grid anomalies and failures, this project aims to create a uniquely dynamic structure that only needs a small number of PMUs to interact in a protected blockchain-enabled framework in [Almutairi et al. 2022]. This study offers a novel strategy for allocating μ-PMUs in flexible smart distribution grids considering zero injection nodes and communication system needs [Abdolahi et al. 2021]. The impacts of zero injection buses and traditional metrics for PMU placement are carefully considered by a novel integrated model reported in this article [Khajeh et al. 2015].

Reference [Andreoni et al. 2021] considers single-line and PMU fault-related system observability, either with or without uncertainties. Additionally, it focuses on the effects of potential zero-injection nodes, and a preliminary limitation on the quantity and type of PMU calculations carried out at each node. When used with conventional networks, the suggested technique partitions the network into smaller segments with less reliance, rendering it augments [Elimam et al. 2021]. Global optimal solutions are provided, and the OPP problem is expressed in a direct and precise mathematical manner, guaranteeing the positive quantitative measurements of the corresponding gain multipliers. Additionally, they account for any existing typical measurements, zero injections, and the influence of PMU channel constraints in [Manousakis et al. 2019]. A homogeneous PMU deployment strategy is put forth in this research while considering the validity of zero injection observation [26]. Reference [Ghamsari-Yazdel et al. 2019] recommends deploying phasor measurement devices with the best safety placement and optimum observability reliability. The initial investment and measurement accuracy are both used to distinguish the options requiring the same quantity of PMUs to be deployed because the optimal scheduling framework is thought to be numerous [Abiri et al. 2015].

The primary target of this chapter is to examine the importance of economically placing distribution-stage phasor measurements while considering zero injections to improve system observability. The developed method chooses the ideal PMU position for radial distribution systems taking ZIBs into consideration. This methodology examines voltage estimation using PMU measurements while considering zero injections. The ZIBs lower the system's necessary PMU count, making the network fully visible and cost-effective. The network topology is the only primary consideration while determining the

37

PMU positions. Any installation of voltage regulating equipment, including distributed generation units, has no impact on these positions. This approach can be applied to radial feeder structures regardless of their size or the diversity of X/R ratios.

2.2 PMU placement in distribution network

An integer linear programming (ILP) algorithm is adopted to define the optimal number and location of PMUs. ILP is a mathematical optimization technique wherein specific or entire constrained variables are restricted to be either binary or integers. ILP includes mainly three effective formulations;1) Variables; execute the decisions regarding integer values, 2) constraints; enclose the costs to a manageable region; and 3) the objective function; gets the optimal solution by directing the problem by maximizing or minimizing its function. The objective function and constraints need to be linear consistently in ILP formulation. This technique affirms the accomplishment of complete observability of the network with optimum PMU numbers.

For siting the PMUs optimally, recognizing the ideal sites is the primary phase. In a practical electrical network framework, certain nodes might be distinct and critical, for instance, a node accompanying an overloaded or reasonable predominant site, or could be an upcoming expansion location. Owing to former occasions, at the preferred sites, PMUs could be situated. The non-observable phasors of the system could be observable with few extra PMUs. A binary search algorithm is exploited to explain the PMUs sites optimally, which would permit the complete network to be observable under usual operating events [Yasinzadeh et al. 2018].

- **Optimal PMU placement on full observability while considering regular system operation**

In the observability analysis of power systems, topological and numerical observability are the two main methods that are frequently used. From a mathematical perspective, a system is observable when the rank of the related Jacobian matrix or measurement gain matrix equals the system's unknown states. However, in the case of enormous systems, the numerical observability assessment is often seen as a cognitive expense. It fails to identify the genuine zero diagonal members of the matrix due to potential rounding mistakes. As a result, most articles have used topological methodologies to confirm the system's complete observability [Kim and Kim 2021].

- **Criteria to monitor the buses in any power system**
  - ➢ The phasors voltage/current of the associated bus can be evaluated by a PMU when installed on that bus.
  - ➢ A PMU deployed at bus permits for surveillance of that bus and all neighbouring buses. While PMU can directly measure the voltage magnitude of the node it is equipped with, KCL is used to ascertain the voltage phasor of the connecting node [Huang et al. 2013].
  - ➢ When one bus cannot be observed in the set of ZIB and all associated buses, its values are calculated using Kirchhoff's current law (KCL). Additionally, KCL can be used to determine the value of a set of connected buses that conform to a ZIB.

- **Limitations for ILP when no zero-injection bus is considered**

$$\min \sum_{k=1}^{N} q_k \tag{2.1}$$

$$Subject\ to\ G = PQ \ \geq \ L \tag{2.2}$$

$$Q = [q_1, q_{2,\ldots\ldots\ldots\ldots\ldots} q_n]^T \tag{2.3}$$

$$q_k \ \in \ \{0,1\}, \ k = 1, 2, \ldots\ldots\ldots, Z \tag{2.4}$$

Z is the total number of nodes in the system

Q is the column matrix of PMU position

$$q_k = \begin{cases} 1, \ if\ PMU\ is\ needed\ in\ bus\ k \\ \qquad 0, \ otherwise \end{cases} \tag{2.5}$$

The matrix element of P are as follows,

$$P(i,j) = \begin{cases} 1, \ if\ buses\ i\ and\ j\ are\ connected \\ \qquad\qquad 1, \ i = j \\ 0, \ if\ buses\ i\ and\ j\ are\ not\ connected \end{cases} \tag{2.6}$$

$$L = [\ 1\ 1\ \ldots\ldots..\ 1]^T \tag{2.7}$$

$$g_i = \sum_{j=1}^{N} P_{ij} \ q_j \ \geq 1; \text{ where i = 1, 2, ..., N} \tag{2.8}$$

The observability of the i_{th} bus is determined by g_i, which is determined by the connection matrix P. L is the column matrix, which shows the least number of PMUs to be installed to make the set of buses observable [Koochi et al. 2020].

- **Variation in constraints when ZIBs are taken into consideration**

Certain adjustments must be made to the formulation of restrictions when a single ZIB or a collection of ZIBs is considered. The following are these:

1) The 'g_i' of a specific bus stays the same while not connected to any ZIB.
2) The buses linked to a single ZIB make up " r " members. These can be observed when the " $r - 1$" members are visible.
3) Consequently, it is comprehended that,

$$\sum_{i=1}^{r} g_i \geq r - 1 \qquad (2.9)$$

4) An " r " member set is created when there are " s " numbers of ZIBs, and they are all connected to certain buses. If ' $r - s$' members are observable, then these members are also observable.

$$\sum_{i=1}^{r} g_i \geq r - s \qquad (2.10)$$

5) A bus's occurrence should be kept to a single ZIB when it incident to numerous ZIBs.
6) The new values of P_{new} and L_{new} are acquired when these rules have been instituted.

2.3 Methodology for the formulation for determining the best PMU location in systems with ZIBs

Two hypotheses are being considered if ZIBs are present.

- **Case 1: A single ZIB is present**

The data file containing the line information for the individual bus systems is loaded. After that, computation and display of the connection matrix relating to the line details are generated. If there are no ZIBs, the lower and upper bounds are set to 0 and 1 accordingly, L is given the value 1, and intcon is set as a series of numbers from 1 to the whole number of buses. Once the required assignments have been made, the arguments are passed to the intlinprog function, which returns the ideal PMU number and its locations.

a) As input, the ZIB position is requested. After completing this, an empty array is made to record the buses associated with the injection bus.
b) The value of the input ZIB is designated to the array's first member. A for loop is employed to ascertain the additional buses to the injection bus.

c) A separate array is used to store buses that are connected to the injection bus but not to any other injection buses.

d) Modifications are performed to the arrays mentioned above to make them the same size.

e) The connection information for the buses with no injection is stored in a new connection matrix. Comparable to the values in the original connection matrix, this matrix has similar values.

f) Creating an array that retains information about the connections between buses and injection buses. The elements of these matrices are then added together to produce a 1-dimensional (D) array.

g) For the bus with no injection, a column vector of ones is produced, and a second vector, 'r,' with a value of '$r - 1$,' is constructed for the bus associated with the bus with injection.

h) The injection bus locations total and the connection matrix for no injection are combined and stored as $'P_{new}'$ in a 1-D array. 'L_{new}' is created by concatenating the column vector of ones for no injection and the one for injection buses. Then, steps (c–d) are repeated after passing these values to the intlinprog function.

- **Case 2: Multiple ZIBs are present**

When more than one ZIB is input, Case 1's steps (a) through (c) are repeated for each ZIB until linking buses for all ZIBs are obtained. Iteratively displayed values are recorded in cells for each iteration that relate to the buses connected to each injection bus. The cell is subsequently transformed into a one-dimensional array containing each connecting injection bus. In addition to being sorted, this array is verified for bus duplication. The steps (d-g) are then repeated except for (g), which is altered so that the value of observability for the injection buses is changed to "$r - s$."

The above two cases are explained considering a 10-bus system with zero injection buses (ZIBs) at positions 5, 6 & 9 as an example.
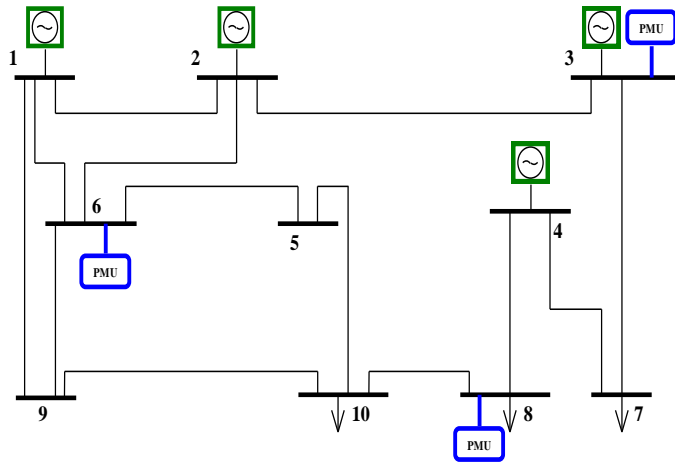
Figure 2.1:10 bus network without zero injection buses
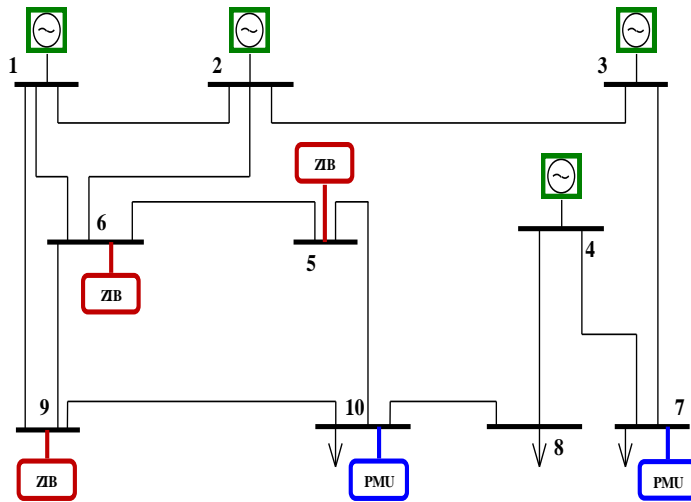
Figure 2.2: 10 bus network with zero injection buses

The initial connection matrix and the corresponding observability matrix is as follows

$$P = \begin{bmatrix} 1 & 1 & 0 & 0 & 0 & 1 & 0 & 0 & 1 & 0 \\ 1 & 1 & 1 & 0 & 0 & 1 & 0 & 0 & 0 & 0 \\ 0 & 1 & 1 & 0 & 0 & 0 & 1 & 0 & 0 & 0 \\ 0 & 0 & 0 & 1 & 0 & 0 & 1 & 1 & 0 & 0 \\ 0 & 0 & 0 & 0 & 1 & 1 & 0 & 0 & 0 & 1 \\ 1 & 1 & 0 & 0 & 1 & 1 & 0 & 0 & 1 & 0 \\ 0 & 0 & 1 & 1 & 0 & 0 & 1 & 0 & 0 & 0 \\ 0 & 0 & 0 & 1 & 0 & 0 & 0 & 1 & 0 & 1 \\ 1 & 0 & 0 & 0 & 0 & 1 & 0 & 0 & 1 & 1 \\ 0 & 0 & 0 & 0 & 1 & 0 & 0 & 1 & 1 & 1 \end{bmatrix} \quad (2.11) \qquad L = \begin{bmatrix} 1 \\ 1 \\ 1 \\ 1 \\ 1 \\ 1 \\ 1 \\ 1 \\ 1 \\ 1 \end{bmatrix} \quad (2.12)$$

With ZIBs at the buses 5, 6 & 9

Buses connected to ZIB 5 are – 6 & 10

42

Buses connected to ZIB 6 are – 1, 2, 5 & 9

Buses connected to ZIB 9 are – 1, 6 & 10

The buses that do not have any injections are 3, 4, 7 & 8.

Hence,
$$\left.\begin{array}{l} g_3 = q_2 + q_3 + q_7 \geq 1 \\ g_4 = q_4 + q_7 + q_8 \geq 1 \\ g_7 = q_3 + q_4 + q_7 \geq 1 \\ g_8 = q_4 + q_8 + q_{10} \geq 1 \end{array}\right\} \qquad (2.13)$$

$$\left.\begin{array}{l} g_6 + g_{10} = q_1 + q_2 + 2q_5 + q_6 + q_8 + 2q_9 + q_{10} \geq 1 \\ g_1 + g_2 + g_5 + g_9 = 3q_1 + 2q_2 + q_3 + q_5 + 4q_6 + 2q_9 + 2q_{10} \geq 2 \\ g_1 + g_6 + g_{10} = 2q_1 + 2q_2 + 2q_5 + 2q_6 + q_8 + 3q_9 + q_{10} \geq 2 \end{array}\right\} \qquad (2.14)$$

Buses with injection are 1, 2, 5, 6, 9 & 10

No: of elements in the injection array set (r) = 6

No: of ZIBs (s) = 3

Therefore $(r - s) = 3$ which means 3 buses of the injection buses need to be observable.

Hence,

$$g_1 + g_2 + g_5 + g_6 + g_9 + g_{10} = 4q_1 + 3q_2 + q_3 + 3q_5 + 5q_6 + q_8 + 4q_9 + 3q_{10} \geq 3$$
$$(2.15)$$

$$\mathrm{P}^{\text{new}} = \begin{bmatrix} 0 & 1 & 1 & 0 & 0 & 0 & 1 & 0 & 0 & 0 \\ 0 & 0 & 0 & 1 & 0 & 0 & 1 & 1 & 0 & 0 \\ 0 & 0 & 1 & 1 & 0 & 0 & 1 & 0 & 0 & 0 \\ 0 & 0 & 0 & 1 & 0 & 0 & 0 & 1 & 0 & 1 \\ 4 & 3 & 1 & 0 & 3 & 5 & 0 & 1 & 4 & 3 \end{bmatrix} \qquad (2.16) \qquad \mathrm{L}^{\text{new}} = \begin{bmatrix} 1 \\ 1 \\ 1 \\ 1 \\ 3 \end{bmatrix} \qquad (2.17)$$

With injection the PMU numbers and PMU locations are determined as follows,

Number of PMUs = 2

Position of PMUs are Q = [0 0 0 0 0 0 1 0 0 1]

Therefore, PMUs are to be positioned in buses 7 and 10. The total PMUs needed for the 10 bus network without considering ZIBs were three and were located in positions 3, 6 and 8.

- **Flowchart of OPP with and without ZIBs**
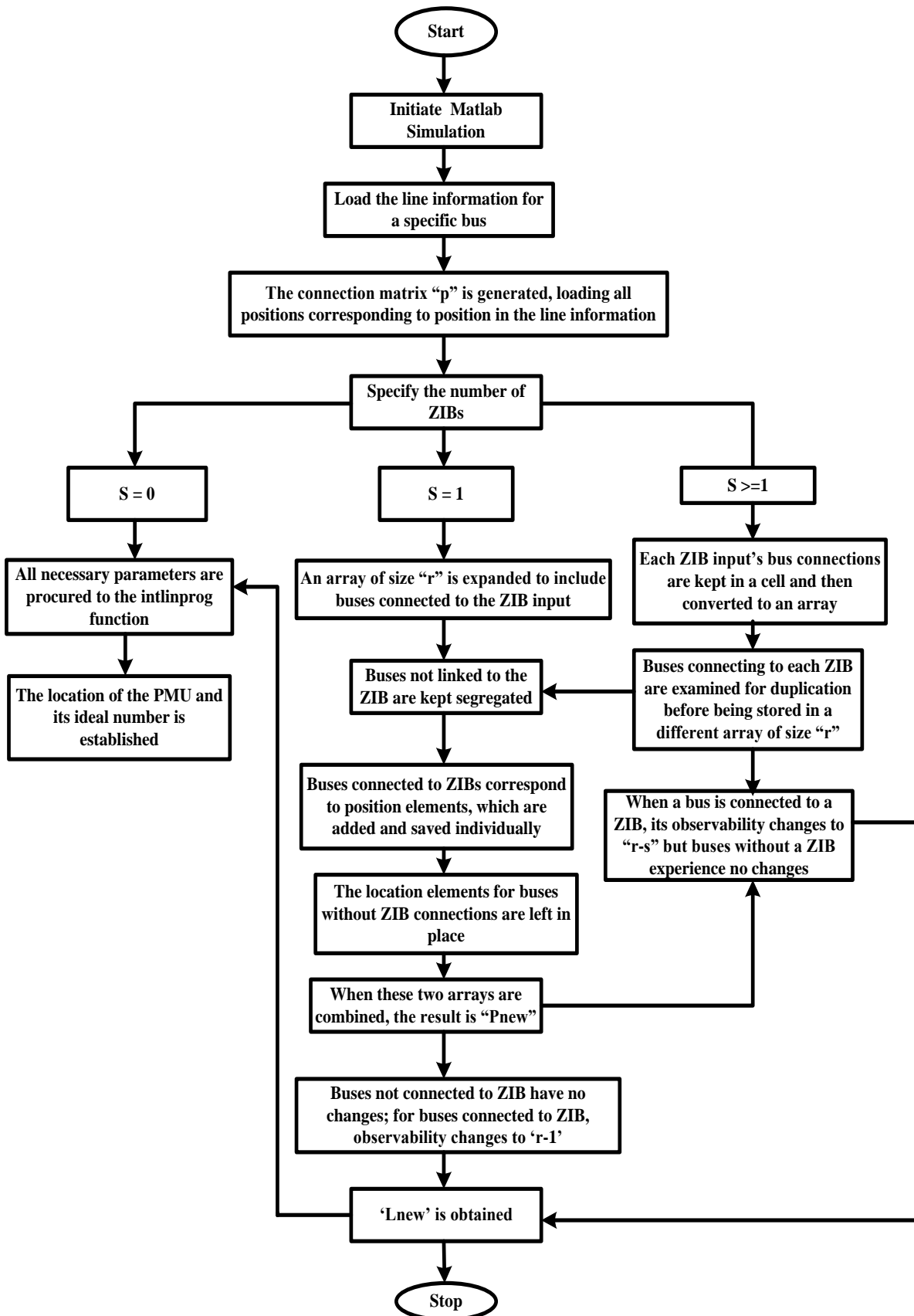
Figure 2.3: Flowchart of OPP with and without ZIB

2.4 Formulation for the voltage estimation using the best PMU location in systems with ZIBs

A generic algorithm is used to evaluate the voltages and currents of the network using PMU-associated nodes. The ZI bus numbers are input to get the new connection matrix. The bus numbers at the end of each adjacent chain and the focal chain of buses make up the enbus vector. First, a voltage of one p.u. (per unit) is assumed on each bus. The line currents are determined by using the enbus vector and KCL for the remaining lines of end buses. Kirchhoff's voltage law (KVL) is used to ascertain the node voltages by working back from the last node to the first node and accessing the line currents from the preceding. This process was repeated using the earlier bus voltages to obtain the line currents. The sequence will be terminated if the variation between the voltage magnitudes is exceedingly tiny. The voltage and line current vectors are utilized to evaluate the voltages and currents at various PMUs by identifying the line matrix with all bus interconnections.

The algorithm below summarizes the steps of the voltage estimation of the radial distribution system considering zero-injection buses using PMUs.

- **Algorithm:** PMU framework for the voltage estimation considering zero injection buses (ZIBs)

Step 1: Start

Step 2: Load the bus specifics and their number in the network

Step 3: Store total no. of zero injection nodes (Z)

Step 4: Find the connection matrix ;   for *l = 1: total*_bus

connection_matrix(l,l) = 1;
end

Step 5: if *Z == 0 (no zero injection nodes)*

Step 6: display the *connection_matrix*

Step 7: input lower & upper bound values

Step 8: Find the best possible PMU locations using *intlinprog*

Step 9: display the *pmu_position*

Step 10: if $Z \neq 0$ *(non zero injection nodes)*

Step 11: *w =* input the *ZI* bus numbers

Step 12: Sort out the network with zero injections and find the injection matrix and new connection matrix with injections(*connectionnewnoinj*)

Step 13: display the *connectionnewnoinj* and repeat steps from 7 to 9

Step 14: Obtain the branch vector and PMU location.

45

Step 15: Get the real and reactive (*Px, Qx*) powers at each bus and line data (*Zx*).

Step 16: Initialize the voltage of each bus as *Vx(l,1) = 1* p.u.

Step 17: Form an *enbus* vector comprising end situated nodes; *enbus = Zeros(m,1)*.

Step 18: Calculate line flows, accounting for end branches and remaining nodes. *Ix(m,1)=conj(abs(app_power)/(abs(Vx(m,1))))*.

Step 19: Use the line currents to estimate the new set of node voltages. *Vxnew=Vx(m,1)*.

Step 20: Execute another assessment of the line currents with the updated node voltages. *Ixnew=[l]*.

Step 21: Continue looping until the difference between the voltages is less than the tolerance.

Step 22: Verify the parameters in the line current and node voltage vectors.

Vx(pmu_node(*k*)), *Ix*(pmu_node(*k*)-1) of the PMU measurement.

Step 23: Print the results of node voltage and line current vectors.

Step 24: Stop.

2.5 Results and discussions

This section explains the findings from the best PMU placement with and without ZIBs and assesses the voltage profile using PMUs. The simulations are executed on the MATLAB platform.

2.5.1 Optimal PMU locations

For full observability of the distribution test feeders, an integer linear programming technique is utilized in the simulation with a minimum number of PMUs with and without ZIBs. Table 2.1 shows the complete observability of these test feeders and the requisite PMU counts and placements for the case studies on the modified IEEE 18-bus, 33-bus, and 69-bus networks. When ZIBs are considered in the design of PMU placement, the necessary number of PMUs is significantly reduced without affecting the system's observability.

Table 2.1 IEEE radial bus networks' optimal PMU bus placements with and without ZIBs

IEEE Test Systems	PMUs count without ZIBs	Positions of PMU	No. of ZIBs	ZIB location	No. of PMUs with ZIBs	Positions of PMU
18	7	1,4,7, 10, 13, 16, 18	3	2,3,7	6	3, 4, 9, 13, 16, 18
33	11	2,5,8,11,14,17, 21,24,27,30,33	2	6, 27	10	2, 5, 8, 11, 14, 17, 21, 24, 29, 32
69	24	2,6,9,14,17,20, 23,26,29,32,35 ,37,40,43,46,4 7,50,52,55,58, 61,64,66,68	20	2, 3, 4, 5, 15, 19. 23, 25, 30, 31, 32, 38, 42, 44, 47, 56, 57, 58,60, 63	16	3 4 6 14 17 20 26 34 41 45 49 51 54 64 66 68

2.5.2 Voltage profile estimation of IEEE bus systems using PMUs

The 18-bus data is provided in [Taher et al., 2011], whereas data for 33 and 69 buses are provided in [Tangi and Gaonkar 2021] and given in appendix.

- **18 bus results**

Figures 2.4 and 2.5 depict the 18-bus radial distribution network with PMUs at designated nodes, both with and without ZI.
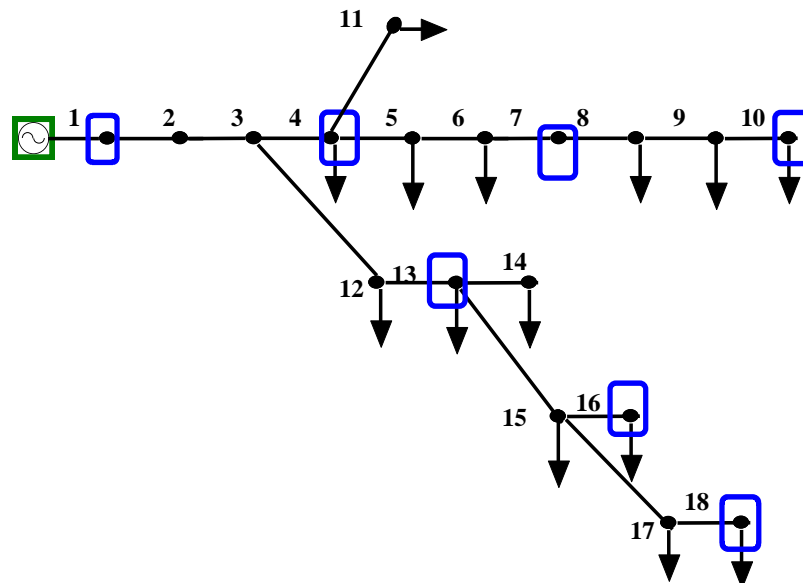
Figure 2.4: ZIB-free modified IEEE 18 bus network
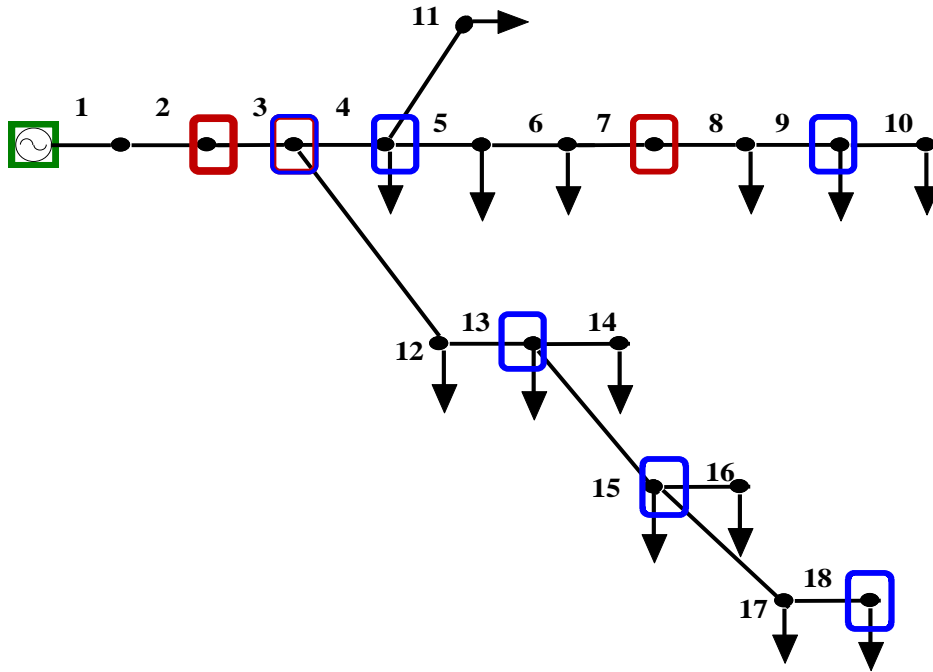
Figure 2.5: ZIB-enabled modified IEEE 18 bus network

Table 2.2 displays the results of comparing the voltage magnitude of an 18-bus system with and without ZIs. The comparison shows that using ZIBs minimizes the number of PMUs deployed in a bus network while retaining its observability. Additionally, Figure 2.6 demonstrates that the usage of ZIBs has no appreciable impact on the voltage profile of the network.

Table 2.2 Voltage magnitudes of modified IEEE 18 bus system at various PMU locations

Without ZIB		With ZIB	
PMU location	Voltage mag. (p.u.)	PMU location	Voltage mag. (p.u.)
1	1	3	0.9989
4	0.9974	4	0.9974
7	0.9925	9	0.9896
10	0.9850	13	0.9899
13	0.9899	16	0.9824
16	0.9824	18	0.9785
18	0.9785	--	--
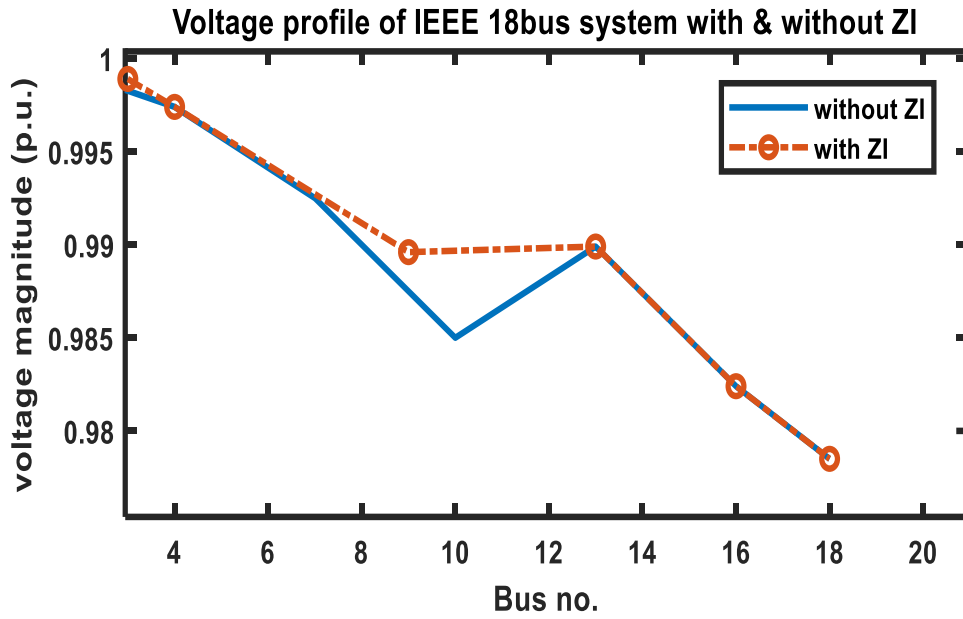
Figure 2.6: Modified IEEE 18 bus system voltage profile with and without ZIBs

- **33 bus results**

Figures 2.7 and 2.8 depict the 33-bus radial distribution network with PMUs at designated nodes, both with and without ZIBs.
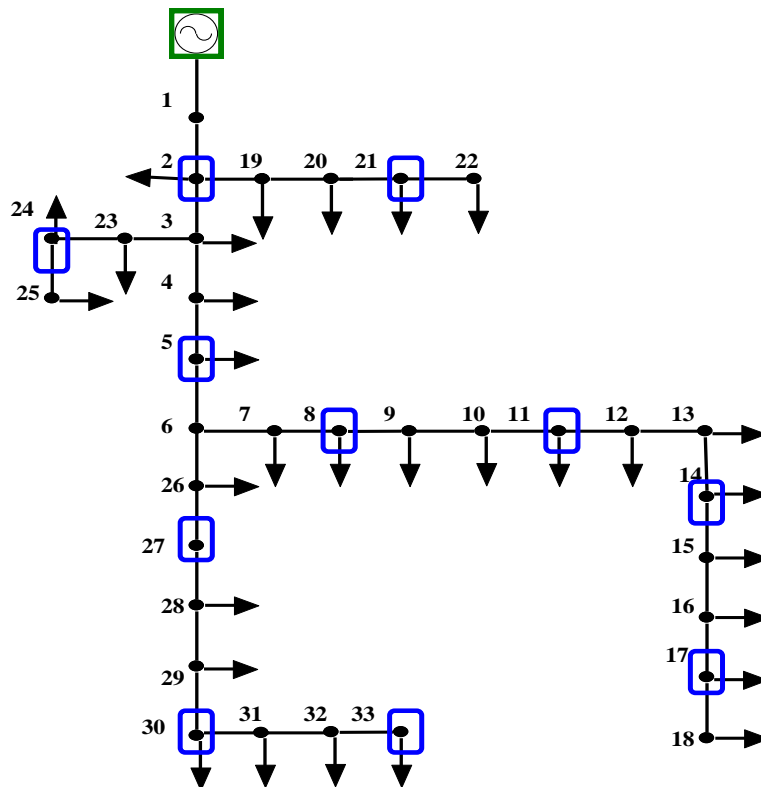
Figure 2.7: IEEE 33 bus network without ZIBs
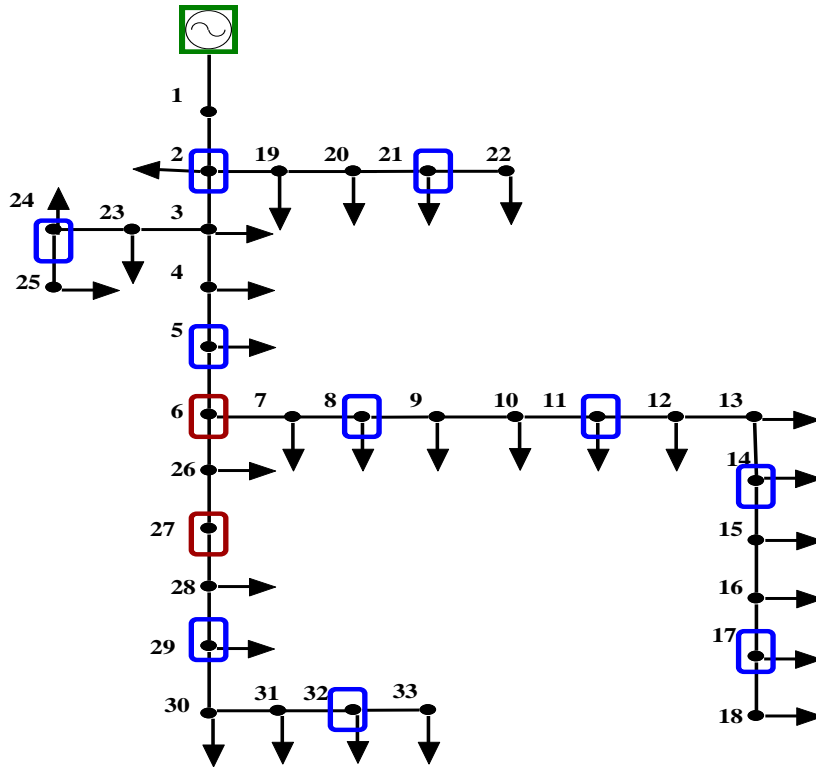
Figure 2.8: IEEE 33 bus network with ZIBs

The results from evaluating the voltage magnitude of a 33-bus system with and without ZIBs are shown in Table 2.3. According to the comparison, employing ZIBs reduces the quantity of PMUs used in a bus network while maintaining its observability. Additionally, Figure 2.9 shows that the voltage profile of the network is unaffected significantly using ZIBs.

Table 2.3 Voltage magnitudes of IEEE 33 bus system at various PMU locations

Without ZIB		With ZIB	
PMU position	Voltage mag. (p.u.)	PMU position	Voltage mag. (p.u.)
2	0.9979	2	0.9979
5	0.9741	5	0.9741
8	0.9476	8	0.9476
11	0.9371	11	0.9371
14	0.9295	14	0.9295
17	0.9261	17	0.9261
21	0.9942	21	0.9942
24	0.9799	24	0.9799
27	0.9553	29	0.9399
30	0.9363	32	0.9328
33	0.9326	--	--
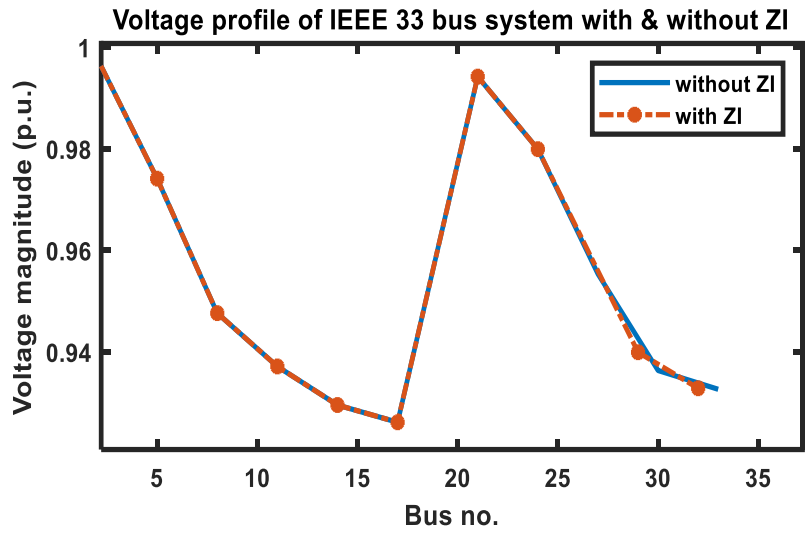
Figure 2.9: IEEE 33 bus system voltage profile with and without ZI

- **69 bus results**

Figures 2.10 and 2.11 depict the 69-bus radial distribution network with PMUs at designated nodes, both with and without ZI.
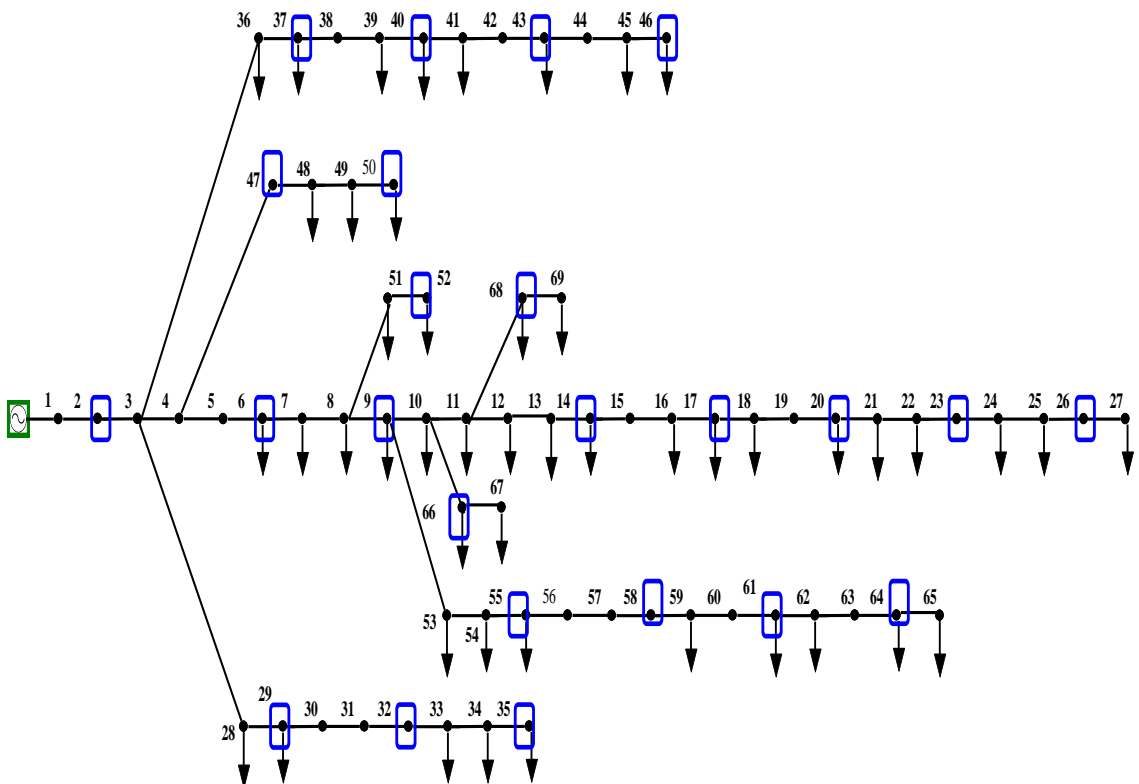
Figure 2.10: IEEE 69 bus network without ZIBs
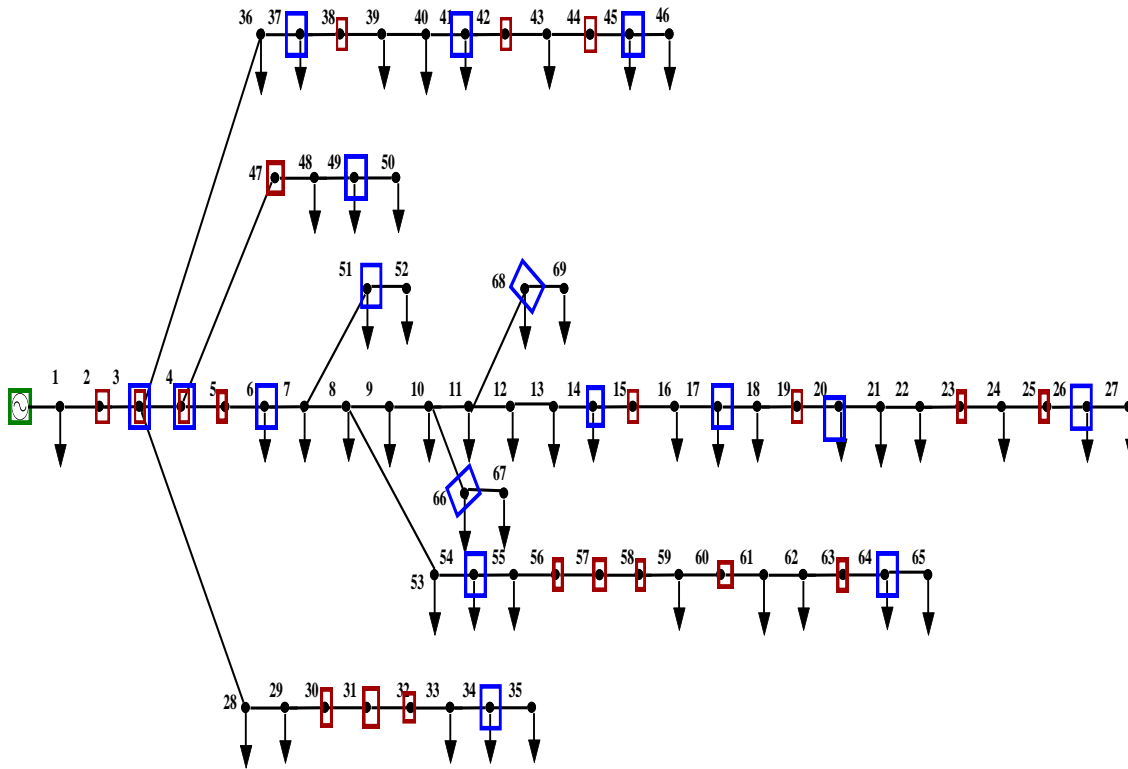
Figure 2.11: IEEE 69 bus network with ZIBs

■ ... PMU bus   ■ ... ZI bus

The findings from comparing the voltage magnitude of a 69-bus system with and without ZIs are shown in Table 2.4. This comparison shows that using ZIBs decreases the number of PMUs employed in a bus network while keeping it observable. Figure 2.12 further shows that the voltage profile of the system is unaffected significantly using ZIBs.

Table 2.4 Voltage magnitudes of IEEE 69 bus system at various PMU locations

Without ZIBs		With ZIBs	
PMU locations	Voltage mag. (p.u.)	PMU location	Voltage mag. (p.u.)
2	1	3	1
6	0.9913	4	0.9999
9	0.9799	6	0.9913
14	0.9632	14	0.9632
17	0.9579	17	0.9579
20	0.9568	20	0.9568
23	0.9559	26	0.9546
26	0.9546	34	0.9993
29	0.9999	41	0.9993
32	0.9997	45	0.999
35	0.9992	49	0.9977
37	0.9999	51	0.9809

40	0.9997	54	0.9746
43	0.9991	64	0.9162
46	0.9990	66	0.9736
47	0.9999	68	0.9699
50	0.9974	--	--
52	0.9809	--	--
55	0.9706	--	--
58	0.9341	--	--
61	0.9184	--	--
64	0.9162	--	--
66	0.9736	--	--
68	0.9699	--	--
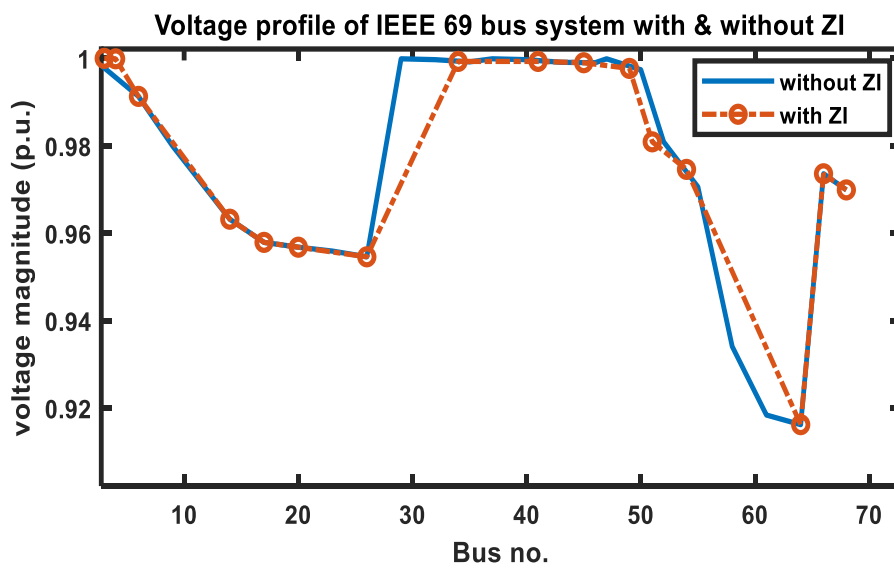
Figure 2.12: IEEE 69 bus system voltage profile with and without ZI

2.6 Conclusion

Given that PMUs are crucial in existing grid networks, this work aims to make choices concerning PMUs' best locations for various configurations simpler. Two strategies are put forth in this study: one aims to determine the distribution network's best observability of PMU sites both with and without ZIBs, and the other assesses the voltage profile with any distribution feeder of a radial nature using PMU technology under the conditions above. It is possible to install the required number of PMUs at diverse locations by leveraging ILP and operating the network normally. Once it is finished, ZIBs in the network are considered to decrease the quantity of PMUs. Results show that, as desired, using ZIBs has no discernible effect on the voltage profile of the system.

Chapter 3

VOLTAGE ESTIMATION OF ACTIVE DISTRIBUTION NETWORK USING PMU TECHNOLOGY WITHOUT CONSIDERING ZERO INJECTION BUS CONSTRAINTS

3.1 Introduction

With the rise of distributed or embedded generation in distribution networks (DN) and local energy producers' involvement, distribution systems have become active and grown more complex. The deregulation market introduced competition among new players, bringing a two-way flow of power in distribution systems. These happenings made the distribution network transform from passive to active configuration; in turn, their difficulty and changing aspects have been built up over time [Gholami et al. 2020]. This scenario demands advanced management systems with accurate monitoring, control, and adequate protection systems for reliable operation, which is a most significant task for the distribution network operators [Gholami et al. 2019]. Distribution networks typically have quite a lot of buses. Nevertheless, it is not practical to furnish all the distribution network nodes with metering equipment from an economic perspective. In this context, DSE (Distribution state estimation) plays a predictable part in the actual measurement and monitoring of distribution networks [Primadianto et al. 2016]. Typically, due to the high R/X value of the distribution network, high DG penetration, lack of proper communication exchange among the nodes, and other factors, the active distribution network's state estimation process is a strenuous task compared to the transmission networks [Dehghanpour et al. 2018].

Various works that have been contributed to the literature to overcome the above issues are discussed as follows. For updating the change of events in the network states of a distribution system, the micro-PMU's recorded data is being used in [Farajollahi et al. 2018]. Multi-area parameter estimation is proposed as a solution for distribution grid monitoring issues in [Pau et al. 2017]; this methodology depends on an improved version of the weighted least squares (WLS) method, which permits to know how the information is shared among the different overlapping nodes with different neighboring zones. An online method to estimate the parameters using PMU measurements based on the least square estimation

technique has been proposed in [Li et al. 2018]. This paper contributes an online estimation technique to measure voltage and current states under high DG penetration [Othman et al. 2019]. Reference [Louis et al. 2020] utilizes error covariance in distribution system state estimation to provide a technique for obtaining optimal measurement locations. A gradient-based multi-area algorithm is proposed for the distribution network state estimation, and it is expressed through a weighted least squares problem in [Zhou et al. 2020]. The authors of [Hong et al. 2020], proposed a methodology to estimate the target bus voltage with known bus information using a supervised learning algorithm. A neural network technique that offers robustness for any restructuring in the network topology discussed in [Zamzam et al. 2020]. A numerical method has been proposed in [Zhang et al. 2020] to classify the distribution system's topology and estimate line parameters. Reference [Dutta et al. 2020] explained a technique for estimating the parameter for unbalanced and un-transposed distribution lines. This work addresses the state estimation problem in an unbalanced distribution system by exploiting virtual reference buses [Langner et al. 2020]. [Singh et al. 2009] recommended a Monte Carlo simulation-based probabilistic technique for placement of meters to reduce the relative errors of estimated voltage and angle of the buses in the network. To identify the best location for meter placement, a site with a significant 2- error ellipse area is considered. An ordinal optimization has been proposed, which gives precise calculations of the possibilities associated with it by decreasing the highness of the search space. As the valuation of the exact objective function is computationally exclusive, they conducted a primary quest to evaluate the approximate objective function; from this, the best results are chosen for the exact objective function [Singh et al. 2011]. The authors in [Nusrat et al. 2012] suggest a stochastic approach for finding the best feasible meter location for state estimation of the distribution network. This method compares the estimation quality with and without placing the meter to check whether a particular site suits the meter location. In [Muscas et al. 2008], the authors proposed a Dynamic programming-based optimization technique for optimal selection and placement of measurement devices. As the uncertainty in the available information risks the operating conditions of the network, they suggested the Monte Carlo method to consider uncertainties in the load demand, network parameters, and measuring devices. Reference [Liu et al. 2014] suggested a Gaussian component combination approach to integrate non-monitored DG generation and estimate the optimal meter placement for the distribution state estimation. The non-monitored DG generation is characterized by non-Gaussian probability density distribution and estimated by the Gaussian Mixture Model. In [Xygkis et al. 2016], the authors used the Fisher Information

matrix method to estimate the unknown states of the system from the available measurement unit data for the best meter placement.

The above literature has contributed valued research work which deals with state estimation of distribution network. The concept of zero injection measurements, in addition to the PMUs, is considered widely for PMU placement problem constraint formulation for the analysis of network observability. Though the zero injections minimize the required number of PMUs, however, the limitations associated with the zero injection Bus (ZIB-neither generation nor load) concept for PMU placement in ADN have not been well addressed. As the distribution networks are heavily loaded, and the loads are highly unpredictable, and also with the gradual evolvement of DG into it, none of the nodes/buses can be ignored for accurate estimation of the states of DN in terms of monitoring, study, and enhance the network's operating condition.

This work aims to propose a methodology for estimating the voltage magnitude of the radial distribution network using PMU technology. An integer linear programming (ILP) algorithm is adopted to define the optimal number and location of PMUs. In addition to the proposed voltage estimation technique, an algorithm is developed to validate the ILP functioning in radial test feeders for complete observability of the system with a minimum number of PMUs. The workflow of this chapter is explained in the following sections as follows. The PMU placement in the distribution network and its validation is discussed in Section 3.2 and 3.3. The proposed voltage profile estimation technique for an active distribution system is explained in section 3.4. In section 3.5 Simulation results of case studies are presented and conclusion is given in section 3.6.

3.2 Observability analysis under normal conditions

In general, the placement of PMUs is primarily based on the topological observability of the power system, which refers to the ability to estimate the state variables (voltage phasors) at all nodes of the system using available measurements. The placement algorithm aims to ensure that there is sufficient redundancy and coverage of measurements to achieve observability. Whether a power system is balanced or unbalanced does not significantly affect the basic principles of PMU placement algorithms. These algorithms primarily focus on achieving topological observability rather than balancing conditions. The algorithms consider factors such as the network structure, system topology, available measurements, and the desired observability requirements to determine the optimal placement locations for PMUs.

This work uses a topological method to authenticate the observability of the entire power distribution network [Almunif et al. 2020]. It is acceptable, if the bus type and topology of the network are identified to site the placing PMUs optimally. The incidence matrix represents the bus interconnection of the network. The matrix E exemplifies the correlation in the buses by lines/branches of the system. If E and L constitute the connectivity matrix and total nodes of the network, E_p is a L x L matrix, and the elements ($[e]_{pq}$) of the matrix are explained in equation (3.1) [Chauhan et al. 2019].

$$[e]_{pq} = \begin{cases} 1, & if \ p=q \\ 1, & if \ buses \ p \ and \ q \ are \ linked \\ 0, & else \end{cases} \tag{3.1}$$

The interrelation setting of the PMUs at the p_{th} placement bus is explicated by equation (3.2).

$$y_p = \begin{cases} 1, & if \ a \ PMU \ is \ situated \ at \ p_{th} \ bus \\ 0, & else \end{cases} \tag{3.2}$$

The objective function of this scenario to achieve complete system observability by optimal placement of PMUs is explained by equation (3.3) [Babu et al., 2018].

$$\min \sum_{p=1}^{L} y_p, \quad p = 1, 2, 3........, L \tag{3.3}$$

An 11-bus radial distribution feeder is considered to elucidate the observability of the whole system and is demonstrated in Figure 3.1.
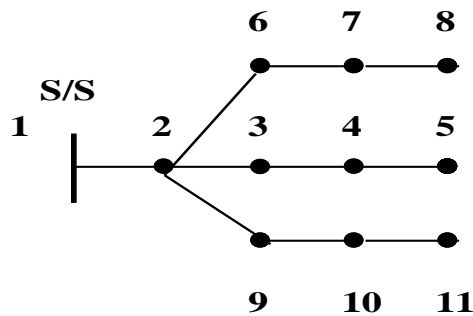
Figure 3.1: 11-Bus Radial Test Feeder Topology

The incidence matrix associated to Figure 3.1 is indicated in equation (3.4).

$$E = \begin{bmatrix} 1 & 1 & 0 & 0 & 0 & 0 & 0 & 0 & 0 & 0 & 0 \\ 1 & 1 & 1 & 0 & 0 & 1 & 0 & 0 & 1 & 0 & 0 \\ 0 & 1 & 1 & 1 & 0 & 0 & 0 & 0 & 0 & 0 & 0 \\ 0 & 0 & 1 & 1 & 1 & 0 & 0 & 0 & 0 & 0 & 0 \\ 0 & 0 & 0 & 1 & 1 & 0 & 0 & 0 & 0 & 0 & 0 \\ 0 & 1 & 0 & 0 & 0 & 1 & 1 & 0 & 0 & 0 & 0 \\ 0 & 0 & 0 & 0 & 0 & 1 & 1 & 1 & 0 & 0 & 0 \\ 0 & 0 & 0 & 0 & 0 & 0 & 1 & 1 & 0 & 0 & 0 \\ 0 & 1 & 0 & 0 & 0 & 0 & 0 & 0 & 1 & 1 & 0 \\ 0 & 0 & 0 & 0 & 0 & 0 & 0 & 0 & 1 & 1 & 1 \\ 0 & 0 & 0 & 0 & 0 & 0 & 0 & 0 & 0 & 1 & 1 \end{bmatrix} \tag{3.4}$$

- **Problem constraints of the system**

By presuming, the nodes/buses at which PMUs are situated are assigned with adequate input data to compute the voltage and current phasors of the network. A node in the network is observable; at the minimum, one measuring unit is situated at the advised site or at any of its adjacent nodes. Hence, the p_{th} node observability is described by equation (3.5) [Koochi et al. 2020].

$$h_p = \sum_{q=1}^{L} e_{pq} y_q \geq 1, \quad p = 1, 2, 3 \ldots \ldots, L \tag{3.5}$$

The restructured form of equation (3.5) in matrix form is given below:

$$H = EY \geq s \tag{3.6}$$

$$\text{where, } Y = \left[y_{1,} \ y_{2,} \ y_{3,} \ \ldots \ldots, \ y_L \right]^T_{L \times 1} \tag{3.7}$$

$$s = [1, 1, \ldots \ldots, 1]^T_{L \times 1} \tag{3.8}$$

$$H = \left[h_{1,} \ h_{2,} \ \ldots \ldots, \ h_L \right]^T_{L \times 1} \tag{3.9}$$

The requisite constraints to assure the full observability of the 11-bus feeder from Figure 3.1, are given by equation (3.10).

$$\begin{cases} h1 = y1 + y2 \geq 1 \\ h2 = y1 + y2 + y3 + y6 + y9 \geq 1 \\ h3 = y2 + y3 + y4 \geq 1 \\ h4 = y3 + y4 + y5 \geq 1 \\ h5 = y4 + y5 \geq 1 \\ h6 = y2 + y6 + y7 \geq 1 \\ h7 = y6 + y7 + y8 \geq 1 \\ h8 = y7 + y8 \geq 1 \\ h9 = y2 + y9 + y10 \geq 1 \\ h10 = y9 + y10 + y11 \geq 1 \\ h11 = y10 + y11 \geq 1 \end{cases} \tag{3.10}$$

From the above expression, a plus ("+") sign represents arithmetical summation, and one ("1") signifies that at least one variable in the summation is expected to be non-zero. For instance, the inequality constraint from the expression (3.7) specifies that at the least one measuring unit intended to be placed at the first or second node (or the two of) for bus one to have complete observability. The solution for optimal PMU placement of figure 3.1, using ILP is $Y = \begin{bmatrix} 1 & 0 & 0 & 1 & 0 & 0 & 1 & 0 & 0 & 1 & 0 \end{bmatrix}^T$, ensures the entire system observable by employing PMUs at buses 1, 4, 7, and 10. The algorithm below encapsulates the steps for the optimum PMU location.

- **Algorithm for optimum PMU location**

---

1. Initialize the variables
2. Enter the details of load data and total number of buses of the designated network
3. Build the incidence matrix (E)
4. Input the constraints to set bounds for lower and upper limits
4. Execute the *intlinprog* function to acquire the optimal PMUs number and corresponding locations
6. Present the PMU number and positions
7. end

3.3 Validation of optimal placement problem (OPP)

Validation was done for the results obtained by creating an algorithm using MATLAB code that checks whether all the buses are connected to the PMUs, which is the whole purpose of an optimal placement solution. All the PMU buses and the remaining buses are sorted into two different arrays and checking all the buses connected to PMU buses through branch array and collecting them in Val array (Val array is initiated as a null array and filled with the bus numbers that are connected to the PMU buses). The system is fully observable if all the remaining bus numbers are there in the Val array; if not, the system is not fully observable, and the PMU optimal locations which are identified would be wrong. Step by detailed step methodology of the validation process of optimal placement is explained in below algorithm.

- **Algorithm for validation of optimal placement problem**

---

1) Input the number of buses (n), branches (b), PMU bus locations (p), remaining buses (r)
2) Initialize $i = 1, r = 1, j = 1$

3) if PMU*[i] = 1* then

   PMUbus *[j] = i*

   j = j+1

   i = i +1

4) else rembus*[r] = i*

   r = r + 1

   i = i + 1

   end

5) if   *i < = n* then

   go to step 2

6) else initialize *i = 1, a=1*

7) initialize *j = 1*

8) Check for each PMU bus element in the branch array's first column and then second column PMUbus [*i*] = branch [*j,2*] and PMUbus [*i*] = branch [*j*]

9) If PMU bus elements are found in branch array, include the other elements in the row into val array, val[*a*] = branch [*j,1*]and val[*a*] = branch [*j,2*]

10) end

11) end

12) Initialize *i = 1, c=1*

13) initialize *j = 1*

14) if rembus[*i*] = val [*j*] then

15) check[*c*] = rembus [*i*]

   c= c+1

   j = j+1

16) else go to step 24

17) if *j < = r* then

18) go to step 21

19) else *i = i + 1*

20) end

21) end

22) if *i < = r* then

22) go to *step 20*

23) else if check = rembus then

24) Given system is fully Observable

25) else Given system is not fully Observable

26) end

27) end

3.4 Methodology of PMU measurement setup for voltage profile estimation

A generalized code for N number of buses is developed to give the PMU nodes' voltages and the currents in the branches connected to PMUs. End_bus array consists of all the bus numbers of the ones at the end of every lateral chain (chains of buses which are not the main chain, but are connected to it) and buses' main chain (chain of buses from the source). Firstly, voltage is assumed at every bus as 1 p.u. (Per Unit). The currents are calculated in branches of end buses using the end_bus array and using Kirchhoff's current law for the remaining ones. Then proceeded to find voltages at the buses by going backward, from the end buses to the first bus by using branch currents from before, in Kirchhoff's voltage law and then finding the branch currents again by using the bus voltages from before and the loop goes on. The voltage magnitudes from this set and the next set, and if the difference is extremely low (<0.0001), this set would be the desired result, and the loop will be stopped. The voltage magnitudes and currents at PMUs are found by checking the branch array with all the bus connections and finding the magnitudes of voltages and currents for the same in the voltage magnitude array and branch currents array, respectively. The methodology of the PMU measurement setup process is explained in the following algorithm.

- **Algorithm for PMU measurement setup**

1) Start

2) Get the PMU locations and branch array.

3) Get the active, reactive *(Pa, Qa)* powers at each bus and branch impedances *(Z)*.

4) Initialize voltage at every bus as *V(j,1) = 1 p.u.*

5) Create Endbus array consisting of all the end located buses Endbus = zeros(*j,1*).

6) Calculate branch currents using the branch impedance for end branches and then
    for remaining ones *i(j,1)=conj(abs(apparent power)/abs(v(j,1)))*.

7) Calculate new bus voltages using the branch currents *Vnew=V(j,1)*.

8) Find the branch currents again using the new bus voltages *inew=[i]*

9) Find the branch currents again using the new bus voltages

10) Continue the loop until the difference between the voltage sets is very low(<tolerance)

11) Currents and voltages at PMUs are found by checking for the connections in the branch

12) Check for the corresponding values in bus voltage and branch current array
   V(pmubus(k)), ii(pmubus(k)-1).

13) Display the bus voltage and branch current arrays

14) Stop

3.5 Results and discussion

The results of optimal PMU placement and their validation, voltage profile estimation with and without DG using PMUs are explained in this section.

3.5.1 Optimal PMU locations

The simulation is done using an ILP technique for complete observability of the distribution test feeders with minimal number of PMUs. MATLAB programming is used to perform the case studies on IEEE 33-bus, 69-bus, and modified 119-bus network, respectively. The whole observability of these test feeders with the requisite PMU numbers and their locations are shown in Table 3.1.

Table 3.1: Optimal PMU nodes for IEEE radial bus systems

IEEE Test System	No. of PMUs	PMU located buses	CPU time (sec)
33 bus	11	2,5,8,11,14,17, 21,24,27,30,33	0.389279
69 bus	24	2,6,9,14,17,20,23,26,29,32,35, 37,40,43,46,47,50,52,55,58,61, 64,66,68	0.407024
119 bus	42	3,5,8,11,14,17,20,23,26,29,32, 34,37,39,42,45,48,51,54,56,59, 62,63,67,70,73,76,78,81,84,87, 90,91,94,98,101,104,107,110, 113,115,118	0.435688

From Table 3.1, it is noticed that for the network to be fully observable, there is no necessity of locating PMUs at all the buses in the system. Henceforth, as the least number of PMUs are needed, it is economical, adequate, and effective in obtaining optimal placement and system observability. In this work an ILP technique based on integer feasibility (IF) is considered to determine whether an optimal solution has been achieved or not. In the IF based ILP approach, the decision variables are usually restricted to integer values, if all variables are determined to have integer values, it is typically a strong indication that an optimal solution has been reached and suggests that the solution aligns with the desired optimization goals. However, if any variables have fractional values, it suggests that

the solution is not yet optimal and further iterations are required. As the solution sets from the test results are presented in the Table 3.1 exclusively contains integer values, it is indicative that the obtained solutions are optimal.

3.5.2 Validation results of PMU locations

The Validation results of PMU Locations of 33, 69 and 119 radial test systems are presented in Table 3.2. As both the check and rem_bus arrays are the same in all test systems, given systems are completely observable.

Table 3.2: Validation results of PMU locations in radial distribution test systems

IEEE Test system	Pmu_bus	Rem_bus	Val_array	Check_array
33 bus	[2,5,8,11,14,17, 21,24,27,30,33]	[1,3,4,6,7,9,10,1 2,13,15,16,18,1 9,20,22,23,25,2 6,28,29,31,32]	[3,6,9,12,15,18,19,22,2 5,28,31,1,4,7,10,13,16, 20,23,26,29,32]	[1,3,4,6,7,9,10,12,13, 15,16,18,19,20,22,23, 25,26,28,29,31,32]
69 bus	[2,6,9,14,17,20, 23,26,29,32,35, 37,40,43,46,47, 50,52,55,58,61, 64,66,68]	[1,3,4,5,7,8,10,1 1,12,13,15,16,1 8,19,21,22,24,2 5,27,28,30,31,3 3,34,36,38,39,4 1,42,44,45,48,4 9,51,53,54,56,5 7,59,60,62,63,6 5,67,69]	[3,7,10,15,18,21,24,27, 30,33,38,41,44,48,53,5 6,59,62,65,67,69,1,5,8, 13,16,19,22,25,28,31,3 4,36,39,42,45,4,49,51,5 4,57,60,63,11,12]	[1,3,4,5,7,8,10,11,12, 13,15,16,18,19,21,22, 24,25,27,28,30,31,33, 34,36,38,39,41,42,44, 45,48,49,51,53,54,56, 57,59,60,62,63,65,67, 69]
119 bus	[3,5,8,11,14,17, 20,23,26,29,32, 34,37,39,42,45, 48,51,54,56,59, 62,63,67,70,73, 76,78,81,84,87, 90,91,94,98,101 ,104,107,110,11 3,115,118]	[1,2,4,6,7,9,10,1 2,13,15,16,18,1 9,21,22,24,25,2 7,28,30,31,33,3 5,36,38,40,41,4 3,44,46,47,49,5 0,52,53,55,57,5 8,60,61,64,65,6 6,68,69,71,72,7 4,75,77,79,80,8 2,83,85,86,88,8 9,92,93,95,96,9 7,100,102,103,1 05,106,108,109, 111,112,114,11 6,117]	[6,9,12,15,18,21,24,27, 30,35,40,43,46,49,52,5 7,60,64,68,71,74,77,79, 82,85,88,91,92,95,96,9 9,102,105,108,111,112, 116,2,4,7,10,13,16,19,2 2,25,28,31,33,36,38,41, 44,47,50,53,55,58,61,1, 66,69,72,75,65,80,83,8 6,89,90,93,97,100,103, 106,109,112,114,117]	[1,2,4,6,7,9,10,12,13, 15,16,18,19,21,22,24, 25,27,28,30,31,33,35, 36,38,40,41,43,44,46, 47,49,50,52,53,55,57, 58,60,61,64,65,66,68, 69,71,72,74,75,77,79, 80,82,83,85,86,88,89, 92,93,95,96,97,99,10 0,102,103,105,106,10 8,109,111,112,114,11 6,117]

3.5.3 PMU measurement setup results of voltage profile estimation

The PMUs are installed in the distribution network test systems based on the results obtained from the optimal PMU locations, as discussed in section 3.2. It is observed that the results obtained from PMU measurements are close to forward backward sweep method (FBS) results. The rated line voltage for all test systems is considered 12.66 kV and Base MVA =100. The detailed system data for 33 bus and 69 bus are reported in [Mishra et al. 2014], 119 bus data is reported in [Ghasemi et al. 2018] and given in appendix.

- **33 bus system PMU readings with and without DG and shunt capacitor (SC)**

The 33-bus radial distribution network is shown in Figure 3.2. The total load of this system is 4369 kVA with PF = 0.85. The network has four DGs placed at buses 14, 17, 21, and 32 with a total DG capacity of 371.5 kW and 230 kVAR and two SCs are placed at buses 24 and 30 with a rating of 600 kVAR and 750 kVAR, respectively.
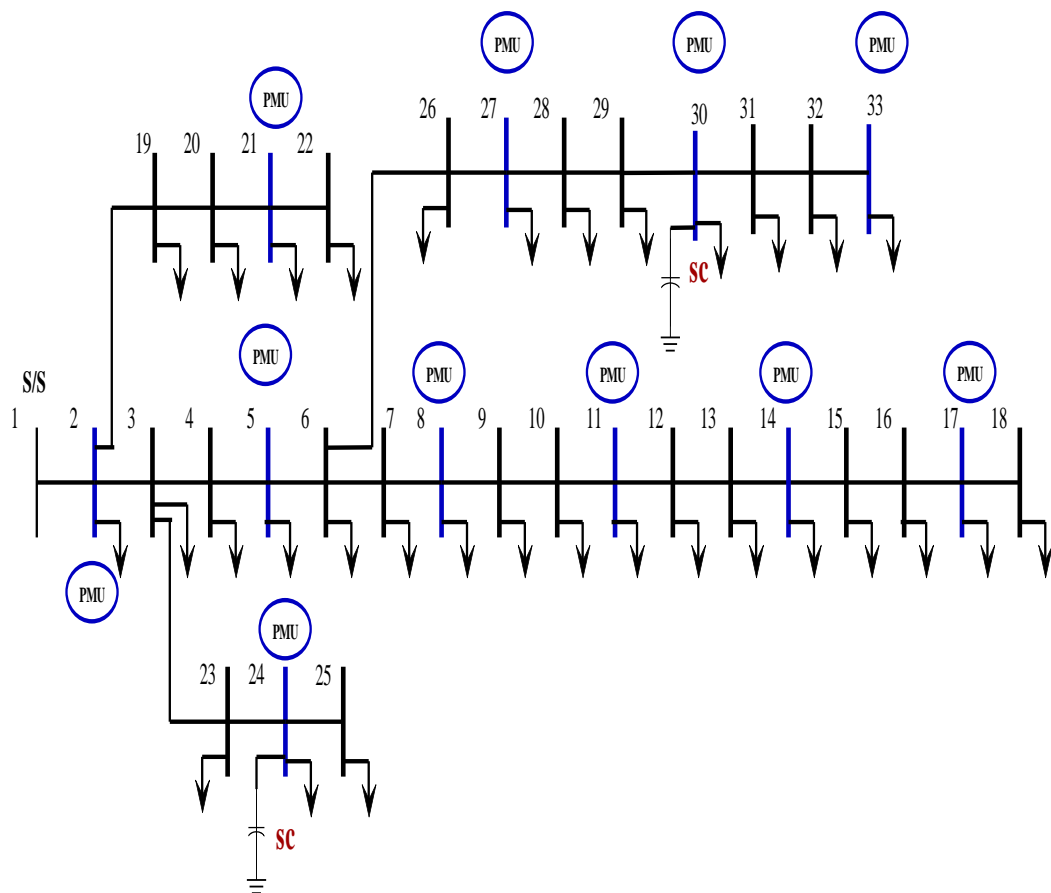
Figure 3.2: 33 bus system with PMUs, DG, and SC

Table 3.3 gives the comparative voltage magnitude results of 33 bus radial distribution network using PMU setup and FBS load flow algorithm. It is observed that the PMU set up results match with the FBS load flow algorithm.

65

Table 3.3: Comparison of 33 bus radial system voltage magnitude results of PMU measurement setup with FBS algorithm

Bus Location	Voltage Magnitude (p.u.) using PMU setup			Voltage Magnitude (p.u.) using FBS algorithm		
	Without DG and SC	With DG	With DG and SC	Without DG and SC	With DG	With DG and SC
2	0.9979	0.9981	0.9983	0.9978	0.9980	0.9982
5	0.9741	0.9764	0.9799	0.9742	0.9763	0.9797
8	0.9476	0.9527	0.9583	0.9475	0.9526	0.9580
11	0.9371	0.9440	0.9497	0.9370	0.9438	0.9496
14	0.9295	0.9384	0.9440	0.9296	0.9382	0.9440
17	0.9261	0.9351	0.9408	0.9260	0.9350	0.9406
21	0.9942	0.9954	0.9957	0.9940	0.9952	0.9956
24	0.9799	0.9809	0.9814	0.9798	0.9808	0.9816
27	0.9553	0.9592	0.9660	0.9553	0.9592	0.9658
30	0.9363	0.9419	0.9547	0.9360	0.9415	0.9545
33	0.9326	0.9391	0.9519	0.9325	0.9390	0.9518

Figure 3.3 displays the voltage profile of the 33-bus radial distribution system using PMU data. With the DG installation, the voltages at all nodes are improved to an extent.
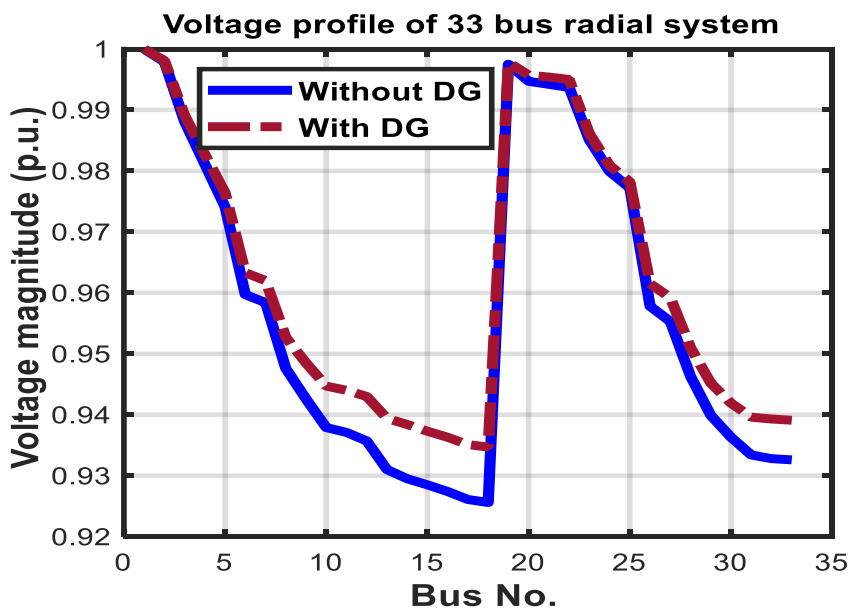
Figure 3.3: 33 bus radial System's voltage profile with and without DG using PMU data

The voltage estimation analysis is done further by installing SCs along with the DGs in the network. Figures 3.4, 3.7, and 3.10 show a remarkable enhancement in the voltage profile with the SCs installation and DGs in ADN, and the losses are reduced by a significant amount, which improved the overall voltage profile of the network.
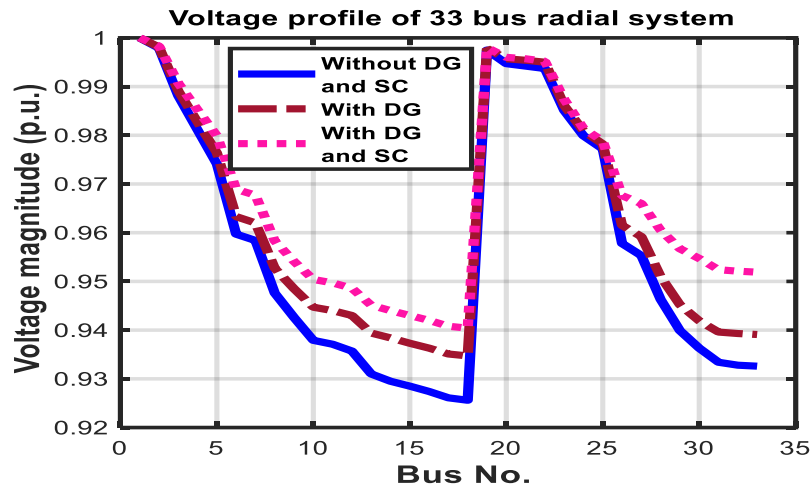
Figure 3.4: 33 bus radial System's voltage profile with and without DG and SC using PMU data

- **69 bus system PMU readings with and without DG and SC**

The 69-bus radial distribution system is shown in Figure 3.5. The total load of this system is 2223 kVA with PF = 0.89. The network has five DGs placed at buses 49, 50, 61, 64, and 69 with a total DG capacity of 400 kW and 230 kVAR, and three SCs are placed at buses 12, 21, and 61 with a rating of 300 kVAR, 150 kVAR, and 450 kVAR, respectively.
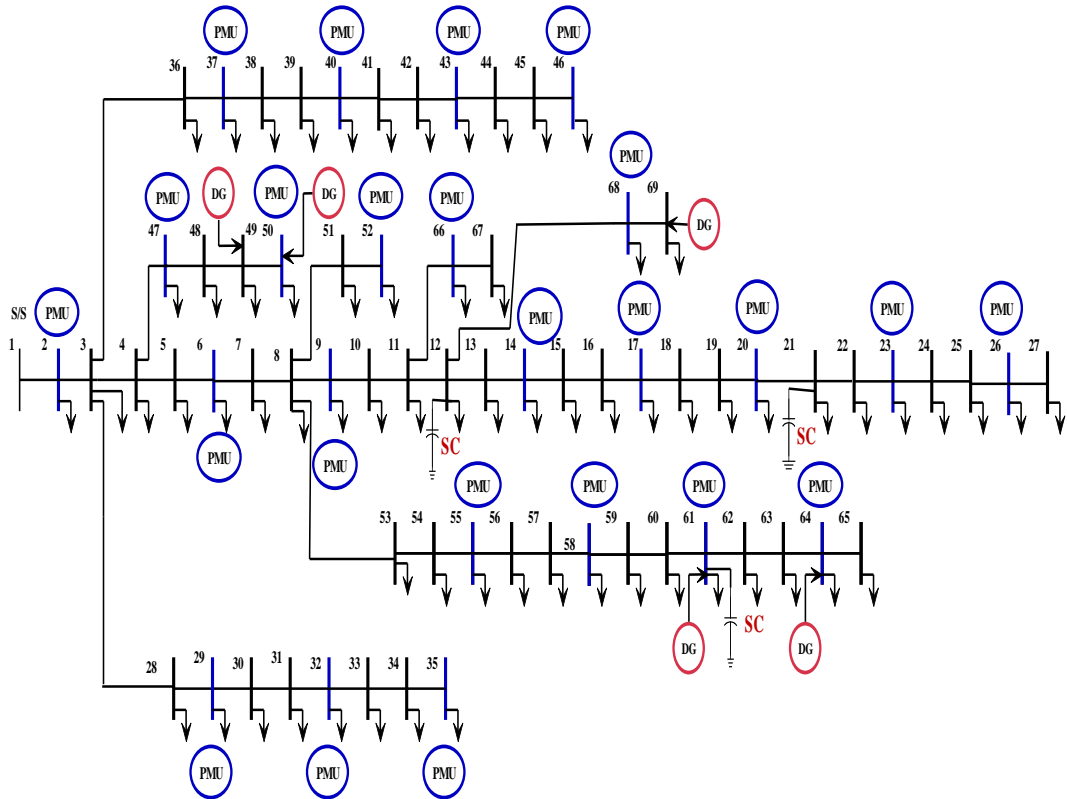
Figure 3.5: 69 bus system with PMUs, DG, and SC

Table 3.4 gives the comparative voltage magnitude results of 69 bus radial distribution network using PMU setup and FBS load flow algorithm. It is observed that the PMU set up results are similar to the FBS load flow algorithm.

Table 3.4: Comparison of 69 bus radial system voltage magnitude results of PMU measurement setup with FBS Algorithm

Bus Location	Voltage Magnitude (p.u.) using PMU setup			Voltage Magnitude (p.u.) using FBS Algorithm		
	Without DG and SC	With DG	With DG and SC	Without DG and SC	With DG	With DG and SC
2	1	1	1	1	1	1
6	0.9913	0.9918	0.9922	0.9912	0.9917	0.9920
9	0.9799	0.9810	0.9820	0.9798	0.9808	0.9818
14	0.9632	0.9640	0.9645	0.9634	0.9638	0.9644
17	0.9579	0.9588	0.9593	0.9578	0.9589	0.9591
20	0.9568	0.9576	0.9582	0.9565	0.9575	0.9580
23	0.9559	0.9568	0.9573	0.9557	0.9566	0.9572
26	0.9546	0.9555	0.9560	0.9547	0.9553	0.9561
29	0.9999	0.9999	0.9999	0.9998	0.9998	0.9997
32	0.9997	0.9997	0.9997	0.9997	0.9997	0.9997
35	0.9992	0.9992	0.9992	0.9990	0.9990	0.9990
37	0.9999	0.9999	0.9999	0.9997	0.9997	0.9997
40	0.9997	0.9997	0.9998	0.9995	0.9995	0.9997
43	0.9991	0.9991	0.9991	0.9990	0.9990	0.9990
46	0.9990	0.9990	0.9990	0.9989	0.9989	0.9989
47	0.9999	0.9999	0.9999	0.9998	0.9998	0.9999
50	0.9974	0.9979	0.9980	0.9972	0.9975	0.9979
52	0.9809	0.9819	0.9829	0.9805	0.9820	0.9827
55	0.9706	0.9725	0.9745	0.9706	0.9725	0.9743
58	0.9341	0.9393	0.9453	0.9340	0.9395	0.9451
61	0.9184	0.9252	0.9329	0.9185	0.9255	0.9327
64	0.9162	0.9235	0.9312	0.9160	0.9233	0.9311
66	0.9736	0.9745	0.9751	0.9735	0.9742	0.9750
68	0.9699	0.9706	0.9710	0.9695	0.9702	0.9709

Figure 3.6 displays the PMU data voltage profile of the 69-bus radial distribution system with and without DG. With the DG integration into the network, all the node voltages are boosted to a higher value.
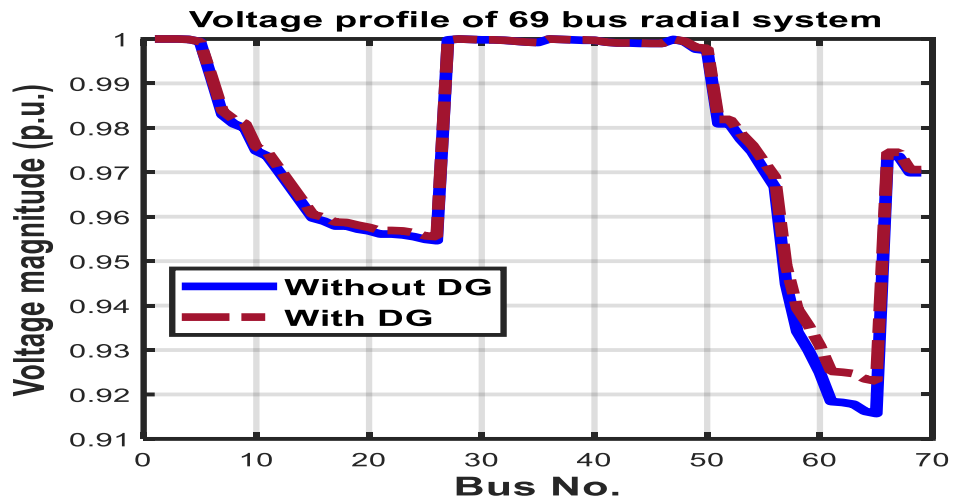
Figure 3.6: 69 bus radial system's voltage profile with and without DG
using PMU data
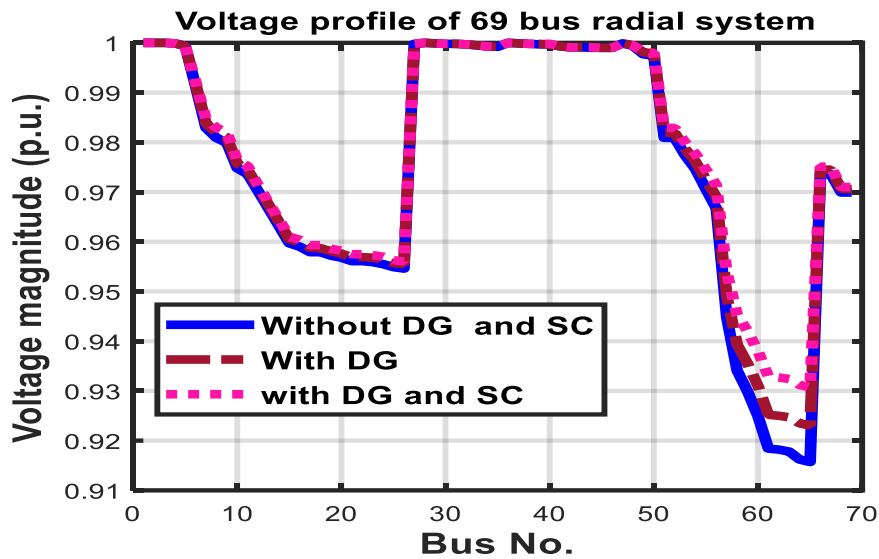
Figure 3.7: 69 bus radial system's voltage profile with and without DG and SC using PMU data

- **119 bus system PMU readings with and without DG and SC**

The 119-bus radial distribution network is shown in Figure 3.8. The total load of this system is 28,392 kVA with PF = 0.79. The network has six DGs placed at buses 20, 28, 42, 50, 74, and 111, with a total DG capacity of 3406 kW and 2556 kVAR, and six SCs are placed at buses 32, 36, 54, 63, 80, and 102 with a rating of 450 kVAR, 450 kVAR, 600 kVAR, 450 kVAR, 450 kVAR, and 300 kVAR respectively.

69
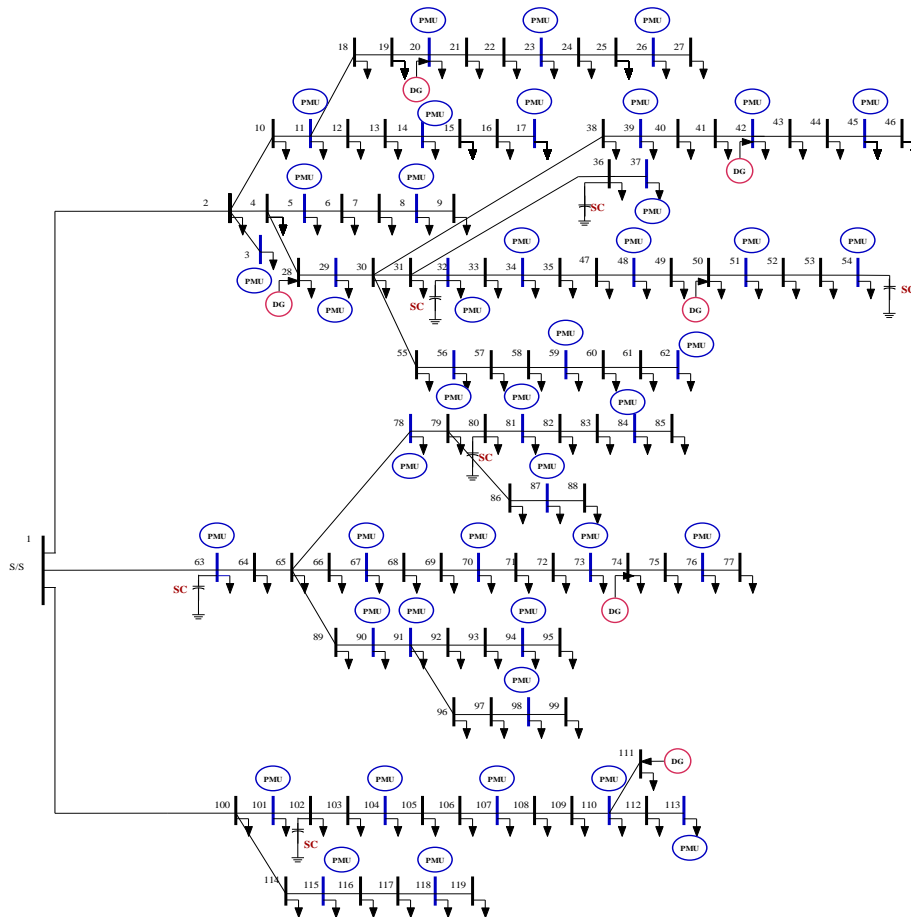
Figure 3.8: 119 Bus System with PMUs, DG, and SC

Figure 3.9 shows the 119-bus radial distribution system's voltage profile measured from PMU data with and without DG. With the incorporation of DG, all node voltages are improved to an extent. Table 3.5 compares the voltage magnitude results of the 119-bus radial distribution network using PMU setup and FBS load flow algorithm. It is witnessed that the PMU setup results are almost identical with the FBS load flow algorithm.
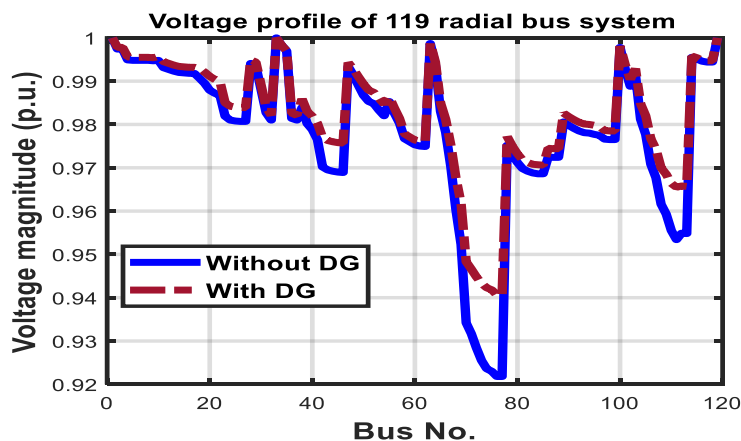
Figure 3.9: 119 bus radial system's voltage profile with and without DG using PMU data
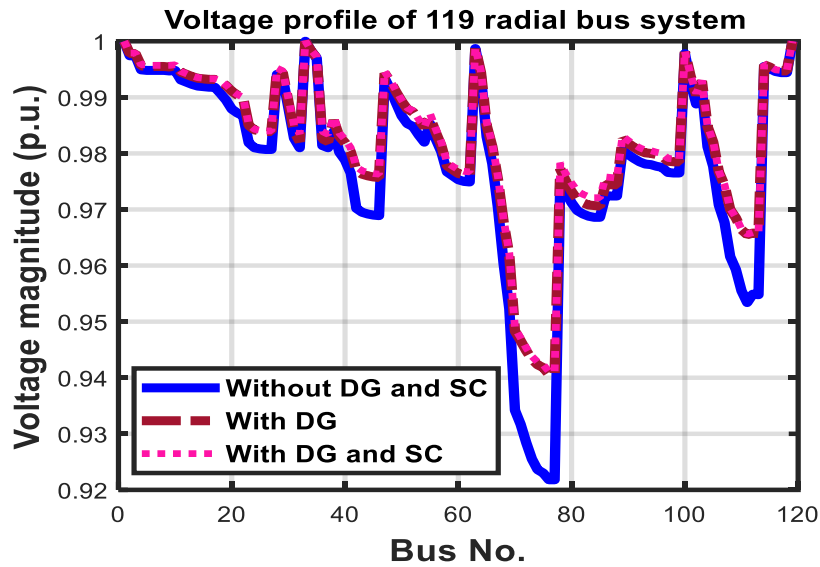
Figure 3.10: 119 bus radial system's voltage profile with and without DG and SC using PMU data

Table 3.5: Comparison of 119 bus radial system voltage magnitude results of PMU measurement setup with FBS algorithm

Bus Location	Voltage magnitude (p.u.) using PMU setup			Voltage magnitude (p.u.) using FBS Algorithm		
	Without DG and SC	With DG	With DG and SC	Without DG and SC	With DG	With DG and SC
3	0.9974	0.9978	0.9979	0.9972	0.9975	0.9978
5	0.9948	0.9955	0.9958	0.9945	0.9954	0.9957
8	0.9948	0.9955	0.9957	0.9947	0.9953	0.9956
11	0.9931	0.9945	0.9946	0.9930	0.9945	0.9945
14	0.9920	0.9934	0.9935	0.9918	0.9932	0.9933
17	0.9918	0.9932	0.9933	0.9916	0.9932	0.9933
20	0.9879	0.9911	0.9912	0.9875	0.9906	0.9910
23	0.9819	0.9850	0.9851	0.9817	0.9848	0.9850
26	0.9807	0.9839	0.9840	0.9805	0.9837	0.9838
29	0.9935	0.9944	0.9947	0.9932	0.9942	0.9944
32	0.9810	0.9821	0.9835	0.9809	0.9822	0.9833
34	0.9983	0.9983	0.9984	0.9984	0.9984	0.9984
37	0.9810	0.9821	0.9834	0.9808	0.9819	0.9832
39	0.9802	0.9830	0.9836	0.9800	0.9828	0.9834
42	0.9702	0.9770	0.9776	0.9703	0.9771	0.9774
45	0.9690	0.9758	0.9764	0.9692	0.9756	0.9763
48	0.9914	0.9928	0.9930	0.9912	0.9925	0.9928
51	0.9853	0.9879	0.9881	0.9855	0.9880	0.9880
54	0.9820	0.9847	0.9847	0.9817	0.9845	0.9846
56	0.9826	0.9838	0.9844	0.9825	0.9836	0.9840
59	0.9760	0.9771	0.9777	0.9762	0.9770	0.9775
62	0.9749	0.9761	0.9767	0.9747	0.9760	0.9765

63	0.9987	0.9988	0.9989	0.9985	0.9987	0.9988
67	0.9703	0.9753	0.9758	0.9700	0.9752	0.9755
70	0.9342	0.9483	0.9488	0.9340	0.9482	0.9485
73	0.9255	0.9433	0.9438	0.9253	0.9430	0.9435
76	0.9218	0.9406	0.9411	0.9219	0.9407	0.9409
78	0.9752	0.9772	0.9783	0.9751	0.9770	0.9781
81	0.9698	0.9718	0.9733	0.9696	0.9715	0.9730
84	0.9686	0.9707	0.9721	0.9684	0.9704	0.9720
87	0.9724	0.9744	0.9757	0.9722	0.9743	0.9755
90	0.9798	0.9818	0.9823	0.9796	0.9817	0.9822
91	0.9791	0.9811	0.9816	0.9789	0.9809	0.9814
94	0.9780	0.9800	0.9805	0.9775	0.9797	0.9804
98	0.9765	0.9785	0.9790	0.9764	0.9786	0.9788
101	0.9928	0.9938	0.9940	0.9925	0.9935	0.9938
104	0.9812	0.9848	0.9849	0.9810	0.9845	0.9847
107	0.9677	0.9743	0.9744	0.9675	0.9742	0.9744
110	0.9555	0.9664	0.9665	0.9552	0.9666	0.9663
113	0.9548	0.9657	0.9658	0.9548	0.9655	0.9656
115	0.9951	0.9954	0.9955	0.9952	0.9957	0.9954
118	0.9944	0.9947	0.9948	09940	0.9945	0.9947

Table 3.6 gives the total loss reduction of active and reactive powers of 33, 69, and 119 bus radial networks with and without DG and SC integration. The table shows a reduction of 35.79 kW and 25.63 kVAR with DG and 78.28 kW and 54.26 kVAR with DG and SC in 33 bus system, similarly a reduction of 32.3 kW and 15.3 KVAR with DG and 63.89 kW and 29.15 kVAR with DG and SC in 69 bus system, and 238.48 kW and 150.89 kVAR with DG and 267.42 kW and 186.38 kVAR reduction in 119 bus system. The percentage of total power loss reduction is given in Table 3.7.

Table 3.6: Comparison of load flow results of various IEEE radial distribution networks using PMU data

	33 bus radial system			69 bus radial system			119 bus radial system		
	Without DG and SC	With DG	With DG and SC	Without DG and SC	With DG	With DG and SC	Without DG and SC	With DG	With DG and SC
Total P_{loss} (kW)	195.54	159.75	117.26	227.96	195.66	164.07	766.55	528.07	499.13
Total Q_{loss} (kVAR)	136.98	111.35	82.72	103.19	87.89	74.04	585.03	431.11	398.65
No. of Iteration count	4	4	4	4	4	4	4	4	4
Computation time (Sec)	0.1448	0.1838	0.2087	0.7329	0.8225	0.6453	0.2729	0.6508	0.2544

Table 3.7: Percentage reduction of power loss of radial distribution systems with DG integration using PMU data

Percentage reduction in active and reactive power losses after DG and SC integration						
Power loss reduction (%)	33 bus system		69 bus system		119 bus system	
	With DG	With DG and SC	With DG	With DG and SC	With DG	With DG and SC
Total P_{loss}	18.301	40.03	14.16	28.02	31.11	34.88
Total Q_{loss}	18.70	39.61	14.83	28.24	26.30	31.85

3.6 Conclusion

In this work, the proposed methodology is effective in the state estimation of any active radial distribution network. This technique gives real-time information of distribution networks with DG integration and allied problems in monitoring the system states, unlike the traditional distribution network planning method. PMU is a real-time monitoring equipment that evaluates the voltage phasor of the node installed on and the neighbouring line current phasors attached to it. This capability of PMU, in turn, makes all its direct neighbouring buses observable. Various distribution network test systems are analysed for a steady-state voltage estimation using the proposed PMU based online estimation technique. An integer Linear Programming approach has been discussed on standard radial distribution systems for optimal PMU allocation. The novelty in this work lies in utilizing the ILP technique to address the specific problem of PMU placement in radial distribution test feeders. Additionally, the work introduces an algorithm that validates the complete observability of the system, which further strengthens the reliability and accuracy of the obtained results. This algorithm contributes to the overall novelty of the work, as it ensures that the selected PMU locations provide comprehensive observability of the system, enhancing the effectiveness of the monitoring and control capabilities. While the ILP technique itself is not novel, its application to determine optimal PMU locations in radial distribution test feeders, along with the development of an algorithm for complete observability, represents a unique contribution to the field. Two methodologies are suggested in this work: to validate the complete observability of the distribution network with the optimal number of PMUs, and another one is to estimate the voltage profile of any radial distribution system. The performance of the suggested estimation methodology is validated

with the FBS load flow algorithm on distribution test systems with and without DG and SC interconnection, and it is observed that the results obtained from PMU based measurements are close to the former method results.

Chapter 4

MULTI-AGENT BASED COORDINATED VOLTAGE REGULATION TECHNIQUE IN AN UNBALANCED DISTRIBUTION NETWORK

4.1 Introduction

The continuous enlargement of the distribution network due to increasing load demand and substantial evolution of distributed generation (DG) is one of the critical research areas in the electrical engineering domain. DG penetration into distribution networks transforms them from passive to active systems, which could impact the entire power system's dynamics, particularly the distribution networks [Nasr-Azadani et al. 2014]. Power electronic voltage source inverters are frequently used to interface DG systems. Power quality will be a significant challenge in networks with increased power electronics interfacing with DGs and loads and increased nonlinear loads. Among the many power quality challenges, unbalanced voltage is one of the most serious [Nejabatkhah et al. 2015]. Voltage regulation becomes difficult when network voltages are unbalanced because the unbalanced voltage's negative-sequence component causes oscillations with a double fundamental frequency in both reactive and active power injections [Kabiri et al. 2015], moreover, an unbalanced network can support less photovoltaic (PV) generation before the critical voltage limit is reached [Weckx et al. 2015].

Based on strong and weak mutual Var compensation effects, a novel inter-phase coordinated consensus technique is proposed in this paper to overcome the voltage regulation challenges arising from imbalanced photovoltaic systems [Wang et al. 2020]. In coordination with the distribution system operator, an ideal hierarchical control technique is proposed for handling reactive power injection of electrical Vehicle chargers located geologically nearby. This system uses a linear quadratic regulator (LQR) that prevents voltage sag/swell [Mejia-Ruiz et al. 2021]. Voltage source converters (VSCs) are used as reactive power sources in the proposed controller. It coordinates with conventional controllers without substantially modifying the current distribution grid's control and operation architecture in [Ahmed et al., 2019]. The distributed voltage control scheme based on the time-graded control strategy is presented. In case of regulative need, the coordination scheme allows adjusting control devices of the photovoltaic plants to operate first and then

other devices according to the time synchronization schedule [Chamana et al. 2016]. In [Ranamuka et al. 2018], a novel controller parameter tuning method is proposed based on a virtual-time delay scheme to moderate the adverse effects of simultaneous and non-simultaneous operations of traditional voltage regulating devices and distributed generation units. Reference [Chamana et al. 2018], an innovative multi-phase zonal-based coordination method is proposed to control network voltages within limits and mitigate the overuse of regulating devices. The authors of [Bedawy et al. 2019], presented an integrated multi-agent system architecture where each voltage regulator is treated as an independent control agent that operates based on changes in the network topology to minimize voltage deviations. This research provides a hybrid online approach for optimum coordination of plug-in electric vehicles (PEVs) that performs voltage regulation and improves voltage imbalance with local auxiliary voltage assistance through dynamic PEV switching [Jabalameli et al. 2020]. An on-load tap changer's post-contingency slow-timescale curative activities are coordinated with solar inverters and battery energy storage system's fast-timescale curative activities using a multi-time scale optimization method in [Zafar et al. 2019]. The differential evolution optimization technique is used to elucidate the coordination between electric vehicles and distributed generations to improve the distribution system's performance [Islam et al. 2020]. A two-stage stochastic approach using the co-optimization method is presented to handle short and long-time period voltage issues in [Guo et al. 2021]. This paper provides a two-level coordination model for distributed generation and soft open point scheduling in unbalanced distribution networks, considering their regulating capacities in [Wang et al. 2019]. In this study, a multi-objective optimization model is used to coordinate between the operation of fast and slow voltage regulators [Zhang et al. 2018].

This chapter discusses the developed MAS (Multi-Agent System) based coordinated technique for the operation of DGs and SCs in an unbalanced distribution network. The MAS scheme provides a mechanism for operating the DGs and SCs optimally whenever voltage regulation is necessary. The existing DGs and switchable capacitors in the UDN are used to minimize the voltage deviation and unbalanced percentage; hence no external regulators are not needed, which reduces the cost incurring towards the use of auxiliary regulators. The usage of PMUs helps to monitor the electrical parameters (voltage/current) via a conjoint time basis for synchronization, which helps the MAS controller get its agent's data at specified timestamp events. The proposed technique is simulated on an IEEE 3-phase, 25 bus unbalanced radial distribution network and the specified results show that the proposed

method is capable of minimize voltage deviation, power loss, and voltage and current balance factors and improves the overall network's voltage profile.

4.2 Feeder modelling of 3-phase unbalanced distribution network

Inherently, distribution systems are unbalanced. To avoid catastrophic errors due to internal imbalances in the system, careful analysis of the distribution system with a detailed component model is required. Since the distribution network is made up of single, two and three phases non-converting phase line serving unbalanced loads, need to maintain mutual and self-impedance conditions of the line conductors and take into account the path of return conductor to earth for imbalanced current. Using modified Carson equations [Kryonidis et al. 2020], a 4x4 primitive impedance matrix can be written for a three-phase feeder with neutral, shown in Figure 4.1.
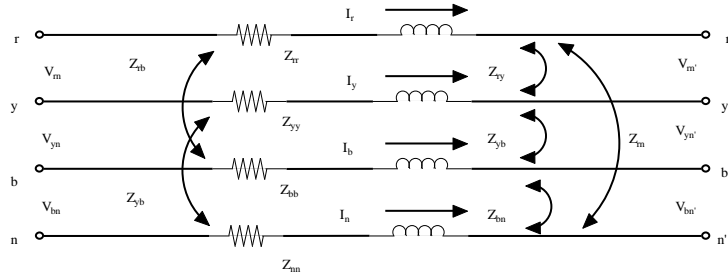
Figure 4.1: Three- Phase line section model

$$\text{Primitive impedance matrix} = [Z_{rybn}] = \begin{bmatrix} Z_{rr} & Z_{ry} & Z_{rb} & Z_{rn} \\ Z_{yr} & Z_{yy} & Z_{yr} & Z_{yn} \\ Z_{br} & Z_{by} & Z_{bb} & Z_{bn} \\ Z_{nr} & Z_{ny} & Z_{nb} & Z_{nn} \end{bmatrix} \tag{4.1}$$

Thus, the receiving end voltages are related to the sending end side of network depicted in Figure 4.1, as

$$\begin{bmatrix} V_r \\ V_y \\ V_b \\ V_n \end{bmatrix} = \begin{bmatrix} V_{r\prime} \\ V_{y\prime} \\ V_{b\prime} \\ V_{n\prime} \end{bmatrix} + \begin{bmatrix} Z_{rr} & Z_{ry} & Z_{rb} & Z_{rn} \\ Z_{yr} & Z_{yy} & Z_{yr} & Z_{yn} \\ Z_{br} & Z_{by} & Z_{bb} & Z_{bn} \\ Z_{nr} & Z_{ny} & Z_{nb} & Z_{nn} \end{bmatrix} * \begin{bmatrix} I_r \\ I_y \\ I_b \\ I_n \end{bmatrix} \tag{4.2}$$

Distance values between conductors, specific standard configuration and phase order is considered as per standard configurations. Because distribution circuits are multi-grounded (i.e. the neutral is firmly grounded at each convenient point), the voltage drop

$$V_n - V_{n\prime} = 0 \tag{4.3}$$

The basic 4 x 4 impedance matrix in (2.4) is bring down to a 3 x 3 matrix known as Phase impedance matrix. Each phase impedance component in the matrix form using the Kron's reduction method is given by

$$z_{ik} = Z_{ik} - (Z_{in} * Z_{nk})/Z_{nn} \tag{4.4}$$

Here, the grounding effect is considered using the modified matrix element z_{ij} instead of Z_{ij}. So the phase impedance matrix is given as

$$[Z_{ryb}] = \begin{bmatrix} Z_{rr-n} & Z_{ry-n} & Z_{rb-n} \\ Z_{yr-n} & Z_{yy-n} & Z_{yb-n} \\ Z_{br-n} & Z_{by-n} & Z_{bb-n} \end{bmatrix} \tag{4.5}$$

Now, the receiving end voltage relative to the sending end voltage of the feeder is displayed in Figure 4.1.

$$\begin{bmatrix} V_r \\ V_y \\ V_b \end{bmatrix} = \begin{bmatrix} V_{r\prime} \\ V_{y\prime} \\ V_{b\prime} \end{bmatrix} + \begin{bmatrix} Z_{rr-n} & Z_{ry-n} & Z_{rb-n} \\ Z_{yr-n} & Z_{yy-n} & Z_{yb-n} \\ Z_{br-n} & Z_{by-n} & Z_{bb-n} \end{bmatrix} \tag{4.6}$$

The relevant load current injection I_{Li} for bus i is calculated as a function of bus voltage V_i.

$$I_{ir} = \left(\frac{P_{ir} + jQ_{ir}}{V_{ir}} \right)^* \tag{4.7}$$

$$I_{iy} = \left(\frac{P_{iy} + jQ_{iy}}{V_{iy}} \right)^* \tag{4.8}$$

$$I_{ib} = \left(\frac{P_{ib} + jQ_{ib}}{V_{ib}} \right)^* \tag{4.9}$$

Power fed into the phase-r of line (Figure 4.1) at the sending end bus is $V_r.(I_r)^*$ and at the receiving end bus is $V_{r\prime}.(I_r)^*$. Therefore, real and reactive power losses for phase-r in the line may be written as:

$$SL_r = PL_r + jQL_r = V_r.(I_r)^* - V_{r\prime}.(I_r)^* \tag{4.10}$$

Similarly, for phase–y and phase-b

$$SL_y = PL_y + jQL_y = V_y.(I_y)^* - V_{y\prime}.(I_y)^* \tag{4.11}$$

$$SL_b = PL_b + jQL_b = V_r.(I_b)^* - V_{b\prime}.(I_b)^* \tag{4.12}$$

- **Integration of DG**

Consider a 3-phase radial distribution networks with N_B branches and a DG is to be placed at node i and β be a set of branches connected between the source and node i. It is known that, the DG supplies active power (P_{Gi}^{DG}) to the systems, but in case of reactive power (Q_{Gi}^{DG}) it is depend upon the source of DG, either it is supplies to the systems or consume from the systems. Due to this there will be a change in the active and reactive component of current of branch set β. The current of other branches are unaffected by the DG [Hung et al. 2010]. The total apparent power of phase r, at ith node:

$$SL_{ri} = \sum PL_{ri} + jQL_{ri} \qquad i = 1, \dots .. N_B \tag{4.13}$$

Similarly, for phase–y and phase-b

$$SL_{yi} = \sum PL_{yi} + jQL_{yi} \qquad i = 1, \dots .. N_B \tag{4.14}$$

$$SL_{bi} = \sum PL_{bi} + jQL_{bi} \qquad i = 1, \dots .. N_B \tag{4.15}$$

The current at ith node of phase r, y and b are:

$$IL_{ri} = IL_{ri}^{without\_DG} = \left(\frac{SL_{ri}}{V_{ri}}\right)^* \tag{4.16}$$

$$IL_{yi} = IL_{yi}^{without\_DG} = \left(\frac{SL_{yi}}{V_{yi}}\right)^* \tag{4.17}$$

$$IL_{bi} = IL_{bi}^{without\_DG} = \left(\frac{SL_{bi}}{V_{bi}}\right)^* \tag{4.18}$$

With the incorporation of DG model, the active and reactive power demand of a 3-phase feeder at i^{th} node at which a DG unit is placed is modified by:

$$PL_{ri}^{with\_DG} = PL_{ri}^{without\_DG} - PG_{ri}^{DG} \; ; \; QL_{ri}^{with\_DG} = QL_{ri}^{without\_DG} \mp QG_{ri}^{DG} \tag{4.19}$$

$$PL_{yi}^{with\_DG} = PL_{yi}^{without\_DG} - PG_{yi}^{DG} \; ; \; QL_{yi}^{with\_DG} = QL_{yi}^{without\_DG} \mp QG_{yi}^{DG} \tag{4.20}$$

$$PL_{bi}^{with\_DG} = PL_{bi}^{without\_DG} - PG_{bi}^{DG} \; ; \; QL_{bi}^{with\_DG} = QL_{bi}^{without\_DG} \mp QG_{bi}^{DG} \tag{4.21}$$

The DG power at ith node of a 3- phase feeder:

$$S_{ri}^{DG} = \sum P_{Gri}^{DG} \pm j \, Q_{Gri}^{DG} \qquad i = 1, \dots \dots N_B \tag{4.22}$$

$$S_{yi}^{DG} = \sum P_{Gyi}^{DG} \pm j\, Q_{Gyi}^{DG} \qquad i = 1, \ldots\ldots N_B \qquad (4.23)$$

$$S_{bi}^{DG} = \sum P_{Gbi}^{DG} \pm j\, Q_{Gbi}^{DG} \qquad i = 1, \ldots\ldots N_B \qquad (4.24)$$

The total apparent power and load current with DG integration at i[th] node of a 3-phase feeder:

$$S_{ri} = SL_{ri} - S_{ri}^{DG} \qquad (4.25)$$

$$S_{yi} = SL_{yi} - S_{yi}^{DG} \qquad (4.26)$$

$$S_{bi} = SL_{bi} - S_{bi}^{DG} \qquad (4.27)$$

$$I_{Lr} = I_{Lri}^{with\_DG} = \left(\frac{SL_{ri} - S_{ri}^{DG}}{V_r}\right)^* \qquad (4.28)$$

$$I_{Ly} = I_{Lyi}^{with\_DG} = \left(\frac{SL_{yi} - S_{yi}^{DG}}{V_y}\right)^* \qquad (4.29)$$

$$I_{Lb} = I_{Lbi}^{with\_DG} = \left(\frac{SL_{ri} - S_{ri}^{DG}}{V_b}\right)^* \qquad (4.30)$$

The updated network power of a 3- phase feeder can be expressed in matrix form.

$$[S_{ri}] = [SL_{ri}] - [S_{ri}^{DG}] \qquad (4.31)$$

$$[S_{yi}] = [SL_{yi}] - [S_{yi}^{DG}] \qquad (4.32)$$

$$[S_{bi}] = [SL_{bi}] - [S_{bi}^{DG}] \qquad (4.33)$$

4.3 Effect of unbalance in the distribution network

Unbalanced distribution networks (UDNs) must be carefully analysed to minimize undesirable implications from internal unbalances and the incorporation of intermittent sources such as DG. Power electronic voltage source inverters are frequently used to interface DG systems. Power quality will be a significant challenge in networks with increased power electronics interfacing with DGs and loads and increased nonlinear loads. Among the many power quality challenges, unbalanced voltage is one of the most serious. Voltage regulation becomes difficult when network voltages are unbalanced because the unbalanced voltage's negative-sequence component causes oscillations with a double fundamental frequency in both reactive and active power injections, moreover, an unbalanced network can support less photovoltaic (PV) generation before the critical voltage limit is reached.

- **Voltage unbalance**

When the line or phase voltages in a three-phase system deviate from their nominal balance state, voltage unbalance condition occurs. A significant imbalance could drastically reduce equipment life cycles, speed up the additional component cycle, and significantly increase network operating and maintenance costs. The less unbalanced there is, the more desirable it is. According to IEEE standards, the percentage unbalance of voltage and current is given in (4.34) & (4.35) defined as follows [Wang et al. 2020].

$$V_{unf} = \frac{V_2}{V_1} * 100\%$$

(4.34)

- **Current unbalance**

Current unbalance is caused by load deficiencies, which travel to the transformer and generate three-phase voltage unbalance. Even slight voltage imbalances considerably disrupt the current waveform on all the loads connected at the transformer level.

$$I_{unf} = \frac{I_2}{I_1} * 100\%$$

(4.35)

The +ve (positive) and –ve (negative) sequence components of voltage and current are $V_1, I_1 \ and \ V_2, I_2$, respectively, while the voltage and current imbalance factors are V_{unf}, I_{unf}. As per standards, the nodes with $V_{unf} \leq 3\% \ and \ I_{unf} \leq 20\%$ are presumed to be normal operating range [Yao et al. 2020].

Historically, distribution networks were passive and radial, ensuring stability under most conditions; therefore, designing distribution networks did not need to consider stability concerns. Nonetheless, as the load imbalance and DG penetration of networks grow, their contribution to network security increases over time. As a result, voltage regulation is essential in these circumstances.

A sensitivity-based voltage regulation solutions based on the MAS coordinated algorithm is implemented to overcome the aforementioned problems. For this study, two sensitivity techniques are being investigated as follows. Sensitivity approach for DG selection and capacitor selection.
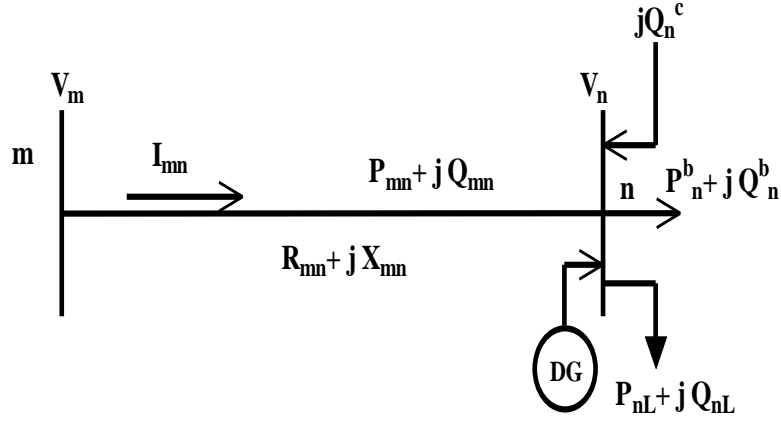
Figure 4.2: Single line diagram of an electrical distribution network's equivalent branch [Yao et al., 2020].

4.4 Sensitivity matrix of DG for voltage regulation

In an unbalanced distribution network, voltage profile optimization is a significant challenge that can perform by selecting the optimal DG units. Therefore, satisfactory results can only be obtained if assigned to the most appropriate nodes. Nonetheless, determining the optimal voltage-sensitive bus installed for DG selection is difficult. Voltage sensitivity analysis has been addressed in various ways in the literature. This section describes the evaluation of buses that are the most sensitive to DG selection. Equations (4.36) and (4.37) represent the real and reactive power of a node in a 'k' bus network [Mendonca et al. 2019; Jhala et al. 2017; Zad et al. 2018].

$$P_m = |V_m| \sum_{n=1}^{K} |Y_{mn}||V_n| \cos(\theta_{mn} - \delta_m + \delta_n)$$

$$for \ j = 1, 2, 3....k \qquad (4.36)$$

$$Q_m = -|V_m| \sum_{n=1}^{K} |Y_{mn}||V_n| \sin(\theta_{mn} - \delta_m + \delta_n)$$

$$for \ j = 1, 2, 3....k \qquad (4.37)$$

From equations (4.36) & (4.37), k is the number of nodes to a specific node, and $|V_n|, |V_m|$ are the voltage magnitudes of the nth, mth nodes, and δ_m, δ_n are the voltage phase angles at node m, n, and $|Y_{mn}|, \theta_{mn}$ are the node admittance magnitude and angle.

For the k-bus network, equations (4.36) and (4.37) represent 2n active power flow equations. Taking the partial derivative of (4.37) to voltage yields equations (4.38) and (4.39).

$$\frac{\partial Q_m}{\partial |V_m|} = -2|V_m||Y_{mn}|\sin\theta_{mn} - \sum_{n\neq m}|V_n||Y_{mn}|\sin(\theta_{mn} - \delta_m + \delta_n) \qquad (4.38)$$

$$\frac{\partial Q_m}{\partial |V_m|} = -|V_m||Y_{mn}|\sin(\theta_{mn} - \delta_m + \delta_n) \quad for\, n \neq m \qquad (4.39)$$

As a result, the change in voltage equation at a node 'm' in response to the change in P and Q on every system node 'n' is reduced to (4.40)

$$\partial |V_m| \cong \sum_{n=1}^{K}(\frac{\partial |V_m|}{\partial P_n}*dP_n + \frac{\partial |V_m|}{\partial Q_n}*dQ_n) \qquad (4.40)$$

The decoupled load flow nodal equation is expressed in matrix form as follows:

$$[dV] = [\frac{\partial V}{\partial Q}][d\,Q] \qquad (4.41)$$

Equation (4.42) shows that the best DG corresponds to node m' is the one with the highest sensitivity value.

$$[dV_m] = [\frac{\partial V_m}{\partial Q_n}][d\,Q_n] \qquad (4.42)$$

4.5 Loss sensitivity factor (LSF) matrix for capacitor selection

Loss sensitivity analysis identifies the network's sensitive buses to install shunt capacitors (SCs) [Dixit et al., 2018]. The buses with the highest LSF values are regarded as the most sensitive buses in the network. Equations (4.43) and (4.44) can indicate the active and reactive power losses that have occurred throughout branch "mn", respectively.

$$P_{loss[mn]} = \frac{\left((P_n^b[eqi])^2 + (Q_n^b[eqi])^2\right) \times R_{mn}}{(V_n)^2} \qquad (4.43)$$

$$Q_{loss[mn]} = \frac{\left((P_n^b[eqi])^2 + (Q_n^b[eqi])^2\right) \times X_{mn}}{(V_n)^2} \qquad (4.44)$$

By taking partially derivative Eqs. (4.43) and (4.44) with regard to reactive power injection, the LSF value of every node in a distribution system is derived as follows.

83

$$LSF = \frac{dP_{Loss[mn]}}{dQ_n^b[eqi]} = \frac{2 \times Q_n^b[eqi] \times R_{mn}}{(\mathrm{V}_n)^2} \qquad (4.45)$$

Buses with high LSF values are designated as sensitive buses for the installation of shunt capacitors.

4.6 Proposed methodology

Multi-Agent Systems (MAS), the focus of this research, comprises autonomous entities called agents. Agents collaborate to complete tasks, but their intrinsic ability to learn and make independent judgments allows them to be more flexible. Through encounters with the other agents and the environment, agents learn new situations and activities. Agents then use their knowledge to identify and execute activities in the environment to achieve their tasks. MAS is highly suited to tackling problems in various technological applications due to its adaptability [Dorri et al. 2018]. For the analysis of this proposed study, MAS architecture is divided into two sections: Agent control process and Management control process (Task manager).

- **Agent control**

The DG and SC agents will have access to the details of the network's installed DG and SCs and will regulate voltage locally. When a coordinated operation of voltage regulators is required, they interact with the MAS controller, which passes the duties to the agents to complete.

- **Management control**

The management controller receives data from the PMU agent and communicates with each DG/SC agent as needed.

PMU agent is a real-time monitoring device that continuously measures and stores data from the agents in the distribution network [Yasinzadeh et al. 2018].
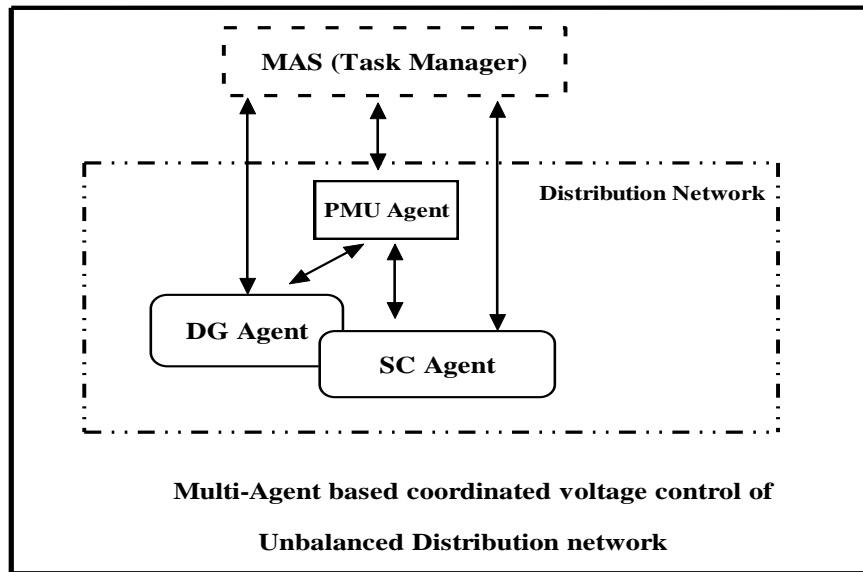
Figure 4.3: Block diagram of coordinated operation of voltage regulators in an active UDN using MAS architecture

4.6.1 Algorithm for voltage regulation of UDN using DG agent, based on sensitivity approach

The following steps are used in the DG agent-based strategy for optimal selection of DGs for voltage regulation and loss minimization.

1. Input the line and bus data of the unbalanced network.

2. Conduct a load flow analysis to determine the base case parameters for bus voltages, line losses, and voltage and current unbalance factors.

3. Create a vector G(x) is an exact replica of the given bus network and add all the branches as edges.

4. Add the reactance of every branch as edge weight and find the shortest path from bus m to n add their corresponding weights.

5. Multiply 'Xmn' with 'Qn' and keep summing

6. Repeat the steps 4 to 5 for every bus to obtain their sensitivities

7. Calculate the sensitivity values of all DG connected buses and sort them in descending order and store the values in voltage sensitive matrix Vs (y).

8. The DG Agent chooses the highest sensitive value from Vs (y) matrix and picks those DGs for voltage regulation.

9. Repeat step 2 for each DG selection and check the bus voltages to ensure they are within the range (i.e., $0.95 \leq Vn \leq 1.05$ $p.u.$), reduction of total loss and unbalance factors etc.

10. if satisfied results are achieved

11. end the simulation

12. Print the PMU results

13. else select the next highest value from step 7 and repeat the steps 8 to 12.

14. end.

4.6.2 Algorithm for voltage regulation of UDN using SC agent, by means of loss sensitivity factor (LSF) approach

The SC agent-based approach for optimal selection of SCs problem to minimize the loss takes the following steps.

1. Input the data for the branch and load, as well as the bus voltage limitations.

2. Compute the $P_{loss}[mn]$ and $Q_{loss}[mn]$ using load flow analysis.

3. Determine the sensitivity of real power loss to reactive power injection at each bus.

4. Organize the nodes according to their highest sensitivity levels and store the values in LSF (z) vector.

5. The SC Agent chooses the highest sensitive value LSF vector and selects those SCs for loss minimization.

6. Check if the shunt capacitors' total compensation (Qnc) is less or equivalent to the network's net reactive load (QnL).

7. go to step 2 and check for the bus voltages are within the limits, reduction of loss and unbalance factors etc.

8. if the results are satisfied

9. end the simulation

10. Print the PMU results

11. else select the next highest value from step 5 and repeat the steps 6 to 10.

12. stop

4.6.3 Coordinated operation of voltage regulators in active UDN using MAS topology

The management controller collects the values from the Vs and LSF vectors and are sorted and passes the maximum values to ptr[Vsmax] and ptr[LSFmax] vectors, respectively. The ptr vectors include the DG/SC memory location and initiate them to participate in voltage regulation. The MAS controller passes a logic "rand" function to coordinate SCs and DGs for optimal operation if voltage regulation is not achieved.
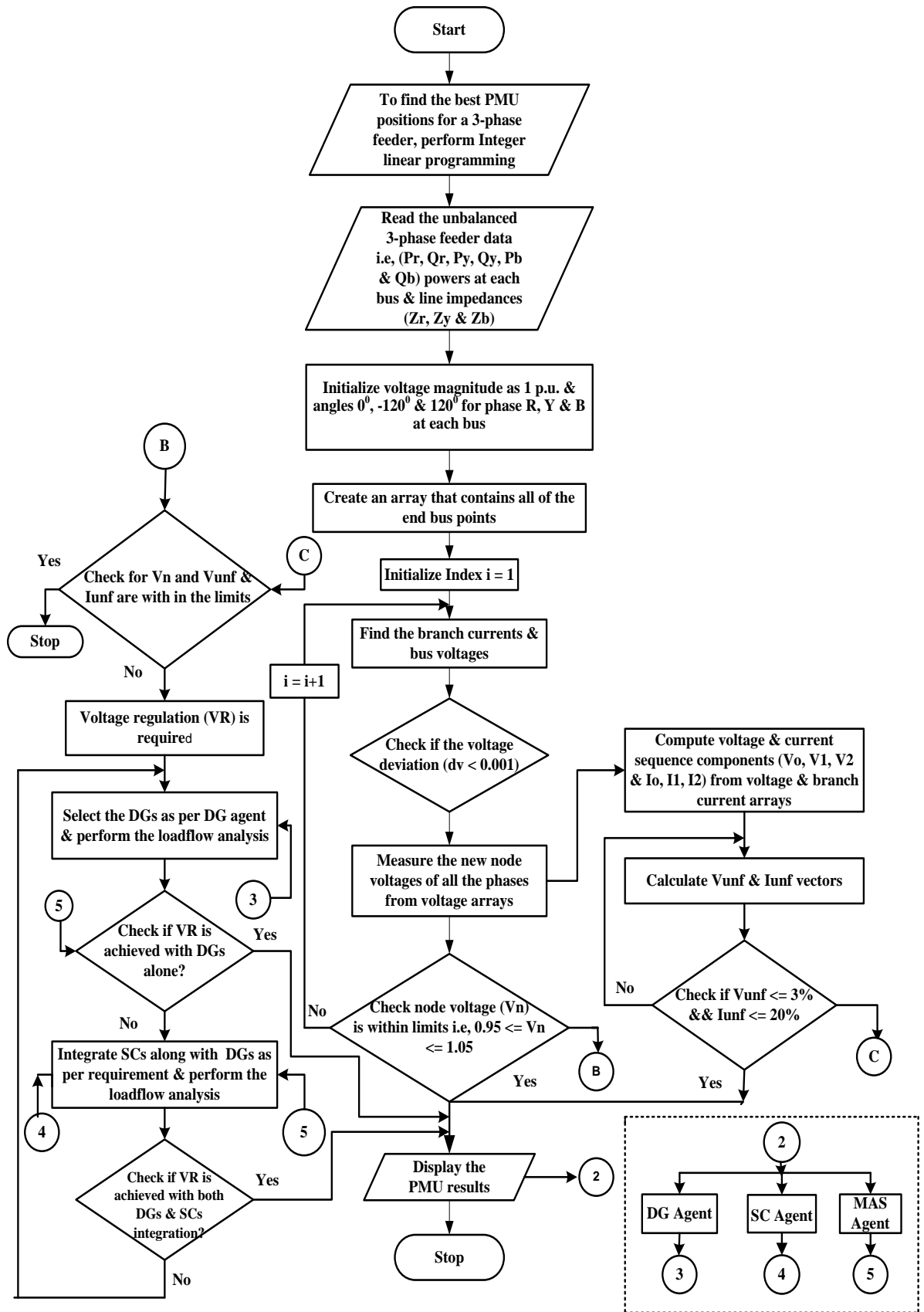
Figure 4.4: Flowchart of coordinated operation of voltage regulators in an active UDN
using MAS architecture

87

4.7 Results and discussion

The proposed methodology is being used on a 25-bus, unbalanced 3-phase radial distribution system. The rated line voltage of the system is 4.16 kV and the base MVA is 100. The detailed system data is reported in [Taher et al. 2014] and given in appendix. An ILP analysis is utilized to identify the best PMU location of the test system. By implementing MATLAB programming, the simulation is done for comprehensive system observability. Table 4.1 shows the necessary number of PMUs and their positions in the test feeder for total system observability.
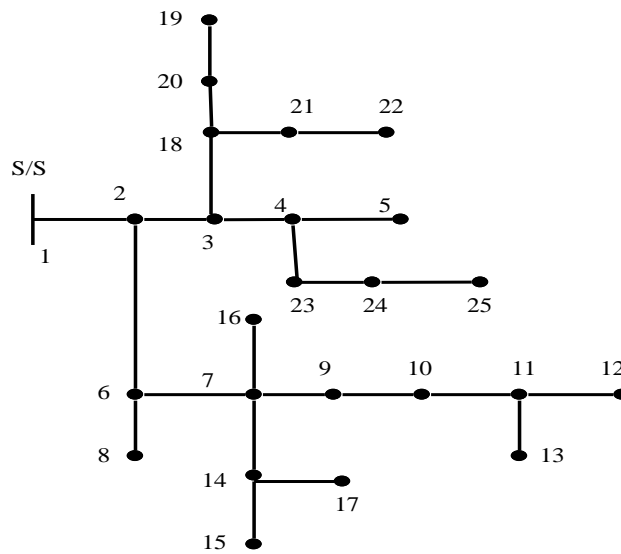
Figure 4.5: A single line representation of an unbalanced 25 bus, radial distribution system

Table 4.1: Recommended PMU locations of a 25-bus unbalanced radial distribution system

Number of PMUs	PMU installed nodes
9	1,4,7,8,11,14,20,22,25

The percentage unbalance in the 3-phase feeder is considered as follows. It is assumed that the load in the R-phase remains the same as in a balanced system, and Y-phase load is reduced by x % while B-phase load is increased by y % from the base case.

The case study analysis considers three scenarios: a system without voltage regulators, DG integration, and SC and DG integration. A detailed discussion of each scenario follows.

- **Scenario1 - Without DG and SC**

In this case, the percentage of load unbalance is taken in steps of 10%, 20%, 30% & 40% to observe the effect of unbalance in the system without DG/SC integration. With 10% in the load unbalance, the total load of phase R is 1333.8 kVA, phase Y is 1226.2 kVA & phase B is 1465.9 kVA, with 20% in the load unbalance, the total load of phase R is 1333.8 kVA, phase Y is 1089.96 kVA & phase B is 1599.23 kVA, with 30% in the load unbalance, the total load of phase R is 1333.8 kVA, phase Y is 953.71 kVA & phase B is 1732.50 kVA, & with 40% in the load unbalance, the total load of phase R is 1333.8 kVA, phase Y is 817.47 kVA & phase B is 1865.77 kVA, with power factor (PF) = 0.8.
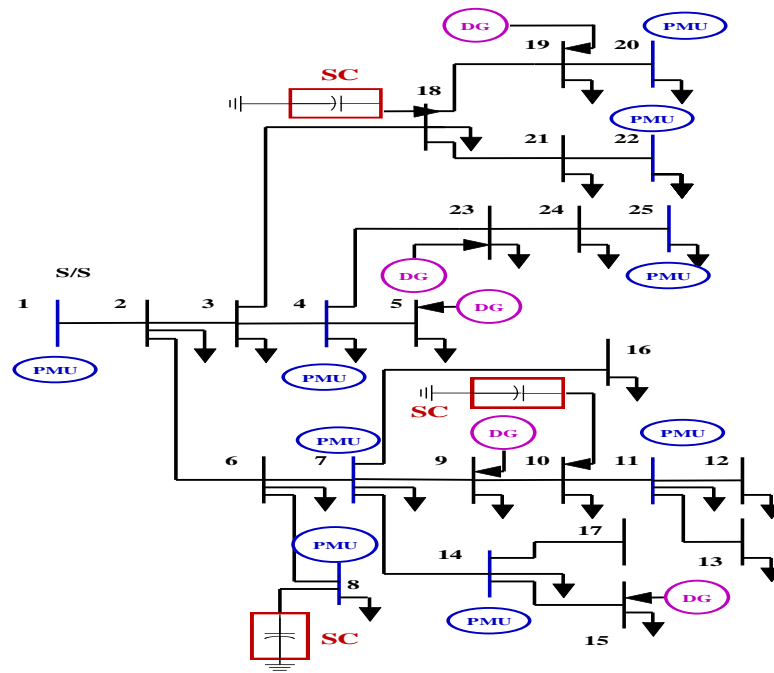
Figure 4.6: Modified diagram of 25 bus unbalanced, radial distribution test system with DGs, SCs & PMUs

Table 4.2 presents voltage magnitudes without DG and SC. Figure 4.7 shows the voltage profile of 25 bus unbalanced 3-phase radial feeder networks without DG and SC using PMU setup.

From the test results of scenario 1, as there is no change in load, the voltage profile of phase-R remains the same compared with the other two phases of the 3-phase feeder. The voltage profile of phase Y improved as the unbalance percentage increased, whereas the phase-B voltage magnitude profile is reduced with the increase in the percentage unbalance. Despite improvements in some phase voltage profiles, these unbalances caused some node voltage to fall below specifications, increasing the total power loss of the system.

Table 4.2 Voltage magnitude (p.u.) results of unbalanced loading without DG and SC
based on PMU data

PMU installed bus no.	25 Bus unbalanced, 3-phase radial feeder voltage magnitude (p.u.) using PMU setup without DG and SC											
	with 10% Unbalance			with 20% Unbalance			with 30% Unbalance			with 40% Unbalance		
	V_{Rph}	V_{Yph}	V_{Bph}	V_{Rph}	V_{Yph}	V_{Bph}	V_{Rph}	V_{Yph}	V_{Bph}	V_{Rph}	V_{Yph}	V_{Bph}
1	1.0000	1.0000	1.0000	1.0000	1.0000	1.0000	1.0000	1.0000	1.0000	1.0000	1.0000	1.0000
4	0.9479	0.9522	0.9418	0.9483	0.9579	0.9355	0.9487	0.9636	0.9292	0.9491	0.9691	0.9227
7	0.9322	0.9377	0.9238	0.9327	0.9453	0.9155	0.9332	0.9527	0.9070	0.9338	0.9600	0.8984
8	0.9491	0.9532	0.9427	0.9495	0.9589	0.9365	0.9499	0.9645	0.9302	0.9503	0.9699	0.9237
11	0.9156	0.9219	0.9046	0.9163	0.9314	0.8941	0.9170	0.9407	0.8834	0.9176	0.9498	0.8725
14	0.9251	0.9314	0.9159	0.9257	0.9397	0.9067	0.9263	0.9479	0.8974	0.9269	0.9559	0.8878
20	0.9434	0.9483	0.9353	0.9438	0.9545	0.9283	0.9443	0.9606	0.9213	0.9447	0.9667	0.9141
22	0.9420	0.9467	0.9348	0.9425	0.9531	0.9277	0.9429	0.9594	0.9206	0.9434	0.9656	0.9134
25	0.9432	0.9484	0.9371	0.9436	0.9546	0.9303	0.9441	0.9607	0.9234	0.9445	0.9667	0.9164
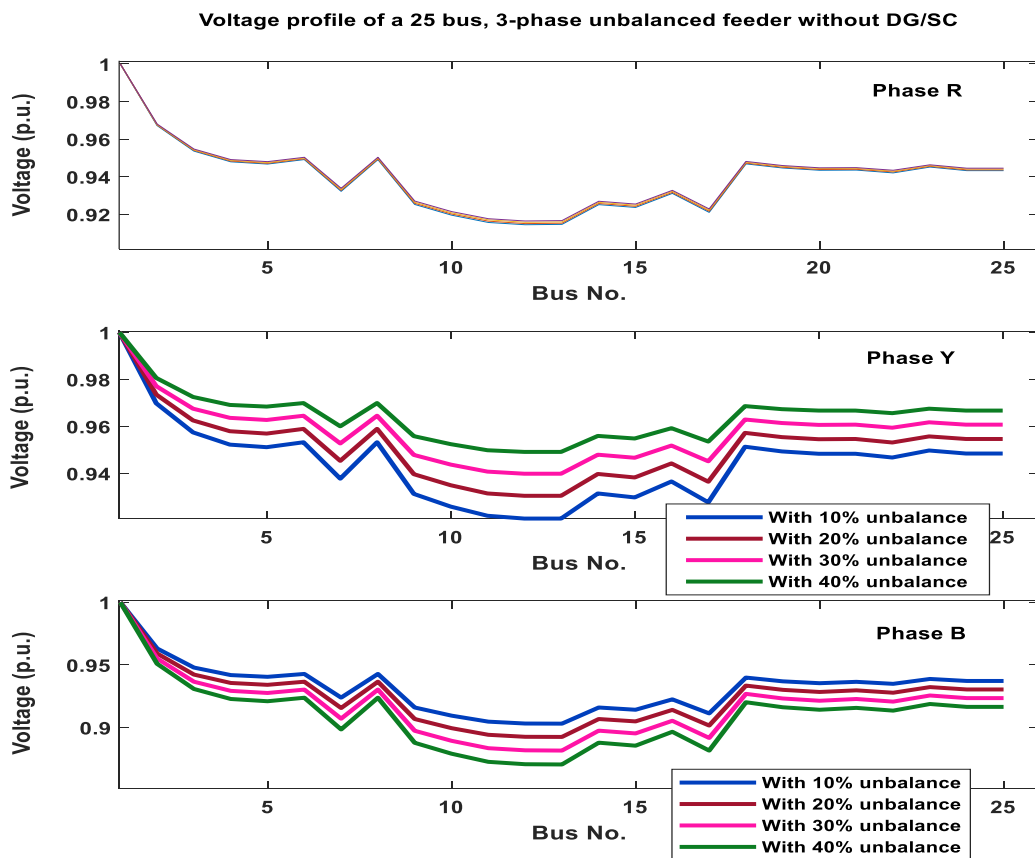
Figure 4.7: Voltage profile of a 25 bus, 3-phase unbalanced feeder without DG and SC

Also, the analysis is being extended further by calculating the voltage and current unbalance factors of the above cases are tabulated in Table 4.3. It is noticed that the voltage unbalances factors are within the standard limits (i.e., $< 3\%$), but the current unbalance factor is increased to above the limit (i.e., $< 20\%$) in one of the cases as the load unbalance increases.

Table 4.3: Voltage and current unbalance factor (UBF) of a 25-bus unbalanced system with various loading conditions

with 10% system unbalance		with 20% system unbalance		with 30% system unbalance		with 40% system unbalance	
V_{UBF}	I_{UBF}	V_{UBF}	I_{UBF}	V_{UBF}	I_{UBF}	V_{UBF}	I_{UBF}
0.0029	5.5095	0.0015	11.8665	0.0029	17.9968	0.0029	24.4526
0.1891	2.3656	0.3978	4.9548	0.6117	7.4036	0.8213	9.8374
0.2694	0.9455	0.5638	1.8891	0.8627	2.8468	1.1560	4.1245
0.2924	0.3654	0.6271	0.4506	0.9583	0.7349	1.2901	0.9479
0.3054	2.8269	0.6422	6.3522	0.9804	9.9467	1.3214	13.2040
0.2840	2.3226	0.6108	5.9027	0.9414	9.1393	1.2702	12.4299
0.3731	0	0.8086	0	1.2480	0	1.6888	0
0.2840	1.0669	0.6108	2.4920	0.9414	3.7469	1.2702	5.3788
0.4080	1.1124	0.8921	2.0167	1.3791	3.3854	1.8679	4.4321
0.4344	0.5908	0.9597	1.5480	1.4845	2.3649	2.0106	3.1856
0.4618	0.3654	1.0095	0.4886	1.5601	0.7349	2.1154	0.9479
0.4668	0.5965	1.0259	0.6668	1.5866	0.9518	2.1499	1.1692
0.4701	1.2955	1.0308	2.5150	1.5917	3.9756	2.1548	5.2500
0.4091	0.3671	0.8929	0.4227	1.3778	0.7887	1.8602	1.2290
0.4107	0.2197	0.9047	0.4498	1.3973	0.5941	1.8970	0.9479
0.3784	0.7950	0.8213	1.6011	1.2690	2.5352	1.7176	3.1443
0.4371	1.4545	0.9466	2.8592	1.4597	4.0224	1.9701	5.2132
0.3194	0.9747	0.6596	1.3432	1.0013	2.0230	1.3395	2.3394
0.3484	0.3654	0.7041	0.7396	1.0624	0.9518	1.4149	1.1732
0.3658	0.2160	0.7289	0.9312	1.0939	1.5054	1.4566	1.9263
0.3322	0.2638	0.6905	0.3159	1.0494	0.7887	1.4109	1.0069
0.3329	0.4244	0.7007	1.0478	1.0700	1.6367	1.4423	2.0332
0.3143	0.4450	0.6621	0.7612	1.0080	1.0695	1.3615	1.2944
0.3279	0	0.6852	0	1.0433	0	1.3984	0
0.3279	0	0.6852	0	1.0433	0	1.3984	0

- **Scenario2 - With DG**

In this scenario, the percentages of load unbalance are taken as 30 and 40 percent, respectively, and DGs are incorporated as needed at each step of change in unbalance. The DGs are placed at buses 5, 9, 15, 19 & 23 on each phase with 10%, 15% & 20% DG penetration levels are presented in Table 4.4.

Table 4.4 Variation of DG penetration level parameters on each phase of the 3-phase unbalanced distribution system

Percentage DG penetration	Total real & reactive power of DG on phase R		Total real & reactive power of DG on phase Y		Total real & reactive power of DG on phase B	
	Pr_total (kW)	Qr_total (kVAR)	Py_total (kW)	Qy_total (kVAR)	Pb_total (kW)	Qb_total (kVAR)
10 %	107.33	79.2	107.33	81.3	107.33	79
15 %	160.995	118.8	163.995	121.95	160.995	118.5
20 %	214.66	158.4	218.66	162.6	214.66	158

Figures 4.8 & 4.9 show the voltage profile, Table 4.5 & 4.7 compares voltage magnitude measurements, and Table 4.6 & 4.8 compares the voltage and current unbalance factors of the test system with and without DG considering 30% and 40% unbalance loading, whereas Table 4.8 presents the total power loss of the network.

Table 4.5 Voltage magnitude (p.u.) results of the test system with 30% unbalanced loading, DG using PMU measurement

PMU installed bus no.	Voltage magnitude (p.u.) using PMU setup with 30% unbalance loading, with and without DG											
	without DG/SC			with 10% DG			with 15% DG			with 20% DG		
	V_{Rph}	V_{Yph}	V_{Bph}	V_{Rph}	V_{Yph}	V_{Bph}	V_{Rph}	V_{Yph}	V_{Bph}	V_{Rph}	V_{Yph}	V_{Bph}
1	1.0000	1.0000	1.0000	1.0000	1.0000	1.0000	1.0000	1.0000	1.0000	1.0000	1.0000	1.0000
4	0.9487	0.9636	0.9292	0.9553	0.9668	0.9416	0.9585	0.9685	0.9477	0.9617	0.9701	0.9538
7	0.9332	0.9527	0.9070	0.9393	0.9557	0.9189	0.9423	0.9572	0.9246	0.9453	0.9587	0.9303
8	0.9499	0.9645	0.9302	0.9546	0.9668	0.9393	0.9569	0.9680	0.9438	0.9592	0.9691	0.9482
11	0.9170	0.9407	0.8834	0.9238	0.9441	0.8968	0.9272	0.9458	0.9033	0.9305	0.9474	0.9097
14	0.9263	0.9479	0.8974	0.9331	0.9513	0.9105	0.9364	0.9529	0.9170	0.9397	0.9546	0.9233
20	0.9443	0.9606	0.9213	0.9508	0.9639	0.9339	0.9541	0.9656	0.9400	0.9573	0.9672	0.9461
22	0.9429	0.9594	0.9206	0.9489	0.9624	0.9321	0.9518	0.9639	0.9377	0.9547	0.9653	0.9432
25	0.9441	0.9607	0.9234	0.9513	0.9643	0.9371	0.9548	0.9661	0.9438	0.9584	0.9679	0.9505
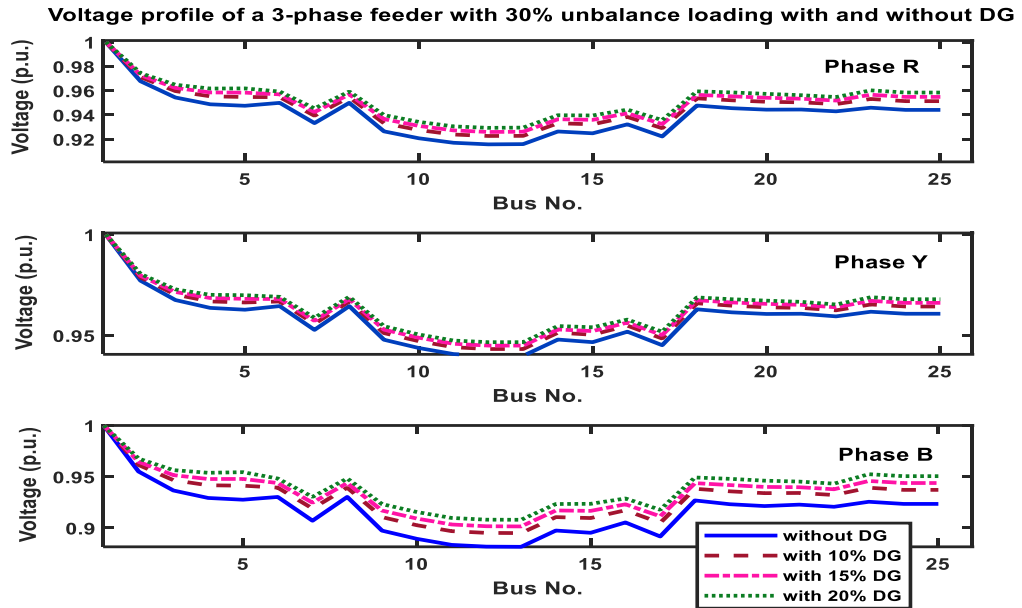
Figure 4.8: Voltage profile of a 3-phase feeder with 30% unbalance loading, with and without DG

Table 4.6 Voltage and current unbalance factors with 30% unbalance loading & various DG penetration levels

without DG/SC		with 10% DG		with 15% DG		with 20% DG	
V_{UBF}	I_{UBF}	V_{UBF}	I_{UBF}	V_{UBF}	I_{UBF}	V_{UBF}	I_{UBF}
0.0029	17.9968	0.0029	16.0814	0.0029	14.7420	0.0029	13.6286
0.6117	7.4036	0.4786	5.7669	0.4099	5.2360	0.3532	3.8410
0.8627	2.8468	0.6528	1.6164	0.5529	1.0489	0.4575	0.3857
0.9583	0.7349	0.7062	0.1207	0.5799	0.2030	0.4588	1.1605
0.9804	9.9467	0.7016	9.0846	0.5691	8.8760	0.4385	8.3034
0.9414	9.1393	0.7500	8.6685	0.6636	7.9712	0.5729	7.5291
1.2480	0	1.0003	0	0.8845	0	0.7689	0
0.9414	3.7469	0.7500	3.4586	0.6636	3.0899	0.5729	2.8606
1.3791	3.3854	1.1043	3.5710	0.9743	3.8095	0.8433	3.8627
1.4845	2.3649	1.2101	2.4124	1.0754	2.5735	0.9454	2.9823
1.5601	0.7349	1.2833	0.8281	1.1485	0.8834	1.0184	0.9484
1.5866	0.9518	1.3083	1.0725	1.1704	1.1442	1.0404	1.2283
1.5917	3.9756	1.3102	3.4586	1.1782	3.1456	1.0453	2.7319
1.3778	0.7887	1.1060	0.3902	0.9759	0.5559	0.8449	1.0080
1.3973	0.5941	1.1021	0.6694	0.9596	0.7141	0.8188	0.7666
1.2690	2.5352	1.0212	2.8567	0.9035	3.0475	0.7877	2.9929
1.4597	4.0224	1.1818	3.8406	1.0504	3.6414	0.9205	3.3235
1.0013	2.0230	0.7646	1.2062	0.6562	0.9911	0.5425	0.5957
1.0624	0.9518	0.8021	1.0725	0.6784	1.1442	0.5566	1.2283
1.0939	1.5054	0.8315	1.4695	0.7096	1.5676	0.5861	1.6829
1.0494	0.7887	0.8158	0.6373	0.7036	0.6798	0.5928	0.7298
1.0700	1.6367	0.8352	1.1073	0.7223	0.6554	0.6102	0.3591
1.0080	1.0695	0.7310	1.0005	0.5952	1.0674	0.4646	1.1458
1.0433	0	0.7636	0	0.6281	0	0.4917	0
1.0433	0	0.7636	0	0.6281	0	0.4917	0

Table 4.7 Voltage magnitude (p.u.) results of PMU data with 40% unbalance loading & DG

Bus Location	Voltage (p.u.) using PMU setup with 40% unbalance loading, with and without DG											
	without DG/SC			with 10% DG			with 15% DG			with 20% DG		
	V_R	V_Y	V_B	V_R	V_Y	V_B	V_R	V_Y	V_B	V_R	V_Y	V_B
1	1.0000	1.0000	1.0000	1.0000	1.0000	1.0000	1.0000	1.0000	1.0000	1.0000	1.0000	1.0000
4	0.9491	0.9691	0.9227	0.9556	0.9715	0.9374	0.9587	0.9727	0.9446	0.9619	0.9738	0.9516
7	0.9338	0.9600	0.8984	0.9397	0.9622	0.9124	0.9427	0.9633	0.9192	0.9456	0.9643	0.9259
8	0.9503	0.9699	0.9237	0.9549	0.9716	0.9345	0.9572	0.9725	0.9398	0.9594	0.9733	0.9450
11	0.9176	0.9498	0.8725	0.9243	0.9523	0.8884	0.9276	0.9535	0.8961	0.9309	0.9547	0.9037
14	0.9269	0.9559	0.8878	0.9335	0.9583	0.9034	0.9368	0.9595	0.9110	0.9401	0.9607	0.9185
20	0.9447	0.9667	0.9141	0.9511	0.9690	0.9290	0.9543	0.9702	0.9362	0.9575	0.9714	0.9433
22	0.9434	0.9656	0.9134	0.9492	0.9677	0.9269	0.9521	0.9688	0.9335	0.9550	0.9699	0.9400
25	0.9445	0.9667	0.9164	0.9516	0.9693	0.9326	0.9551	0.9706	0.9405	0.9585	0.9719	0.9482
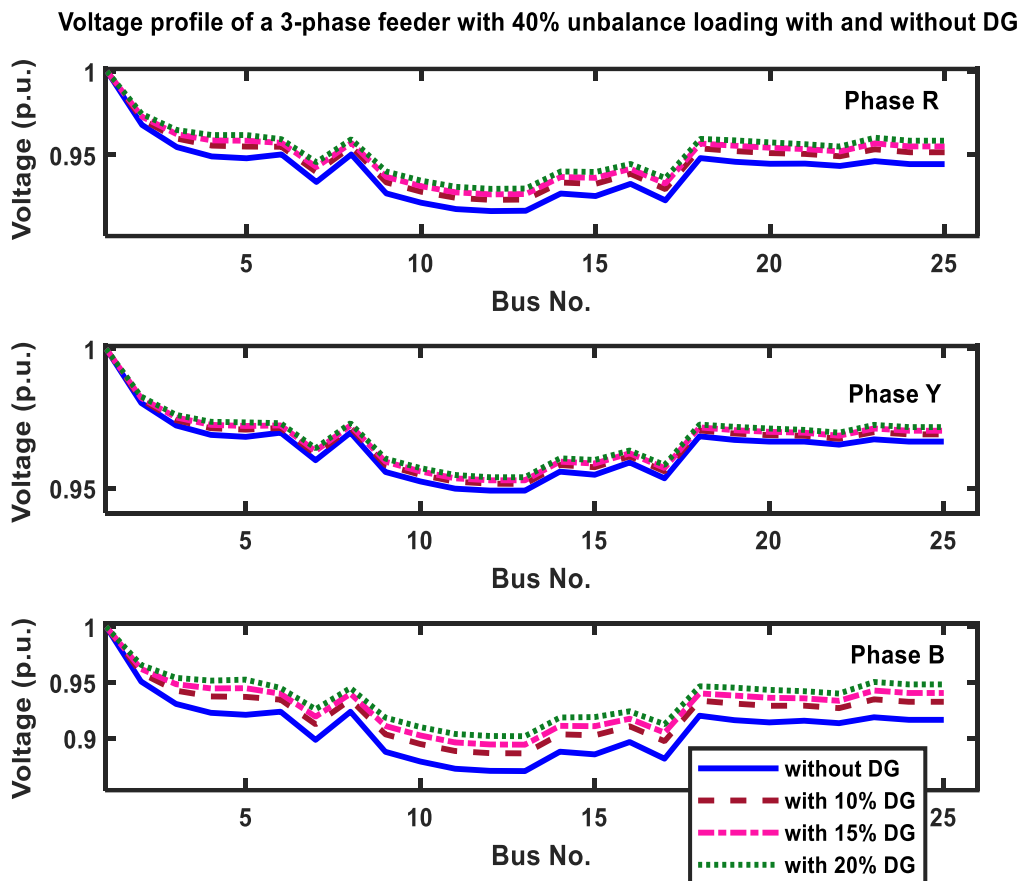
Figure 4.9: Voltage profile of a 3-phase feeder with 40% unbalance loading, with and without DG

Table 4.8 Voltage and current unbalance factor with 40% unbalance loading with various DG penetration levels

without DG/SC		with 10% DG		with 15% DG		with 20% DG	
V_{UBF}	I_{UBF}	V_{UBF}	I_{UBF}	V_{UBF}	I_{UBF}	V_{UBF}	I_{UBF}
0.0029	24.4526	0.0029	21.6642	0.0029	19.9715	0.0029	18.4623
0.8213	9.8374	0.6411	8.0299	0.5548	6.9854	0.4723	5.3043
1.1560	4.1245	0.8802	2.3803	0.7460	1.4294	0.6143	0.4842
1.2901	0.9479	0.9456	0.1213	0.7822	0.4844	0.6216	1.4724
1.3214	13.2040	0.9427	12.4614	0.7687	11.9517	0.5885	11.5074
1.2702	12.4299	1.0156	11.7546	0.8906	11.0613	0.7706	10.6972
1.6888	0	1.3561	0	1.1998	0	1.0395	0
1.2702	5.3788	1.0156	4.6841	0.8906	4.4333	0.7706	3.8794
1.8679	4.4321	1.4957	4.7966	1.3190	5.1340	1.1478	5.0108
2.0106	3.1856	1.6367	3.6227	1.4585	3.8015	1.2793	4.0918
2.1154	0.9479	1.7394	1.0780	1.5581	1.1539	1.3796	1.2420
2.1499	1.1692	1.7742	1.3297	1.5908	1.4232	1.4096	1.5319
2.1548	5.2500	1.7759	4.8484	1.5941	4.2062	1.4172	3.9093
1.8602	1.2290	1.4947	0.0867	1.3161	0.7750	1.1416	1.3003
1.8970	0.9479	1.4935	1.0780	1.3025	1.1539	1.1109	1.2420
1.7176	3.1443	1.3832	3.5758	1.2267	3.8273	1.0689	3.8416
1.9701	5.2132	1.5998	5.0685	1.4212	4.8753	1.2466	4.4794
1.3395	2.3394	1.0256	1.4667	0.8771	0.9995	0.7286	0.5430
1.4149	1.1732	1.0693	1.3342	0.9024	1.4281	0.7376	1.5371
1.4566	1.9263	1.1100	2.1906	0.9414	2.3447	0.7749	2.2713
1.4109	1.0069	1.0944	1.1450	0.9447	1.2256	0.7958	1.3192
1.4423	2.0332	1.1256	1.3724	0.9730	0.6609	0.8251	0.6748
1.3615	1.2944	0.9846	1.4720	0.8027	1.5756	0.6242	1.6959
1.3984	0	1.0247	0	0.8432	0	0.6621	0
1.3984	0	1.0247	0	0.8432	0	0.6621	0

Table 4.9 Total power loss of 25-bus, unbalanced 3-phase radial distribution system with DG

Percentage Unbalance loading	% DG penetration	Net real power loss (kW)	Net reactive power loss (kVAR)
30%	without DG	219.03	161.25
	10% DG	168.59	124.11
	15% DG	146.68	107.99
	20% DG	126.86	93.39
40%	without DG	244.58	180.06
	10% DG	166.15	122.32
	15% DG	147.73	108.76
	20% DG	123.49	90.56

From the test results of scenario 2, as the DG penetration levels increase, the voltage profiles of the three phases are improved, and the total power losses are reduced. The voltage & current unbalance factors are also within the standard limits. Nevertheless, some node voltages in each phase are still below the lower limit. Hence, a further improvement of voltage regulation is desirable.

- **Scenario3 - With DG and SC**

In scenario 3, the percentage of load unbalance is considered the same as in previous cases. SCs with ratings of 300 kVAR, 150 kVAR, and 300 kVAR have been installed at buses 8, 10, and 18 together with the existing DGs to improve the system conditions further from the above two scenarios.

Figures 4.10 and 4.11 depict the voltage profile, while Tables 4.10 and 4.12 compare voltage magnitude measurements, and Tables 4.11 and 4.13 compare the voltage and current unbalance factors of the test system with and without DG under 30 percent and 40 percent unbalance loading, respectively. Table 4.14 represents the network's total power loss.

Table 4.10 Voltage magnitude (p.u.) results of PMU data with 30% unbalance loading, DG & SC

| PMU installed bus no.	Voltage magnitude (p.u.) using PMU setup with 30% unbalance loading, with & without DG & SC											
	without DG/SC			with 10% DG & SC			with 15% DG & SC			with 20% DG & SC		
	V_{Rph}	V_{Yph}	V_{Bph}	V_{Rph}	V_{Yph}	V_{Bph}	V_{Rph}	V_{Yph}	V_{Bph}	V_{Rph}	V_{Yph}	V_{Bph}
1	1.0000	1.0000	1.0000	1.0000	1.0000	1.0000	1.0000	1.0000	1.0000	1.0000	1.0000	1.0000
4	0.9487	0.9636	0.9292	0.9699	0.9761	0.9645	0.9730	0.9777	0.9703	0.9761	0.9793	0.9760
7	0.9332	0.9527	0.9070	0.9582	0.9676	0.9539	0.9611	0.9690	0.9592	0.9639	0.9705	0.9645
8	0.9499	0.9645	0.9302	0.9752	0.9799	0.9733	0.9774	0.9810	0.9774	0.9796	0.9822	0.9814
11	0.9170	0.9407	0.8834	0.9469	0.9585	0.9441	0.9502	0.9601	0.9501	0.9534	0.9617	0.9560
14	0.9263	0.9479	0.8974	0.9520	0.9631	0.9459	0.9553	0.9648	0.9518	0.9585	0.9664	0.9577
20	0.9443	0.9606	0.9213	0.9695	0.9759	0.9624	0.9727	0.9775	0.9682	0.9758	0.9791	0.9739
22	0.9429	0.9594	0.9206	0.9676	0.9744	0.9606	0.9704	0.9758	0.9659	0.9733	0.9772	0.9710
25	0.9441	0.9607	0.9234	0.9659	0.9737	0.9601	0.9694	0.9754	0.9665	0.9728	0.9772	0.9728
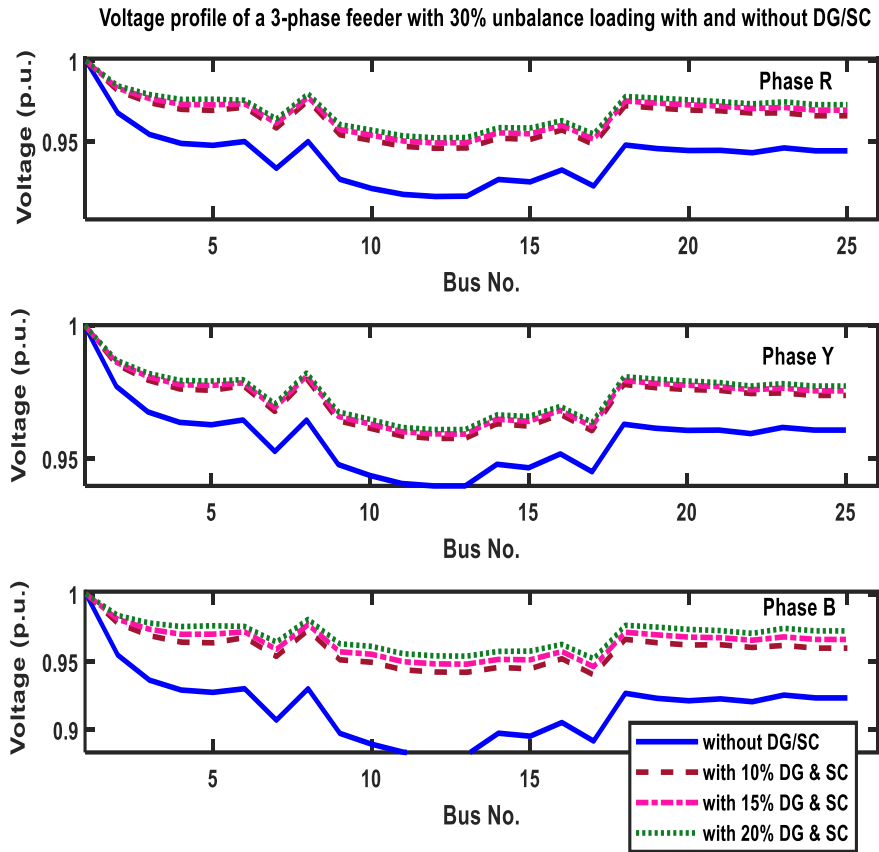
Figure 4.10: Voltage profile of a 3-phase feeder with 30% unbalance loading, with & without DG and SC

Table 4.11 Voltage and current unbalance factor with 30% unbalance loading, DG & SC

without DG/SC		with 10% DG & SC		with 15% DG & SC		with 20% DG & SC	
V_{UBF}	I_{UBF}	V_{UBF}	I_{UBF}	V_{UBF}	I_{UBF}	V_{UBF}	I_{UBF}
0.0029	17.9968	0.0029	20.0693	0.0029	20.2489	0.0029	20.6302
0.6117	7.4036	0.4707	6.2916	0.4448	5.5364	0.4269	5.3925
0.8627	2.8468	0.6133	1.7878	0.5694	1.2505	0.5384	0.4786
0.9583	0.7349	0.6424	0.1527	0.5877	0.2558	0.5519	1.4401
0.9804	9.9467	0.6442	13.7393	0.5849	14.6342	0.5485	15.0371
0.9414	9.1393	0.7958	11.6509	0.7618	11.2109	0.7413	11.6629
1.2480	0	1.0598	5.3002	1.0106	5.4400	0.9754	5.7511
0.9414	3.7469	0.8617	8.8505	0.8375	9.2172	0.8217	9.7694
1.3791	3.3854	1.2582	8.7809	1.2074	9.1044	1.1741	9.6250
1.4845	2.3649	1.4553	2.9238	1.4129	3.1059	1.3778	3.2835
1.5601	0.7349	1.4686	1.0480	1.4154	1.1133	1.3748	1.1769
1.5866	0.9518	1.4750	1.3573	1.4232	1.1133	1.3809	1.1769
1.5917	3.9756	1.4707	3.6908	1.4169	3.9504	1.3742	3.0859

1.3778	0.7887	1.1087	0.4938	1.0458	0.7006	0.9980	1.2509
1.3973	0.5941	1.0991	0.8471	1.0329	0.8999	0.9838	0.9514
1.2690	2.5352	1.0613	3.2009	1.0134	3.4003	0.9716	3.2414
1.4597	4.0224	1.1447	4.4233	1.0830	4.4224	1.0255	4.7568
1.0013	2.0230	0.7157	1.4478	0.6694	1.2490	0.6415	0.6535
1.0624	0.9518	0.7271	1.0480	0.6759	1.1133	0.6385	1.1769
1.0939	1.5054	0.7467	2.1725	0.6898	2.3079	0.6492	2.1668
1.0494	0.7887	0.7403	0.8065	0.6924	0.8567	0.6553	0.9057
1.0700	1.6367	0.7500	1.1582	0.7025	0.9657	0.6597	0.3141
1.0080	1.0695	0.6643	1.2662	0.6013	1.3450	0.5553	1.4220
1.0433	0	0.6931	0	0.6226	0	0.5771	0
1.0433	0	0.6931	0	0.6226	0	0.5771	0

Table 4.12 Voltage magnitude (p.u.) results of PMU data with 40% unbalance loading, DG & SC

| PMU installed bus no.	Voltage magnitude (p.u.) using PMU setup with 40% unbalance loading, with & without DG & SC											
	without DG/SC			with 10% DG & SC			with 15% DG & SC			with 20% DG & SC		
	V_{Rph}	V_{Yph}	V_{Bph}	V_{Rph}	V_{Yph}	V_{Bph}	V_{Rph}	V_{Yph}	V_{Bph}	V_{Rph}	V_{Yph}	V_{Bph}
1	1.0000	1.0000	1.0000	1.0000	1.0000	1.0000	1.0000	1.0000	1.0000	1.0000	1.0000	1.0000
4	0.9491	0.9691	0.9227	0.9701	0.9791	0.9623	0.9732	0.9802	0.9691	0.9763	0.9814	0.9757
7	0.9338	0.9600	0.8984	0.9586	0.9717	0.9506	0.9614	0.9728	0.9569	0.9642	0.9738	0.9630
8	0.9503	0.9699	0.9237	0.9755	0.9823	0.9715	0.9777	0.9831	0.9763	0.9799	0.9839	0.9811
11	0.9176	0.9498	0.8725	0.9474	0.9638	0.9401	0.9506	0.9650	0.9471	0.9538	0.9662	0.9540
14	0.9269	0.9559	0.8878	0.9525	0.9680	0.9420	0.9556	0.9691	0.9490	0.9588	0.9703	0.9559
20	0.9447	0.9667	0.9141	0.9699	0.9788	0.9600	0.9729	0.9800	0.9668	0.9760	0.9811	0.9735
22	0.9434	0.9656	0.9134	0.9679	0.9775	0.9580	0.9707	0.9786	0.9642	0.9735	0.9796	0.9702
25	0.9445	0.9667	0.9164	0.9662	0.9769	0.9576	0.9696	0.9782	0.9651	0.9730	0.9794	0.9724
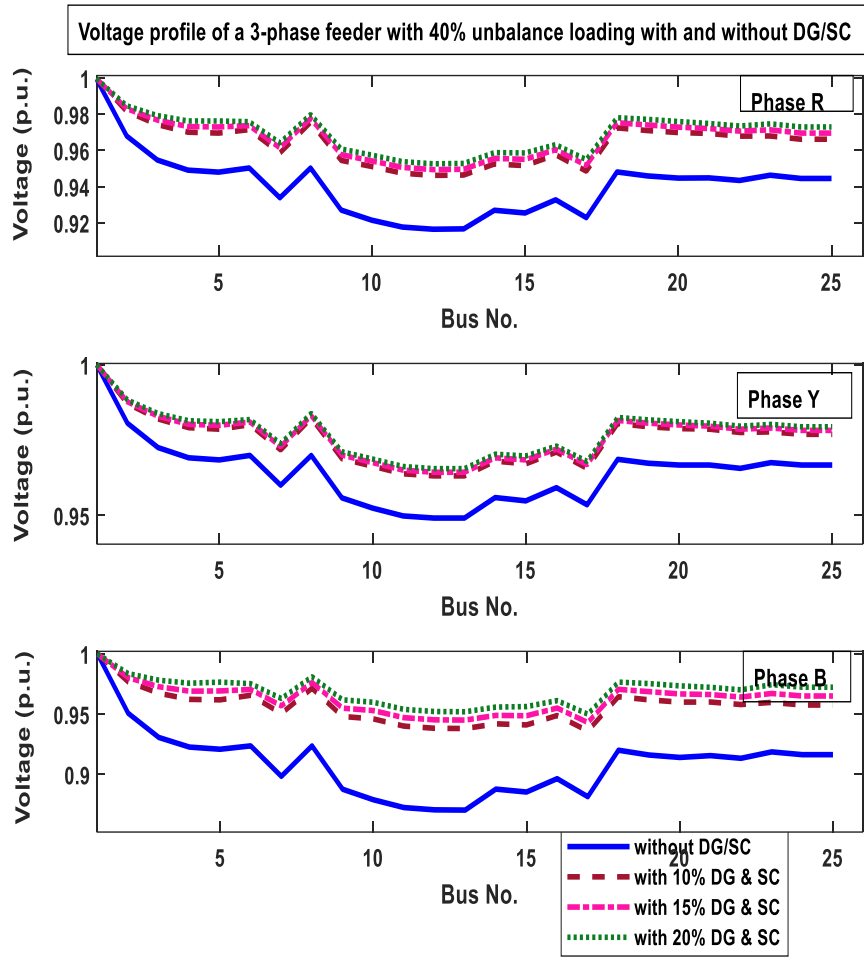
Figure 4.11: Voltage profile of a 3-phase feeder with 40% unbalance loading, with & without DG and SC

Table 4.13 Voltage and current unbalance factor with 40% unbalance loading, DG & SC

without DG/SC		with 10% DG & SC		with 15% DG & SC		with 20% DG & SC	
V_{UBF}	I_{UBF}	V_{UBF}	I_{UBF}	V_{UBF}	I_{UBF}	V_{UBF}	I_{UBF}
0.0029	24.4526	0.0029	25.8652	0.0029	25.9904	0.0029	26.4678
0.8213	9.8374	0.6059	8.3613	0.5732	7.8290	0.5468	7.7024
1.1560	4.1245	0.7992	2.7162	0.7424	1.5991	0.7050	1.0395
1.2901	0.9479	0.8416	0.1532	0.7667	0.6068	0.7202	1.8186
1.3214	13.2040	0.8435	17.4282	0.7648	17.9326	0.7152	18.9253
1.2702	12.4299	1.0132	14.5172	0.9653	14.3547	0.9349	14.5299
1.6888	0	1.3389	7.1196	1.2739	7.5540	1.2183	8.0166
1.2702	5.3788	1.0913	10.2344	1.0621	10.9847	1.0383	11.3566
1.8679	4.4321	1.5737	10.4761	1.5032	10.5582	1.4497	11.2048
2.0106	3.1856	1.8022	4.0280	1.7382	4.2737	1.6840	4.1677
2.1154	0.9479	1.8306	1.0518	1.7561	1.1160	1.6958	1.1844
2.1499	1.1692	1.8448	1.3623	1.7685	1.4454	1.7075	1.5339
2.1548	5.2500	1.8444	5.5485	1.7644	5.1249	1.7011	4.8494
1.8602	1.2290	1.4141	0.1096	1.3278	0.9708	1.2615	1.6060
1.8970	0.9479	1.4087	1.0518	1.3180	1.1160	1.2465	1.1844

99

1.7176	3.1443	1.3499	4.0940	1.2798	4.0144	1.2233	4.2603
1.9701	5.2132	1.4741	5.9654	1.3814	5.9250	1.3001	6.4833
1.3395	2.3394	0.9374	2.0889	0.8752	1.2521	0.8367	0.4873
1.4149	1.1732	0.9533	1.6860	0.8827	1.7889	0.8368	1.8985
1.4566	1.9263	0.9708	2.7742	0.9018	2.9434	0.8489	2.8227
1.4109	1.0069	0.9709	1.4470	0.9049	1.5352	0.8604	1.6293
1.4423	2.0332	0.9919	1.7343	0.9187	1.0091	0.8677	0.4645
1.3615	1.2944	0.8729	1.8602	0.7853	1.9737	0.7310	2.0946
1.3984	0	0.9053	0	0.8120	0	0.7536	0
1.3984		0.9053		0.8120		0.7536	

Table 4.14 Total power loss of 25-bus, unbalanced 3-phase radial distribution system with DG and SC

Percentage Unbalance loading	% DG penetration	Net real power loss (kW)	Net reactive power loss (kVAR)
30%	without DG	219.03	161.25
	10% DG & SC	119.36	87.87
	15% DG & SC	106.89	78.69
	20% DG & SC	96.16	70.79
40%	without DG	244.58	180.06
	10% DG & SC	130.48	96.06
	15% DG & SC	116.13	85.50
	20% DG & SC	104.01	76.57

From the results of the three scenarios, it is observed that without voltage regulating devices, as the load unbalancing increases in the distribution network, most of the node voltage magnitudes are below the lower limit. Though the voltage unbalances factors are within the acceptable limits, the current unbalance factors are beyond the limit. When DGs and SCs are integrated into the network, considerable losses are minimized. The voltage profile is improved by bringing all node voltage magnitudes within limits. Also, the percentages of voltage and current imbalance factors are dropped compared to the unregulated scenario.

4.8 Conclusion

This work analyses a 3-phase, 25-bus unbalanced distribution network for steady-state performance. This research provides an effective and efficient coordinated voltage control mechanism based on the MAS approach. The scheme optimizes the voltage profile to

minimize the unbalance, voltage deviation, and losses in an active UDN. The DG/SC agents have the sensitivity indices of all DGs and SCs linked in the network and allow voltage regulation to be made locally on the most sensitive nodes. When a coordinated action of voltage regulators is desired, they communicate with the MAS controller, which then delegates the tasks to the agents based on the available information from the PMU agent database. Thus, coordinated voltage regulation is accomplished by optimally choosing the exact number of devices, eliminating the need for other voltage regulators in the network. As the PMUs are already installed in the network, a separate memory unit for the MAS structure can be avoided, making the scheme cost-effective. The voltage and current parameters of the network are measured using an online estimation technique based on PMU. A PMU allows one to measure the voltage phasor of the bus in real-time and the current phasor of all lines connected to the bus. Due to this capability of PMU, all buses adjacent to it are observable. The optimum PMU allocation on the test system is elucidated using an integer linear programming approach. An improved voltage profile of the system and a substantial reduction in voltage and current imbalance and power loss are exhibited as a result of optimal operations of DGs and SCs in the network.

Chapter 5

Conclusions and scope for future work

5.1 Conclusions

The primary objective of the work described is to simplify the process of selecting optimal locations for Phasor Measurement Units (PMUs) in existing distribution networks. PMUs are essential for monitoring and controlling power systems, but determining the best locations for them can be complex. The study proposes two strategies: one for determining optimal observability of PMU sites considering the presence or absence of Zero Injection Buses (ZIBs), and another for assessing the voltage profile of radial distribution feeders using PMU technology. These strategies aim to provide insights and solutions for effective PMU placement and voltage profile analysis in distribution networks. To streamline the process of determining optimal PMU locations, the study utilizes Integer Linear Programming (ILP) and considers normal network operation. This approach facilitates the installation of the required number of PMUs at diverse locations, enhancing the overall monitoring and control capabilities of the grid network. The study's findings suggest that the use of ZIBs has no significant effect on the voltage profile of the system, allowing for a reduction in the number of PMUs without compromising accuracy or stability.

To overcome the limitations associated with ZIBs and ensure effective state estimation, the study proposes a methodology specifically designed for active radial distribution networks. This technique provides real-time information on distribution networks with Distributed Generation (DG) integration and addresses challenges related to monitoring system states. The study presents two methodologies for distribution network analysis: validating complete observability using the optimal number of PMUs and estimating the voltage profile of a radial distribution system. The performance of the proposed voltage profile estimation methodology is evaluated by comparing its results with those obtained using the traditional FBS load flow algorithm. The evaluation is conducted on distribution test systems, considering cases with and without DG and SC interconnections. The findings indicate that the voltage profile estimations obtained from the methodology, which relies on PMU measurements, closely align with the results obtained from the traditional algorithm. This

suggests that the estimated voltage profiles accurately capture the behaviour of the distribution system.

Furthermore, the integration of DG within distribution networks can have significant implications for the dynamics of the entire power system. One of the challenges associated with DG integration is the occurrence of power quality issues, particularly unbalanced voltage. Unbalanced voltages introduce oscillations caused by the presence of negative sequence components, which can adversely affect the stability and performance of the distribution network. Managing the voltage profile in an unbalanced network becomes crucial to mitigate the impact on distributed generation. To address these challenges, the work focuses on analysing a specific scenario involving a 3-phase, 25-bus unbalanced distribution network for steady-state performance. The Multi-Agent System (MAS) approach is employed as a distributed control framework that utilizes autonomous agents to collaboratively achieve a common goal. The voltage control scheme developed aims to optimize the voltage profile of the unbalanced distribution network by minimizing parameters such as unbalance, voltage deviation, and losses. The scheme optimizes these factors to improve the overall performance and stability of the active UDN. The MAS approach involves DG/SC agents with sensitivity indices for all DGs and SCs in the network, enabling local voltage regulation at sensitive nodes. When coordinated action is required, agents communicate with a centralized MAS controller. The MAS controller delegates tasks based on information from the PMU agent database, coordinating voltage regulation actions for optimal system performance. This approach achieves coordinated voltage regulation by optimizing the number of devices, eliminating the need for additional voltage regulators. Utilizing existing PMUs in the network makes the scheme cost-effective, as it avoids the requirement for a separate memory unit. The proposed methodology utilizes PMUs for real-time measurement of voltage and current parameters in the network, and an Integer Linear Programming approach is employed to determine the optimal allocation of PMUs. This enables improved voltage profiles, reduced imbalances, and minimized power losses through optimized operations of DGs and SCs in the network.

5.2 Scope for future work

The research that is being presented in this work can be broadened to:

- This study considers radial topologies when evaluating the distribution networks' voltage magnitude utilizing PMU technology. Thus, meshed topologies can be included in this work.

- Along with DG and SCs, the coordinated online voltage regulation using the MAS scheme for smart grids can be made available for other voltage-regulating devices like OLTC and Energy storage devices.

- Full observability analysis and state estimation of the distribution network in case of various contingencies and PMU loss.

LIST OF PUBLICATIONS

Journals:

1. Tangi, S., & Gaonkar, D. N. (2021), "Voltage Estimation of Active Distribution Network Using PMU Technology." *IEEE Access*, *9*, 100436-100446.

2. Tangi, S., & Gaonkar, D. N. (2022), "Multi - Agent-based Coordinated Voltage regulation Technique in an Unbalanced Distribution System, "International Transactions on Electrical Energy Systems." (Under review; Manuscript id: 88562208)

3. Tangi, S., & Gaonkar, D. N. (2023), "Smart distribution network voltage estimation using PMU technology considering zero injection constraints, "*Energies*." (Under review; Manuscript id: 2486913)

Conferences:

1. Tangi, S., & Gaonkar, D. N. (2020). "Optimal Phasor Measurement Units Placement in Radial Distribution Networks Using Integer Linear Programming." *Proc., of 3rd Int. Conf. on Computer Networks and Inventive Communication Technologies (ICCNCT - 2020),* Coimbatore, India. 1021-1031. https://doi.org/10.1007/978-981-15-9647-6_81.

2. Tangi, S., Gaonkar, D. N., & Bhargav, S. (2021). "Voltage Regulation of Smart Distribution Network using Sensitivity Analysis based DG placement." *Proc., of 7th Int. Conf. on Electronics, Computing and Communication Technologies (IEEE CONECCT),* Bangalore, India, 1-6.

BIBLIOGRAPHY

Abdolahi, A., Taghizadegan, N., Banaei, M. R., and Salehi, J. (2021). "A reliability-based optimal µ-PMU placement scheme for efficient observability enhancement of smart distribution grids under various contingencies." *IET Science, Measurement & Technology*, 15(8), 663-680.

Abiri, E., Rashidi, F., and Niknam, T. (2015). "An optimal PMU placement method for power system observability under various contingencies." *International transactions on electrical energy systems*, 25(4), 589-606.

Adeyanju, O. M., Canha, L. N., Rangel, C. A. S., and do Prado, J. C. (2021). "Semi-decentralized and fully decentralized multiarea economic dispatch considering participation of local private aggregators using meta-heuristic method." *International Journal of Electrical Power & Energy Systems*, 128, 106656.

Ahmed, M., Bhattarai, R., Hossain, S. J., Abdelrazek, S., and Kamalasadan, S. (2019). "Coordinated voltage control strategy for voltage regulators and voltage source converters integrated distribution system." *IEEE Transactions on Industry Applications*, 55(4), 4235-4246.

Almasabi, S., and Mitra, J. (2019). "A fault-tolerance based approach to optimal PMU placement." *IEEE Transactions on Smart Grid*, 10(6), 6070-6079.

Almunif, A., and Fan, L. (2020). "Optimal PMU placement for modeling power grid observability with mathematical programming methods." *International Transactions on Electrical Energy Systems*, 30(2), e12182.

Almutairi, A., Alrumayh, O., Alyami, S., Albagami, N., and Hossein, M. (2022). "A blockchain-enabled secured fault allocation in smart grids based on µPMUs and UT." *IET Renewable Power Generation*, 16(16), 3496-3506.

Amoateng, D. O., Yan, R., Mosadeghy, M., and Saha, T. K. (2021). "Topology detection in power distribution networks: A PMU based deep learning approach." *IEEE Transactions on Power Systems*, 37(4), 2771-2782.

Andreoni, R., Macii, D., Brunelli, M., and Petri, D. (2021). "Tri-objective optimal PMU placement including accurate state estimation: The case of distribution systems." *IEEE Access*, 9, 62102-62117.

Babu, R., and Bhattacharyya, B. (2018). "An approach for optimal placement of phasor measurement unit for power network observability considering various contingencies." *Iranian Journal of Science and Technology, Transactions of Electrical Engineering*, 42(2), 161-183.

Babu, R., Raj, S., Dey, B., and Bhattacharyya, B. (2021). "Modified branch-and-bound algorithm for unravelling optimal PMU placement problem for power grid observability: a comparative analysis." *CAAI transactions on intelligence technology*, 6(4), 450-470.

Bai, Y., Li, S., Gu, X., and Zhou, G. (2021). "Collaborative planning of resilient backbone grids and PMU placement for power systems." *International Journal of Electrical Power & Energy Systems*, 131, 107106.

Bečejac, V., and Stefanov, P. (2020). "Groebner bases algorithm for optimal PMU placement." *International Journal of Electrical Power & Energy Systems*, 115, 105427.

Bedawy, A., Yorino, N., Mahmoud, K., Zoka, Y., and Sasaki, Y. (2019). "Optimal voltage control strategy for voltage regulators in active unbalanced distribution systems using multi-agents." *IEEE Transactions on Power Systems*, 35(2), 1023-1035.

Bidgoli, H. S., and Van Cutsem, T. (2017). "Combined local and centralized voltage control in active distribution networks." *IEEE Transactions on Power Systems*, 33(2), 1374-1384.

Chamana, M., and Chowdhury, B. H. (2018). "Optimal voltage regulation of distribution networks with cascaded voltage regulators in the presence of high PV penetration." *IEEE Transactions on Sustainable Energy*, 9(3), 1427-1436.

Chamana, M., Chowdhury, B. H., and Jahanbakhsh, F. (2016). "Distributed control of voltage regulating devices in the presence of high PV penetration to mitigate ramp-rate issues." *IEEE Transactions on Smart Grid*, 9(2), 1086-1095.

Chauhan, K., and Sodhi, R. (2019). "Placement of distribution-level phasor measurements for topological observability and monitoring of active distribution networks." *IEEE Transactions on Instrumentation and Measurement*, 69(6), 3451-3460.

Dehghanpour, K., Wang, Z., Wang, J., Yuan, Y., and Bu, F. (2018). "A survey on state estimation techniques and challenges in smart distribution systems. "*IEEE Transactions on Smart Grid*, 10(2), 2312-2322.

Dixit, M., Kundu, P., and Jariwala, H. R. (2018). "Optimal integration of shunt capacitor banks in distribution networks for assessment of techno-economic asset." *Computers & Electrical Engineering*, 71, 331-345.

Dorri, A., Kanhere, S. S., and Jurdak, R. (2018). "Multi-agent systems: A survey. "*IEEE Access*, 6, 28573-28593.

Dua, G. S., Tyagi, B., and Kumar, V. (2021). "Deploying micro-PMUs with channel limit in reconfigurable distribution systems." *IEEE Systems Journal*, 16(1), 832-843.

Dutta, R., Patel, V. S., Chakrabarti, S., Sharma, A., Das, R. K., and Mondal, S. (2020). "Parameter estimation of distribution lines using SCADA measurements." *IEEE Transactions on Instrumentation and Measurement*, 70, 1-11.

Elimam, M., Isbeih, Y. J., El Moursi, M. S., Elbassioni, K., and Al Hosani, K. H. (2021). "Novel Optimal PMU Placement Approach Based on the Network Parameters for Enhanced System Observability and Wide Area Damping Control Capability." *IEEE Transactions on Power Systems*, 36(6), 5345-5358.

Farag, H. E., El-Saadany, E. F., and Seethapathy, R. (2012). "The evolution for voltage and reactive power control in smart distribution systems." *International Journal of Emerging Electric Power Systems*, 13(1).

Farajollahi, M., Shahsavari, A., and Mohsenian-Rad, H. (2018, August). "Tracking state estimation in distribution networks using distribution-level synchrophasor data." In 2018 *IEEE Power & Energy Society General Meeting* (PESGM) (pp. 1-5). IEEE.

Ghamsari-Yazdel, M., reza Najafi, H., and Amjady, N. (2019). "Novel notions of zero injection property of buses in optimal PMU location with efficient observability enhancement focusing on security concepts." *Electric Power Systems Research*, 169, 24-34.

Ghasemi, S. (2018). "Balanced and unbalanced distribution networks reconfiguration considering reliability indices." *Ain Shams Engineering Journal*, 9(4), 1567-1579.

Gholami, M., Abbaspour, A., Fattaheian-Dehkordi, S., Lehtonen, M., Moeini-Aghtaie, M., and Fotuhi, M. (2020). "Optimal allocation of PMUs in active distribution network

considering reliability of state estimation results." *IET Generation, Transmission & Distribution*, 14(18), 3641-3651.

Gholami, M., Abbaspour, A., Moeini-Aghtaie, M., Fotuhi-Firuzabad, M., and Lehtonen, M. (2019). "Detecting the location of short-circuit faults in active distribution network using PMU-based state estimation." *IEEE Transactions on Smart Grid*, 11(2), 1396-1406.

Guo, X. C., Liao, C. S., and Chu, C. C. (2020). "Enhanced optimal PMU placements with limited observability propagations." *IEEE Access*, 8, 22515-22524.

Guo, Y., Wu, W., Zhang, B., and Sun, H. (2013). "An efficient state estimation algorithm considering zero injection constraints." *IEEE Transactions on Power Systems*, 28(3), 2651-2659.

Guo, Y., Zhang, Q., and Wang, Z. (2021). "Cooperative peak shaving and voltage regulation in unbalanced distribution feeders." *IEEE Transactions on Power Systems*, 36(6), 5235-5244.

Hong, G., and Kim, Y. S. (2020). "Supervised learning approach for state estimation of unmeasured points of distribution network." *IEEE Access*, 8, 113918-113931.

Hossein, Z. S., Khodaei, A., Fan, W., Hossan, M. S., Zheng, H., Fard, S. A., and Bahramirad, S. (2020). "Conservation voltage reduction and volt-VAR optimization: Measurement and verification benchmarking." *IEEE Access*, 8, 50755-50770.

Huang, L., Sun, Y., Xu, J., Gao, W., Zhang, J., and Wu, Z. (2013). "Optimal PMU placement considering controlled islanding of power system." *IEEE Transactions on Power Systems*, 29(2), 742-755.

IEEE. C37.118. (2011). "*IEEE Standard for synchro phasors for Power Systems*." 1-61.

Islam, M. R., Lu, H., Hossain, J., and Li, L. (2020). "Multiobjective optimization technique for mitigating unbalance and improving voltage considering higher penetration of electric vehicles and distributed generation." *IEEE Systems Journal*, 14(3), 3676-3686.

Jabalameli, N., and Ghosh, A. (2020). "Online centralized coordination of charging and phase switching of PEVs in unbalanced LV networks with high PV penetrations." *IEEE Systems Journal*, 15(1), 1015-1025.

Jhala, K., Natarajan, B., and Pahwa, A. (2017). "Probabilistic voltage sensitivity analysis (PVSA)—A novel approach to quantify impact of active consumers." *IEEE Transactions on Power Systems*, 33(3), 2518-2527.

Kabiri, R., Holmes, D. G., and McGrath, B. P. (2015). "Control of active and reactive power ripple to mitigate unbalanced grid voltages." *IEEE Transactions on Industry Applications*, 52(2), 1660-1668.

Khajeh, K. G., Bashar, E., Rad, A. M., and Gharehpetian, G. B. (2015). "Integrated model considering effects of zero injection buses and conventional measurements on optimal PMU placement." *IEEE Transactions on Smart Grid*, 8(2), 1006-1013.

Kiio, M. N., Wekesa, C. W., and Kamau, S. I. (2022). "Evaluating performance of a linear hybrid state estimator utilizing measurements from RTUs and optimally placed PMUs." *IEEE Access*, 10, 63113-63131.

Kim, B. H., and Kim, H. (2021). "PMU Optimal Placement Algorithm Using Topological Observability Analysis." *Journal of Electrical Engineering & Technology*, 16(6), 2909-2916.

Koochi, M. H. R., and Hemmatpour, M. H. (2020). "A general PMU placement approach considering both topology and system aspects of contingencies." *International Journal of Electrical Power & Energy Systems*, 118, 105774.

Kryonidis, G. C., Malamaki, K. N. D., Gkavanoudis, S. I., Oureilidis, K. O., Kontis, E. O., Mauricio, J. M., and Demoulias, C. S. (2020). "Distributed reactive power control scheme for the voltage regulation of unbalanced LV grids." *IEEE Transactions on Sustainable Energy*, 12(2), 1301-1310.

Kumar, V. S. S., and Thukaram, D. (2015). "Approach for multistage placement of phasor measurement units based on stability criteria." *IEEE Transactions on Power Systems*, 31(4), 2714-2725.

Langner, A. L., and Abur, A. (2020). "Formulation of three-phase state estimation problem using a virtual reference." *IEEE Transactions on Power Systems*, 36(1), 214-223.

Li, P., Su, H., Wang, C., Liu, Z., and Wu, J. (2018). "PMU-based estimation of voltage-to-power sensitivity for distribution networks considering the sparsity of Jacobian matrix." *IEEE Access*, 6, 31307-31316.

Liao, H., and Milanović, J. V. (2017). "On capability of different FACTS devices to mitigate a range of power quality phenomena." *IET Generation, Transmission & Distribution*, 11(5), 1202-1211.

Liu, J., Ponci, F., Monti, A., Muscas, C., Pegoraro, P. A., and Sulis, S. (2014). "Optimal meter placement for robust measurement systems in active distribution grids." *IEEE Transactions on Instrumentation and Measurement*, 63(5), 1096-1105.

Louis, A., Ledwich, G., Walker, G., and Mishra, Y. (2020). "Measurement sensitivity and estimation error in distribution system state estimation using augmented complex Kalman filter." *Journal of Modern Power Systems and Clean Energy*, 8(4), 657-668.

Lu, C., Wang, Z., Ma, M., Shen, R., and Yu, Y. (2018). "An optimal PMU placement with reliable zero injection observation." *IEEE Access*, 6, 54417-54426.

Luo, X., Akhtar, Z., Lee, C. K., Chaudhuri, B., Tan, S. C., and Hui, S. Y. R. (2014). "Distributed voltage control with electric springs: Comparison with STATCOM." *IEEE Transactions on Smart Grid*, 6(1), 209-219.

Luo, Y., Chen, M., Kang, W., and Sun, X. (2021). "Distributed Event-Triggered Voltage Control with Limited Re-Active Power in Low Voltage Distribution Networks." *Electronics*, 10(2), 128.

Mai, T. T., Nguyen, P. H., Tran, Q. T., Cagnano, A., De Carne, G., Amirat, Y., and De Tuglie, E. (2021). "An overview of grid-edge control with the digital transformation." *Electrical Engineering*, 1-19.

Manbachi, M., Nasri, M., Shahabi, B., Farhangi, H., Palizban, A., Arzanpour, S., and Lee, D. C. (2013). "Real-time adaptive VVO/CVR topology using multi-agent system and IEC 61850-based communication protocol." *IEEE Transactions on Sustainable Energy*, 5(2), 587-597.

Manousakis, N. M., and Korres, G. N. (2019). "Optimal allocation of phasor measurement units considering various contingencies and measurement redundancy." *IEEE Transactions on Instrumentation and Measurement*, 69(6), 3403-3411.

Mejia-Ruiz, G. E., Cárdenas-Javier, R., Paternina, M. R. A., Rodríguez-Rodríguez, J. R., Ramirez, J. M., and Zamora-Mendez, A. (2021). "Coordinated optimal volt/var control for distribution networks via d-pmus and ev chargers by exploiting the eigensystem realization." *IEEE Transactions on Smart Grid*, 12(3), 2425-2438.

Mendonca, T. R., and Green, T. C. (2019). "Distributed active network management based on locally estimated voltage sensitivity." *IEEE Access*, 7, 105173-105185.

Mishra, S., Das, D., and Paul, S. (2014, May). "A simple algorithm for distribution system load flow with distributed generation." *In International Conference on Recent Advances and Innovations in Engineering* (ICRAIE-2014) (pp. 1-5). IEEE.

Moghe, R., Divan, D., Lewis, D., and Schatz, J. (2016). "Turning distribution feeders into STATCOMs." *IEEE Transactions on Industry Applications*, 53(2), 1372-1380.

Mohamed, M. A., Al-Sumaiti, A. S., Krid, M., Awwad, E. M., and Kavousi-Fard, A. (2019). "A reliability-oriented fuzzy stochastic framework in automated distribution grids to allocate μ-PMUs." *IEEE Access*, 7, 33393-33404.

Müller, H. H., Castro, C. A., and Dotta, D. (2020). "Allocation of PMU channels at substations for topology processing and state estimation." *IET Generation, Transmission & Distribution*, 14(11), 2034-2045.

Muscas, C., Pilo, F., Pisano, G., and Sulis, S. (2008). "Optimal allocation of multichannel measurement devices for distribution state estimation." *IEEE Transactions on Instrumentation and Measurement*, 58(6), 1929-1937.

Nasr-Azadani, E., Canizares, C. A., Olivares, D. E., and Bhattacharya, K. (2014). "Stability analysis of unbalanced distribution systems with synchronous machine and DFIG based distributed generators." *IEEE Transactions on Smart Grid*, 5(5), 2326-2338.

Nejabatkhah, F., Li, Y. W., and Wu, B. (2015). "Control strategies of three-phase distributed generation inverters for grid unbalanced voltage compensation." *IEEE Transactions on Power Electronics*, 31(7), 5228-5241.

Nusrat, N., Irving, M., and Taylor, G. (2012, July). "Novel meter placement algorithm for enhanced accuracy of distribution system state estimation." *In 2012 IEEE Power and Energy Society General Meeting* (pp. 1-8). IEEE.

Othman, M. M., Ahmed, M. H., and Salama, M. M. A. (2019). "A novel smart meter technique for voltage and current estimation in active distribution networks." *International Journal of Electrical Power & Energy Systems*, 104, 301-310.

Pal, A., Mishra, C., Vullikanti, A. K. S., and Ravi, S. S. (2017). "General optimal substation coverage algorithm for phasor measurement unit placement in practical systems." *IET Generation, Transmission & Distribution*, 11(2), 347-353.

Patel, C. D., Tailor, T. K., Shukla, S. K., Shah, S., and Jani, S. N. (2022). "Steiner tree-based design of communication infrastructure with co-optimizing the PMU placement for economical design of WAMS." *IEEE Transactions on Instrumentation and Measurement*, 71, 1-11.

Pau, M., Ponci, F., Monti, A., Sulis, S., Muscas, C., and Pegoraro, P. A. (2017). "An efficient and accurate solution for distribution system state estimation with multiarea architecture." *IEEE Transactions on Instrumentation and Measurement*, 66(5), 910-919.

Primadianto, A., and Lu, C. N. (2016). "A review on distribution system state estimation." *IEEE Transactions on Power Systems*, 32(5), 3875-3883.

Procopiou, A. T., and Ochoa, L. F. (2016). "Voltage control in PV-rich LV networks without remote monitoring." *IEEE Transactions on Power Systems*, 32(2), 1224-1236.

Ranamuka, D., Agalgaonkar, A. P., and Muttaqi, K. M. (2016). "Examining the interactions between DG units and voltage regulating devices for effective voltage control in distribution systems." *IEEE Transactions on Industry Applications*, 53(2), 1485-1496.

Ranamuka, D., Agalgaonkar, A. P., and Muttaqi, K. M. (2018). "Innovative Volt/VAr control philosophy for future distribution systems embedded with voltage-regulating devices and distributed renewable energy resources." *IEEE Systems Journal*, 13(3), 3153-3164.

Shankar, R., and Singh, S. (2022). "Development of smart grid for the power sector in India." *Cleaner Energy Systems*, 2, 100011.

Shi, Y., Tuan, H. D., Duong, T. Q., Poor, H. V., and Savkin, A. V. (2019). "PMU placement optimization for efficient state estimation in smart grid." *IEEE Journal on Selected Areas in Communications*, 38(1), 71-83.

Singh, R., Pal, B. C., and Vinter, R. B. (2009). "Measurement placement in distribution system state estimation." *IEEE Transactions on Power Systems*, 24(2), 668-675.

Singh, R., Pal, B. C., Jabr, R. A., and Vinter, R. B. (2011). "Meter placement for distribution system state estimation: An ordinal optimization approach." *IEEE Transactions on Power Systems*, 26(4), 2328-2335.

Taher, S. A., and Karimi, M. H. (2014). "Optimal reconfiguration and DG allocation in balanced and unbalanced distribution systems." *Ain Shams Engineering Journal*, 5(3), 735-749.

Taher, S. A., Hasani, M., and Karimian, A. (2011). "A novel method for optimal capacitor placement and sizing in distribution systems with nonlinear loads and DG using GA." *Communications in Nonlinear Science and Numerical Simulation*, 16(2), 851-862.

Tangi, S., and Gaonkar, D. N. (2021). "Voltage estimation of active distribution network using PMU technology." *IEEE Access*, 9, 100436-100446.

Wang, H., Yan, Z., Shahidehpour, M., Zhou, Q., and Xu, X. (2020). "Optimal energy storage allocation for mitigating the unbalance in active distribution network via uncertainty quantification." *IEEE Transactions on Sustainable Energy*, 12(1), 303-313.

Wang, J., Zhou, N., Chung, C. Y., and Wang, Q. (2019). "Coordinated planning of converter-based DG units and soft open points incorporating active management in unbalanced distribution networks". *IEEE Transactions on Sustainable Energy*, 11(3), 2015-2027.

Wang, L., Yan, R., Bai, F., Saha, T., and Wang, K. (2020). "A distributed inter-phase coordination algorithm for voltage control with unbalanced PV integration in LV systems." *IEEE Transactions on Sustainable Energy*, 11(4), 2687-2697.

Weckx, S., and Driesen, J. (2015). "Load balancing with EV chargers and PV inverters in unbalanced distribution grids." *IEEE Transactions on Sustainable Energy*, 6(2), 635-643.

Xygkis, T. C., Korres, G. N., and Manousakis, N. M. (2016). "Fisher information-based meter placement in distribution grids via the D-optimal experimental design." *IEEE Transactions on Smart Grid*, 9(2), 1452-1461.

Yao, M., Hiskens, I. A., and Mathieu, J. L. (2020). "Mitigating voltage unbalance using distributed solar photovoltaic inverters." *IEEE Transactions on Power Systems*, 36(3), 2642-2651.

Yasinzadeh, M., and Akhbari, M. (2018). "Detection of PMU spoofing in power grid based on phasor measurement analysis." *IET Generation, Transmission & Distribution*, 12(9), 1980-1987.

Zad, B. B., Lobry, J., and Vallée, F. (2018). "A new voltage sensitivity analysis method for medium-voltage distribution systems incorporating power losses impact." *Electric Power Components and Systems*, 46(14-15), 1540-1553.

Zafar, R., Ravishankar, J., Fletcher, J. E., and Pota, H. R. (2019). "Multi-timescale voltage stability-constrained Volt/VAR optimization with battery storage system in distribution grids." *IEEE Transactions on Sustainable Energy*, 11(2), 868-878.

Zamzam, A. S., and Sidiropoulos, N. D. (2020). "Physics-aware neural networks for distribution system state estimation." *IEEE Transactions on Power Systems*, 35(6), 4347-4356.

Zhang, J., Wang, Y., Weng, Y., and Zhang, N. (2020). "Topology identification and line parameter estimation for non-PMU distribution network: A numerical method." *IEEE Transactions on Smart Grid*, 11(5), 4440-4453.

Zhang, M., Wu, Z., Yan, J., Lu, R., and Guan, X. (2022). "Attack-Resilient Optimal PMU Placement via Reinforcement Learning Guided Tree Search in Smart Grids." *IEEE Transactions on Information Forensics and Security*, 17, 1919-1929.

Zhang, Q., Dehghanpour, K., and Wang, Z. (2018)." Distributed CVR in unbalanced distribution systems with PV penetration." *IEEE Transactions on Smart Grid*, 10(5), 5308-5319.

Zhou, X., Liu, Z., Guo, Y., Zhao, C., Huang, J., and Chen, L. (2020). "Gradient-based multi-area distribution system state estimation." IEEE Transactions on Smart Grid, 11(6), 5325-5338.

APPENDIX

IEEE 18 bus system line and load data

Branch No.	Sending end node	Receiving end node	Resistance (ohms)	Reactance (ohms)	P_{Load} (kW)	Q_{Load} (kVAr)
1	1	2	0.0005	0.00344	0	0
2	2	3	0.00312	0.06753	200	120
3	3	4	0.00431	0.01204	400	250
4	4	5	0.00601	0.01677	150	930
5	5	6	0.00316	0.00882	0	0
6	6	7	0.00896	0.02502	800	500
7	7	8	0.00295	0.00824	200	120
8	8	9	0.0172	0.0212	1000	620
9	9	10	0.0407	0.03053	500	310
10	10	11	0.01706	0.02209	1000	620
11	11	12	0.0291	0.03768	300	190
12	12	13	0.02222	0.02877	200	120
13	13	14	0.0480	0.06218	800	500
14	14	15	0.03985	0.0516	500	310
15	15	16	0.0291	0.03768	1000	620
16	16	17	0.03727	0.04593	200	120
17	17	18	0.02208	0.0272	200	120
Base MVA = 10, Base KV = 12.5						

IEEE 33 bus system line and load data

Branch No.	Sending end node	Receiving end node	Resistance (ohms)	Reactance (ohms)	P_{Load} (kW)	Q_{Load} (kVAr)
1	1	2	0.0922	0.0470	0	0
2	2	3	0.4930	0.2511	100	60
3	3	4	0.3660	0.1864	90	40
4	4	5	0.3811	0.1941	120	80

5	5	6	0.8190	0.7070	60	30
6	6	7	0.1872	0.6188	60	20
7	7	8	1.7114	1.2351	200	100
8	8	9	1.03	0.7400	200	100
9	9	10	1.0440	0.7400	60	20
10	10	11	0.1966	0.0650	60	20
11	11	12	0.3744	0.1238	45	30
12	12	13	1.468	1.1550	60	35
13	13	14	0.5416	0.7129	60	35
14	14	15	0.5910	0.5260	120	80
15	15	16	0.7463	0.5450	60	10
16	16	17	1.2890	1.7210	60	20
17	17	18	0.7320	0.5740	90	20
18	18	19	0.1640	0.1565	90	40
19	19	20	1.5042	1.3554	90	40
20	20	21	0.4095	0.4784	90	40
21	21	22	0.7089	0.9373	90	40
22	22	23	0.4512	0.3083	90	40
23	23	24	0.8980	0.7091	420	50
24	24	25	0.8960	0.7011	420	200
25	25	26	0.2030	0.1034	60	200
26	26	27	0.2842	0.1447	60	25
27	27	28	1.0590	0.9337	60	25
28	28	29	0.8042	0.7006	120	20
29	29	30	0.5075	0.2585	200	70
30	30	31	0.9744	0.9630	150	600
31	31	32	0.3105	0.3619	210	70
32	32	33	0.3410	0.5302	60	100
Base MVA = 100, Base kV = 12.66						

IEEE 69 bus system line and load data

Branch No.	Sending end node	Receiving end node	Resistance (ohms)	Reactance (ohms)	P_{Load} (kW)	Q_{Load} (kVAr)
1	1	2	0.0005	0.0012	0	0
2	2	3	0.0005	0.0012	0	0
3	3	4	0.0015	0.0036	0	0
4	4	5	0.0251	0.0294	0	0
5	5	6	0.3660	0.1864	2.6	2.2
6	6	7	0.3811	0.1941	40.4	30
7	7	8	0.0922	0.0470	75	54
8	8	9	0.0493	0.0251	30	22
9	9	10	0.8190	0.2707	28	19
10	10	11	0.1872	0.0619	145	104
11	11	12	0.7114	0.2351	145	104
12	12	13	1.0300	0.3400	8	5
13	13	14	1.0440	0.3450	8	5.5
14	14	15	1.0580	0.3496	0	0
15	15	16	0.1966	0.0650	45.5	30
16	16	17	0.3744	0.1238	60	35
17	17	18	0.0047	0.0016	60	35
18	18	19	0.3276	0.1083	0	0
19	19	20	0.2106	0.0690	1	0.6
20	20	21	0.3416	0.1129	114	81
21	21	22	0.0140	0.0046	5	3.5
22	22	23	0.1591	0.0526	0	0
23	23	24	0.3463	0.1145	28	20
24	24	25	0.7488	0.2475	0	0
25	25	26	0.3089	0.1021	14	10
26	26	27	0.1732	0.0572	14	10
27	27	28	0.0044	0.0108	26	18.6
28	28	29	0.06405	0.1565	26	18.6
29	29	30	0.3978	0.1315	0	0
30	30	31	0.0702	0.0232	0	0

31	31	32	0.3510	0.1160	0	0
32	32	33	0.8390	0.2816	14	10
33	33	34	1.7080	0.5646	9.5	14
34	34	35	1.4740	0.4873	6	4
35	35	36	0.0044	0.0108	26	18.55
36	36	37	0.0640	0.1565	26	18.55
37	37	38	0.1053	0.1230	0	0
38	38	39	0.0304	0.0355	24	17
39	39	40	0.0018	0.0021	24	17
40	40	41	0.7283	0.8509	1.2	1
41	41	42	0.3100	0.3623	0	0
42	42	43	0.0410	0.0478	6	4.3
43	43	44	0.0092	0.0116	0	0
44	44	45	0.1089	0.1373	39.22	26.3
45	45	46	0.0009	0.0012	39.22	26.3
46	46	47	0.0034	0.0084	0	0
47	47	48	0.0851	0.2083	79	56.4
48	48	49	0.2898	0.7091	384.7	274.5
49	49	50	0.0822	0.2011	384.7	274.5
50	50	51	0.0928	0.0473	40.5	28.3
51	51	52	0.3319	0.1114	3.6	2.7
52	52	53	0.1740	0.0886	4.35	3.5
53	53	54	0.2030	0.1034	26.4	19
54	54	55	0.2842	0.1447	24	17.2
55	55	56	0.2813	0.1433	0	0
56	56	57	1.5900	0.5337	0	0
57	57	58	0.7837	0.2630	0	0
58	58	59	0.3042	0.1006	100	72
59	59	60	0.3861	0.1172	0	0
60	60	61	0.5075	0.2585	1244	888
61	61	62	0.0974	0.0496	32	23
62	62	63	0.1450	0.0738	0	0
63	63	64	0.7105	0.3619	227	162

64	64	65	1.0410	0.5302	59	42
65	65	66	0.2012	0.0611	18	13
66	66	67	0.0047	0.0014	18	13
67	67	68	0.7394	0.2444	28	20
68	68	69	0.0005	0.0012	28	20
Base MVA = 100, Base kV = 12.66						

IEEE 119 bus system line and load data

Branch No.	Sending end node	Receiving end node	Resistance (ohms)	Reactance (ohms)	P_{Load} (kW)	Q_{Load} (kVAr)
1	1	2	0.0360	0.013	0	0
2	2	3	0.0330	0.0119	0	0
3	3	4	0.0450	0.0162	133.84	101.1
4	4	5	0.0150	0.054	16.214	11.3
5	5	6	0.0150	0.054	34.315	21.8
6	6	7	0.0150	0.0125	73.016	63.6
7	7	8	0.0180	0.014	144.2	68.6
8	8	9	0.0210	0.063	104.47	61.7
9	9	10	0.1660	0.1344	28.547	11.5
10	10	11	0.1120	0.0789	87.56	51.1
11	11	12	0.1870	0.313	198.2	106.8
12	12	13	0.1420	0.1512	146.8	76
13	13	14	0.1800	0.118	26.04	18.7
14	14	15	0.1500	0.045	52.1	23.2
15	15	16	0.1600	0.18	141.9	117.5
16	16	17	0.1570	0.171	21.87	28.8
17	17	18	0.2180	0.285	33.37	26.4
18	18	19	0.1180	0.185	32.43	25.2
19	19	20	0.1600	0.196	20.234	11.9
20	20	21	0.1200	0.189	156.94	78.5
21	21	22	0.1200	0.0789	546.29	351.4
22	22	23	1.4100	0.723	180.31	164.2

23	23	24	0.2930	0.1348	93.167	54.6
24	24	25	0.1330	0.104	85.18	39.6
25	25	26	0.1780	0.134	168.1	95.2
26	26	27	0.1780	0.134	125.11	150.2
27	27	28	0.0150	0.0296	16.03	24.6
28	28	29	0.0120	0.0276	26.03	24.6
29	29	30	0.1200	0.2766	594.56	522.6
30	30	31	0.2100	0.243	120.62	59.1
31	31	32	0.1200	0.054	102.38	99.6
32	32	33	0.1780	0.234	513.4	318.5
33	33	34	0.1780	0.234	475.25	456.1
34	34	35	0.1540	0.162	151.43	136.8
35	35	36	0.1870	0.261	205.38	83.3
36	36	37	0.1330	0.099	131.6	93.1
37	37	38	0.3300	0.194	448.4	369.8
38	38	39	0.3100	0.194	440.52	321.6
39	39	40	0.1300	0.194	112.54	55.1
40	40	41	0.2800	0.15	53.963	39
41	41	42	1.1800	0.85	393.05	342.6
42	42	43	0.4200	0.246	326.74	278.6
43	43	44	0.2700	0.0972	536.26	240.2
44	44	45	0.3390	0.1221	76.247	66.6
45	45	46	0.2700	0.1779	53.52	39.8
46	46	47	0.2100	0.1383	40.328	32
47	47	48	0.1200	0.0789	39.653	20.8
48	48	49	0.1500	0.0987	66.195	42.4
49	49	50	0.1500	0.0987	73.904	51.7
50	50	51	0.2400	0.1581	114.77	58
51	51	52	0.1200	0.0789	918.37	1205.1
52	52	53	0.4050	0.1458	210.3	146.7
53	53	54	0.4050	0.1458	210.3	56.6
54	54	55	0.3910	0.141	66.68	40.2
55	55	56	0.4060	0.1461	42.207	283.4

56	56	57	0.4060	0.1461	433.74	26.9
57	57	58	0.7060	0.5461	62.1	88.4
58	58	59	0.3380	0.1218	92.46	55.4
59	59	60	0.3380	0.1218	85.188	332.4
60	60	61	0.2070	0.0747	345.3	16.8
61	61	62	0.2470	0.8922	22.5	49.2
62	62	63	0.0280	0.0418	80.551	90.8
63	63	64	0.1170	0.2016	95.86	47.7
64	64	65	0.2550	0.0918	62.92	463.7
65	65	66	0.2100	0.0759	478.8	52
66	66	67	0.3830	0.138	120.94	100.3
67	67	68	0.5040	0.3303	139.11	193.5
68	68	69	0.4060	0.1461	391.78	26.7
69	69	70	0.9620	0.761	27.741	25.3
70	70	71	0.1650	0.06	52.814	38.7
71	71	72	0.3030	0.1092	66.89	395.1
72	72	73	0.3030	0.1092	467.5	239.7
73	73	74	0.2060	0.144	210.3	84.4
74	74	75	0.2330	0.084	66.68	22.5
75	75	76	0.5910	0.1773	42.207	614.8
76	76	77	0.1260	0.0453	433.74	29.8
77	77	78	0.5590	0.3687	62.1	122.4
78	78	79	0.1860	0.1227	92.46	45.4
79	79	80	0.1860	0.1227	85.188	223.2
80	80	81	0.2600	0.139	345.3	162.5
81	81	82	0.1540	0.148	22.5	437.9
82	82	83	0.2300	0.128	80.551	183
83	83	84	0.2520	0.106	95.86	183
84	84	85	0.1800	0.148	62.92	119.3
85	85	86	0.1600	0.182	478.8	28
86	86	87	0.2000	0.23	120.94	26.5
87	87	88	0.1600	0.393	139.11	257.2
88	88	89	0.6690	0.2412	391.78	20.6

89	89	90	0.2660	0.1227	27.741	11.8
90	90	91	0.2660	0.1227	52.814	43
91	91	92	0.2660	0.1227	66.89	34.9
92	92	93	0.2660	0.1227	467.5	66.8
93	93	94	0.2330	0.115	594.85	81.7
94	94	95	0.4960	0.138	132.5	66.5
95	95	96	0.1960	0.18	52.699	16
96	96	97	0.1960	0.18	869.79	60.5
97	97	98	0.1866	0.122	31.349	224.8
98	98	99	0.0746	0.318	192.39	367.4
99	99	100	0.0625	0.0265	65.75	11.7
100	100	101	0.1501	0.234	238.15	30.4
101	101	102	0.1347	0.0888	294.55	47.6
102	102	103	0.2307	0.1203	485.57	350.3
103	103	104	0.4470	0.1608	243.53	449.3
104	104	105	0.1632	0.0588	243.53	168.5
105	105	106	0.3300	0.099	134.25	134.3
106	106	107	0.1560	0.0561	22.71	66
107	107	108	0.3819	0.1374	49.513	83.6
108	108	109	0.1626	0.0585	383.78	419.3
109	109	110	0.3819	0.1374	49.64	135.9
110	110	111	0.2445	0.0879	22.473	387.2
111	111	112	0.2088	0.0753	62.93	173.5
112	112	113	0.2301	0.0828	30.67	898.5
113	113	114	0.6102	0.2196	62.53	215.4
114	114	115	0.1866	0.127	114.57	41
115	115	116	0.3732	0.246	81.292	192.9
116	116	117	0.4050	0.367	31.733	53.3
117	117	118	0.4890	0.438	33.32	90.3
118	118	119	0.0360	0.438	531.28	29.2
Base MVA = 100, Base kV = 12.66						

25 bus system 3-phase unbalanced system data of phase A

Branch No.	Sending end node	Receiving end node	Phase A self-impedance (ohms)	P_{Load} (kW)	Q_{Load} (kVAr)
1	1	2	1.9280 + 1.4194i	0	0
2	2	3	1.9280 + 1.4194i	35	25
3	3	4	1.9280 + 1.4194i	40	30
4	4	5	1.9280 + 1.4194i	50	40
5	5	6	1.9280 + 1.4194i	40	30
6	6	7	1.9280 + 1.4194i	40	30
7	7	8	1.9280 + 1.4194i	60	45
8	8	9	1.9280 + 1.4194i	0	0
9	9	10	1.9280 + 1.4194i	40	30
10	10	11	1.9280 + 1.4194i	60	45
11	11	12	1.9280 + 1.4194i	50	35
12	12	13	1.9280 + 1.4194i	40	30
13	13	14	1.9280 + 1.4194i	35	25
14	14	15	1.9280 + 1.4194i	45	32
15	15	16	1.9280 + 1.4194i	50	35
16	16	17	1.9280 + 1.4194i	35	25
17	17	18	1.9280 + 1.4194i	133.3	100
18	18	19	1.9280 + 1.4194i	40	30
19	19	20	1.9280 + 1.4194i	35	25
20	20	21	1.9280 + 1.4194i	40	30
21	21	22	1.9280 + 1.4194i	60	45
22	22	23	1.9280 + 1.4194i	50	35
23	23	24	1.9280 + 1.4194i	35	25
24	24	25	1.9280 + 1.4194i	60	45
Base MVA = 100, Base kV = 4.16					

25 bus system 3-phase unbalanced system data of phase B

Branch No.	Sending end node	Receiving end node	Phase B self-impedance (ohms)	P_{Load} (kW)	Q_{Load} (kVAr)
1	1	2	1.9308 + 1.4215i	0	0
2	2	3	1.9308 + 1.4215i	40	30
3	3	4	1.9308 + 1.4215i	45	32
4	4	5	1.9308 + 1.4215i	60	45
5	5	6	1.9308 + 1.4215i	40	30
6	6	7	1.9308 + 1.4215i	40	30
7	7	8	1.9308 + 1.4215i	50	40
8	8	9	1.9308 + 1.4215i	0	0
9	9	10	1.9308 + 1.4215i	40	30
10	10	11	1.9308 + 1.4215i	50	40
11	11	12	1.9308 + 1.4215i	60	45
12	12	13	1.9308 + 1.4215i	40	30
13	13	14	1.9308 + 1.4215i	40	30
14	14	15	1.9308 + 1.4215i	35	25
15	15	16	1.9308 + 1.4215i	60	45
16	16	17	1.9308 + 1.4215i	45	32
17	17	18	1.9308 + 1.4215i	133.3	100
18	18	19	1.9308 + 1.4215i	35	32
19	19	20	1.9308 + 1.4215i	40	30
20	20	21	1.9308 + 1.4215i	35	25
21	21	22	1.9308 + 1.4215i	50	35
22	22	23	1.9308 + 1.4215i	60	45
23	23	24	1.9308 + 1.4215i	45	32
24	24	25	1.9308 + 1.4215i	50	30
Base MVA = 100, Base kV = 4.16					

25 bus system 3-phase unbalanced system data of phase C

Branch No.	Sending end node	Receiving end node	Phase C self-impedance (ohms)	P_{Load} (kW)	Q_{Load} (kVAr)
1	1	2	1.9337 + 1.4236i	0	0
2	2	3	1.9337 + 1.4236i	40	30
3	3	4	1.9337 + 1.4236i	45	32
4	4	5	1.9337 + 1.4236i	60	45
5	5	6	1.9337 + 1.4236i	40	30
6	6	7	1.9337 + 1.4236i	40	30
7	7	8	1.9337 + 1.4236i	50	40
8	8	9	1.9337 + 1.4236i	0	0
9	9	10	1.9337 + 1.4236i	40	30
10	10	11	1.9337 + 1.4236i	50	40
11	11	12	1.9337 + 1.4236i	60	45
12	12	13	1.9337 + 1.4236i	40	30
13	13	14	1.9337 + 1.4236i	40	30
14	14	15	1.9337 + 1.4236i	35	25
15	15	16	1.9337 + 1.4236i	60	45
16	16	17	1.9337 + 1.4236i	45	32
17	17	18	1.9337 + 1.4236i	133.3	100
18	18	19	1.9337 + 1.4236i	35	32
19	19	20	1.9337 + 1.4236i	40	30
20	20	21	1.9337 + 1.4236i	35	25
21	21	22	1.9337 + 1.4236i	50	35
22	22	23	1.9337 + 1.4236i	60	45
23	23	24	1.9337 + 1.4236i	45	32
24	24	25	1.9337 + 1.4236i	50	30
Base MVA = 100, Base kV = 4.16					

25 bus system 3-phase unbalanced system mutual impedance data

Branch No.	Phase AB mutual impedance (ohms)	Phase BC mutual impedance (ohms)	Phase CA mutual impedance (ohms)
1	0.0161 + 0.1183i	0.0161 + 0.1183i	0.0161 + 0.1183i
2	0.0161 + 0.1183i	0.0161 + 0.1183i	0.0161 + 0.1183i
3	0.0161 + 0.1183i	0.0161 + 0.1183i	0.0161 + 0.1183i
4	0.0161 + 0.1183i	0.0161 + 0.1183i	0.0161 + 0.1183i
5	0.0161 + 0.1183i	0.0161 + 0.1183i	0.0161 + 0.1183i
6	0.0161 + 0.1183i	0.0161 + 0.1183i	0.0161 + 0.1183i
7	0.0161 + 0.1183i	0.0161 + 0.1183i	0.0161 + 0.1183i
8	0.0161 + 0.1183i	0.0161 + 0.1183i	0.0161 + 0.1183i
9	0.0161 + 0.1183i	0.0161 + 0.1183i	0.0161 + 0.1183i
10	0.0161 + 0.1183i	0.0161 + 0.1183i	0.0161 + 0.1183i
11	0.0161 + 0.1183i	0.0161 + 0.1183i	0.0161 + 0.1183i
12	0.0161 + 0.1183i	0.0161 + 0.1183i	0.0161 + 0.1183i
13	0.0161 + 0.1183i	0.0161 + 0.1183i	0.0161 + 0.1183i
14	0.0161 + 0.1183i	0.0161 + 0.1183i	0.0161 + 0.1183i
15	0.0161 + 0.1183i	0.0161 + 0.1183i	0.0161 + 0.1183i
16	0.0161 + 0.1183i	0.0161 + 0.1183i	0.0161 + 0.1183i
17	0.0161 + 0.1183i	0.0161 + 0.1183i	0.0161 + 0.1183i
18	0.0161 + 0.1183i	0.0161 + 0.1183i	0.0161 + 0.1183i
19	0.0161 + 0.1183i	0.0161 + 0.1183i	0.0161 + 0.1183i
20	0.0161 + 0.1183i	0.0161 + 0.1183i	0.0161 + 0.1183i
21	0.0161 + 0.1183i	0.0161 + 0.1183i	0.0161 + 0.1183i
22	0.0161 + 0.1183i	0.0161 + 0.1183i	0.0161 + 0.1183i
23	0.0161 + 0.1183i	0.0161 + 0.1183i	0.0161 + 0.1183i
24	0.0161 + 0.1183i	0.0161 + 0.1183i	0.0161 + 0.1183i

BIODATA

Swathi Tangi

Research Scholar

Department of Electrical and Electronic Engg.

National Institute of Technology Karnataka, Surathkal

P.O.Srinivasanagar

Mangalore 575025

Phone: +91- 9538410461

Email: swathit.tangi1@gmail.ecom

Permanent address

Swathi Tangi

D/o T. Bhaskararao

Door No. 15-56,

Near High School

Gajularega – 535002

Vizianagaram, Andhrapradesh.

Qualification

B.Tech. (ELectrical Engineering) at St. Theressa Institute of Engg. & Technology, Vizianagaram, AP.

M.Tech. (Power & Energy Systems) at NITK, Surathkal, Karnataka.